# THE COMPLEX REFRACTIVE INDEX OF WATER

A THESIS IN
Physics

Presented to the Faculty of the University
of Missouri-Kansas City in partial fulfillment of
the requirements for the degree

MASTER OF SCIENCE

by
DAVID J. SEGELSTEIN

B.A., Columbia University, 1971
J.D., University of Missouri-Kansas City, 1975

Kansas City, Missouri
1981

THE COMPLEX REFRACTIVE INDEX OF WATER

David J. Segelstein, Master of Science

University of Missouri-Kansas City, 1981

ABSTRACT

A spectrum of the imaginary part of the complex index of refraction for water as a function of wave number was compiled from the literature and theoretical considerations. The spectrum ranged from $10^{-6}$ through $10^{8}$ $cm^{-1}$. The curve was adjusted within the limits of error for the data used until an electronic sum rule gave proper results. The spectrum was then appropriately Fourier transformed to yield the real part of the complex refractive index. The results of several calculations over various ranges were combined into one spectrum over the range $10^{-3}$ through $10^{6}$ $cm^{-1}$. Both real and imaginary parts are presented in graphical and tabular form.

This abstract of 106 words is approved as to form and content.

Marvin R. Querry

Marvin R. Querry

The undersigned, appointed by the Dean of the School of Graduate Studies, have examined a thesis entitled "The Complex Refractive Index of Water," presented by David J. Segelstein, candidate for the degree Master of Science, and hereby certify that in their opinion it is worthy of acceptance.

Marvin R. Querry, Ph.D.
Department of Physics — 30 June 1981 Date

John R. Urani, Ph.D.
Department of Physics — June 30, 1981 Date

Wai Yim Ching, Ph.D.
Department of Physics — June 26, 1981 Date

TABLE OF CONTENTS

LIST OF ILLUSTRATIONS

LIST OF TABLES

ACKNOWLEDGMENTS

I would like to thank the faculty of the Physics Department of the University of Missouri-Kansas City for struggling so tirelessly to bring me to this point. I would especially thank Dr. Marvin Querry, who is the most patient individual I have ever met, for his generous and warm guidance whenever it was requested. I would also express my gratitude to the entire staff of the University of Missouri-Kansas City Computer Center for their kind tolerance of my constant pestering, and for their always competent assistance.

# CHAPTER I

## INTRODUCTION

Water is one of earth's most common and important substances. Information concerning its optical properties is of great significance in many areas of science and engineering. Knowledge of its properties is a first step, for example, in the ability to interpret data on aqueous solutions, including the oceans and the atmosphere. Water is also interesting because it serves as a challenging object for the application of the full analytical power of classical electromagnetic theory. One tool in the analysis of its optical properties is the complex refractive index $N(\nu)$ as a function of wave number:

$$N(\nu) \equiv n(\nu) + ik(\nu) \tag{1.1}$$

where the wave number, $\nu$, is defined as the inverse of wavelength, and has units of $cm^{-1}$. From $N(\nu)$ one can calculate a variety of optical properties such as reflectance, transmittance, emittance, and Mie scattering parameters at any spectral location.

The purpose of the research described in this thesis was a determination of $N(\nu)$ for water throughout the wave number region of from $10^{-3}$ to $10^{6}$ $cm^{-1}$. This corresponds to a frequency range of from $10^{7}$ to $10^{16}$ Hz, a wavelength range of from 100 Å to 10 m. This task has been undertaken previously by other investigators, but not over such a broad spectral region.

Survey of the Literature

In 1973, Hale and Querry[1] reported optical constants for the region 50 to $5 \times 10^4$ $cm^{-1}$ (200 nm to 200 μm wavelength). They compiled a composite spectrum of $k(\nu)$, the extinction coefficient, from 58 sources representing data reported over a span of 81 years prior to their paper. This spectrum was transformed by Kramers-Kronig analysis to a spectrum of $n(\nu)$ for the region reported.

Some of the data used by Hale and Querry were incomplete or postulated. For example, a Gaussian-shaped absorption band was postulated for $k(\nu)$ with a peak in the area of $1.25 \times 10^6$ $cm^{-1}$ (80 Å wavelength). This would be the peak associated with the K-edge for electronic absorption. Also, the higher wave-number side of an absorption peak reported at approximately $1.2 \times 10^5$ $cm^{-1}$ was postulated to be of Gaussian shape and appropriate width. These deficiencies were recognized by Hale and Querry, and were the basis for their implication that more and better data were needed for more accurate determination of $N(\nu)$.

Since the 1973 paper by Hale and Querry, there have been additional compilations of $n(\nu)$, $k(\nu)$, or $\alpha(\nu)$, the latter being the Lambert absorption coefficient. It is defined in terms of $I$, the intensity, as the fractional decrease in intensity over distance:

$$\alpha(\nu) \equiv -\frac{1}{I}\frac{dI}{dx} = 4\pi k(\nu)\nu \qquad (1.2)$$

Of the more recent literature, the following are notable:

A report by Heller, Hamm, Birkhoff, and Painter[2] appeared in

1974. The authors obtained $n(\nu)$, $k(\nu)$, $\varepsilon_r(\nu)$, and $\varepsilon_i(\nu)$, the latter two being the real and imaginary parts of the dielectric function, $\varepsilon(\nu)$, for the range $6.1 \times 10^4$ to $2.1 \times 10^5$ $cm^{-1}$ (48 to 163 nm wavelength). Reflectance was measured and the above constants were calculated by Kramers-Kronig analysis.

A 1975 paper by Downing and Williams[3] reported values for $n(\nu)$, $k(\nu)$, and $\alpha(\nu)$ for the region 10 to 5000 $cm^{-1}$ (2 μm to 1 mm wavelength). The values of $k(\nu)$ were obtained by measurement and by calculation from reflectance data. The results for $n(\nu)$ were determined by either Kramers-Kronig analysis or by calculation from reflectance and phase shift data, depending on whether accurate values of $k(\nu)$ were available for the particular region.

A communication by Kopelevich[4] reported in 1976 discussed the range $1.7 \times 10^4$ to $4 \times 10^4$ $cm^{-1}$ (250 to 600 nm wavelength). The author criticized the values of $k(\nu)$ used by Hale and Querry in their 1973 paper. The claim was that water samples in the measurements relied upon were not pure enough. Kopelevich asserted that lower values of $k(\nu)$ were inherently better because they indicated a more pure sample.

A 1977 report by Afsar and Hasted[5] gave $\alpha(\nu)$, $k(\nu)$, and $n(\nu)$ for the range 6 to 450 $cm^{-1}$ (22 μm to 1.7 mm wavelength). These were calculated from reflectance data obtained by use of a Fourier-transform spectrophotometer, with an improved liquid cell and a more accurately measured reference interferogram, as compared with earlier measurements of the same type.

In a paper published in 1978, Querry, Cary, and Waring[6] reported

values for $\alpha(\nu)$ for the region $1.5 \times 10^4$ to $2.4 \times 10^4$ $cm^{-1}$ (418 to 640 nm wavelength). These were experimental data obtained by a split-pulse laser method of measuring attenuation.

Tam and Patel[7] gave values for $\alpha(\nu)$ for the interval $1.44 \times 10^4$ to $2.24 \times 10^4$ $cm^{-1}$ (446 to 694 nm wavelength) in a paper published in 1979. The technique used was pulsed dye-laser optoacoustic spectroscopy. The method eliminated the detection of spurious attenuation due to scattering.

In addition to the above data, there are relations which can be used to obtain reasonable data for optical constants. For example, in the region below approximately ten $cm^{-1}$, the semi-empirical Cole-Cole equation[8] gives sound values for the real and imaginary parts of the dielectric function. In the neighborhood of the oxygen K-edge, at $4.35 \times 10^6$ $cm^{-1}$, the shape of the absorption curve above and below the discontinuity can be obtained from an empirical equation which gives the mass absorption coefficient as a power of wavelength.[9] One can find the height of the discontinuity from an empirically obtained relationship between the jump in the mass absorption coefficient across the K-edge and the atomic number.[10] Given these determinations, one needs only some data in the vicinity of the discontinuity to fix the position of the curve. These data are available.

## Description of the Research

With the addition of the above data, it was hoped that a more reliable spectrum of $N(\nu)$ could be obtained. The program was, first, to obtain reasonable values for $\alpha(\nu)$, or equivalently $k(\nu)$, from the

literature and the relations mentioned above. These values would span the range from $10^{-6}$ $cm^{-1}$, the end of the spectrum obtained from the Cole-Cole equation, to $10^{15}$ $cm^{-1}$, the region for which the power law relation gives reasonable predictions. The compilation of this $\alpha(\nu)$ spectrum is described in Chapter II.

This spectrum of $\alpha(\nu)$ was tested for accuracy by use of a sum rule describing the contributions of electronic absorption. The spectrum was adjusted in the region from the low wave-number side of the absorption peak at $1.14 \times 10^{5}$ $cm^{-1}$ to the bottom of the K-edge discontinuity. The adjustment was made, well within the experimental error stated for the data used, until the electronic sum rule indicated ten electrons.

The $\alpha(\nu)$ spectrum was then appropriately Fourier transformed to give $n(\nu)$ for the range $10^{-3}$ to $10^{6}$ $cm^{-1}$. The Fourier transform technique is equivalent to conventional Kramers-Kronig analysis, as is shown in Chapter III. The advantage is in the ability to use the digital FAST FOURIER TRANSFORM yielding equivalent results with much less computing time.

The theoretical development of the Kramers-Kronig relations, their extension to a Fourier transform relationship, and the electronic sum rule derivation are presented in Chapter III. The application to direct computation is described in Chapter IV. Spectral values of $N(\nu)$ are presented in tabular and graphical form in Chapter V. The results are discussed in Chapter VI.

## CHAPTER II

## ACQUISITION OF DATA

### The Middle Range

So as not to discard the baby with the bath water, the absorption spectrum used by Hale and Querry was retained except where better data were available. Replacement of data began in the visible region.

A significant area of contention has been the purity of water samples for experimental determination of extinction coefficients in the visible region. The question involves how much intensity is lost due to scattering, a phenomenon which is aggravated by the presence of particles, bubbles, or other impurities. That was the substance of the objection by Kopelevich to the data used by Hale and Querry. The difficulty is neatly avoided by the technique of optoacoustic spectroscopy, as used by Tam and Patel. The method relies on the generation of transient acoustic waves by any material which absorbs a light pulse. Data were obtained by detection and comparison of sound waves over the particular range of frequencies of input light. The light source was a pulsed dye laser. Since there is no reliance on the intensity of light surviving passage through the sample, scattering is not involved. Tam and Patel measured only absorption.

The data of Tam and Patel were incorporated into the spectrum. The next task was to find values for $\alpha(\nu)$ which joined continuously

with that data. At the lower end, $1.44 \times 10^4$ cm$^{-1}$, the data of Tam and Patel joined almost precisely with that of Hale and Querry. Nothing additional was required. At the high end, however, $2.24 \times 10^4$ cm$^{-1}$, there was no real agreement among investigators up to the area of $5 \times 10^4$ cm$^{-1}$. After considering data of many researchers, it was found that the most reasonable and the smoothest curve connecting the two areas was obtained by averaging the data of Lenoble and Saint-Guilly[11] with that quoted by Kopelevich.

The range from $5 \times 10^4$ to $6.49 \times 10^4$ cm$^{-1}$ was left intact with the data of Hale and Querry. There seems to be much agreement as to the values for that region, as is graphically illustrated by Painter, Birkhoff, and Arakawa in Figure 4 of their 1969 paper.[12]

In the range $6.49 \times 10^4$ to $2.06 \times 10^5$ cm$^{-1}$, the data of Heller, Hamm, Birkhoff, and Painter were used because, at the lower end, the curve fit quite accurately in position and shape with the data below that. Also, as this was the region which would have the greatest effect in adjustments to conform to the sum rule, an inability to reach ten electrons while staying within the experimental error quoted by Heller et al. would have indicated that the data there were inappropriate. Because conformity with the sum rule constraint was obtained while remaining well within the error bars, it was evident that the data were appropriate.

The range above $2.06 \times 10^5$ cm$^{-1}$ is discussed under "High Frequency Data" below. For the other extreme, the part of the spectrum from $10^{-6}$ to 5 cm$^{-1}$ is discussed below in the section entitled "Low Frequency Data."

From 5 to 500 cm$^{-1}$, data from Afsar and Hasted were used. Their

work represents probably the first comprehensive investigation of that range of the spectrum. Further, their technique was advanced as compared with earlier measurements.

To join with the data of Afsar and Hasted, the values of $\alpha(\nu)$ obtained by Robertson and Williams[13] fit quite well. In addition, their work was a direct experimental determination of absorption via transmittance measurements. The values of Robertson and Williams were used where they differed from those used by Hale and Querry, namely in the ranges $5\times10^2$ to $10^3$ $cm^{-1}$ and $3.3\times10^3$ to $4\times10^3$ $cm^{-1}$.

Low Frequency Data

The behavior of a polar liquid in an alternating field is treated by Debye in his book Polar Molecules.[14] By calculating the distribution function for orientation of the molecules, Debye obtained the following expressions[15]:

$$\varepsilon' = \varepsilon_o + \frac{\varepsilon_1 - \varepsilon_o}{1 + x^2} \tag{2.1}$$

$$\varepsilon'' = \frac{(\varepsilon_1 - \varepsilon_o)x}{1 + x^2} \tag{2.2}$$

$$x = \left(\frac{\varepsilon_1 + 2}{\varepsilon_o + 2}\right)\omega\tau \tag{2.3}$$

where $\varepsilon' = \varepsilon_r$, $\varepsilon'' = -\varepsilon_i$, $\tau$ = the "relaxation time" for the orientation of the molecules, $\omega$ = the angular frequency of the applied field, $\varepsilon_o$ = the high frequency value for $\varepsilon$, and $\varepsilon_1$ = the static dielectric constant.

The characteristic relaxation time for water at room temperature was calculated by Debye to be approximately $2.5 \times 10^{-11}$ seconds.[16] This corresponds to a wavelength of the order of one cm. In this region, and for longer wavelengths, the Debye equations should yield good predictions, approaching the low frequency limit smoothly.

A significant improvement over the Debye relation was made by Cole and Cole in their paper published in 1941. They first wrote the Debye equations in the form[8]

$$\varepsilon^* = \varepsilon_\infty + \frac{\varepsilon_o - \varepsilon_\infty}{1 + i\omega\tau_o} \tag{2.4}$$

where $\varepsilon^*$ is the complex dielectric function, $\varepsilon_\infty$ is the high frequency limit, and $\varepsilon_o$ is the static limit. Then the authors showed that better results are obtainable by writing[17]

$$\varepsilon^* = \varepsilon_\infty + \frac{\varepsilon_o - \varepsilon_\infty}{1 + (i\omega\tau_o)^{1-\alpha}} \tag{2.5}$$

where $\alpha$ and $\tau_o$ are parameters to be determined.

This equation can be used directly to calculate values for the dielectric function, and hence the complex refractive index, in the vicinity of the frequency corresponding to the relaxation time. Values for the parameters $\varepsilon_o$, $\varepsilon_\infty$, $\tau_o$, and $\alpha$ are available, for example, from Water, a Comprehensive Treatise,[18] there obtained from experimental results. The values of the parameters in that reference were used in the Cole-Cole equation to calculate the extinction coefficient for

the range $10^{-6}$ to 5 $cm^{-1}$.

High Frequency Data

In the soft x-ray region, data are scarce. However, the evidence indicates a relationship of the form[9]

$$\frac{\mu}{\rho} = K\lambda^n Z^m + \frac{\sigma}{\rho} \tag{2.6}$$

for the mass absorption coefficient, $\mu/\rho$. $\sigma/\rho$ is the attenuation due to scattering. This yields, since $\mu = \alpha$,

$$\alpha = \rho K\lambda^n Z^m + \sigma \tag{2.7}$$

or if scattering is subtracted out, $(\alpha-\sigma) \rightarrow \alpha$, and

$$\alpha = A\nu^{-n} \tag{2.8}$$

Thus, the Lambert absorption coefficient is given by some negative power of wave number.

Engström suggests a value for $n$ for the soft x-ray region of somewhat less than three. In the data used for this thesis, $n$ was found to be 2.2297 in the area between $2.1 \times 10^5$ and $4.3 \times 10^6$ $cm^{-1}$ (the latter location being the bottom of the K-edge), a range corresponding to ultra-soft x-rays. Above the K-edge, $n$ was found to be 2.6257.

This power law relationship was applied in the following manner: Data from the National Bureau of Standards[19] were available for the

mass absorption coefficient for the range $8 \times 10^{7}$ to $8 \times 10^{14}$ $cm^{-1}$. These data were extended by extrapolation to the K-edge location at $4.35 \times 10^{6}$ $cm^{-1}$. This only assumes that the power n remains constant from the K-edge discontinuity to the slightly higher wave numbers stated.

The magnitude of the discontinuity was determined from Figures 3 and 4 of Engström's book.[20] Those figures indicate, respectively, the ratio of mass absorption coefficients and the difference between the coefficients on either side of the discontinuity. This fixed the bottom of the K-edge and left only the region between $2.1 \times 10^{5}$ and $4.3 \times 10^{6}$ $cm^{-1}$ to be filled in. (Data were available up to approximately $2.1 \times 10^{5}$ $cm^{-1}$ from the Heller, Hamm, Birkhoff, and Painter work.)

The data were joined between the points $2.1 \times 10^{5}$ $cm^{-1}$ and the bottom of the K-edge by assuming a linear relationship on a plot of the log of the Lambert coefficient versus the log of the wave number. The slope of this line would then correspond to n in the power law relationship.

The data from the paper of Heller et al. could be adjusted within the experimental limits, and a new line would be calculated each time. This gave an efficient means of adjustment while maintaining self-consistency among all the data.

Data for frequencies above $10^{15}$ $cm^{-1}$ were effectively ignored, that being the range in which absorption predominately involves non-atomic/molecular phenomena. Inclusion of these data would have made use of the electronic sum rule impossible as a measure of the accuracy of the absorption spectrum. Further, since optical properties were

calculated only up to $10^6$ $cm^{-1}$, inclusion or exclusion of these data would have had negligible if any effect on the results. The means for evaluation of the sum rule in this region above $10^{15}$ $cm^{-1}$ is described below.

Application of the Sum Rule

Once the new absorption spectrum was completed, the electronic sum rule was applied to test its accuracy. The sum rule, as derived in Chapter III, in SI units, is

$$Z = \left(\frac{4mc^2\varepsilon_o}{n_o e^2}\right)\int_0^\infty \alpha(\nu)d\nu \tag{2.9}$$

where $m$ is the mass of an electron, $c$ is the speed of light in vacuum, $\varepsilon_o$ the permittivity constant, $n_o$ the number of water molecules per cubic meter, and $e$ the electronic charge.

If numerical values of $\alpha(\nu)$ are available up to some appropriate $\nu_{max}$, the integration from $\nu_{max}$ to infinity can be done analytically using the inverse power law relationship described above. The sum rule is written

$$Z = \left(\frac{4mc^2\varepsilon_o}{n_o e^2}\right)\left[\int_0^{\nu_{max}} \alpha(\nu)d\nu + \int_{\nu_{max}}^\infty \alpha(\nu)d\nu\right] \tag{2.10}$$

Writing $\alpha(\nu) = A\nu^{-n}$ for $\nu \geq \nu_{max}$, so that $\alpha(\infty) = 0$, and integrating the second term, we obtain

$$Z = \left(\frac{4mc^2\varepsilon_o}{n_o e^2}\right)\left[\int_0^{\nu_{max}} \alpha(\nu)d\nu \quad + \quad \frac{A\nu_{max}^{-n+1}}{(n-1)}\right] \tag{2.11}$$

Since $A\nu_{max}^{-n} = \alpha(\nu_{max})$, the result is

$$Z = \left(\frac{4mc^2\varepsilon_o}{n_o e^2}\right)\int_0^{\nu_{max}} \alpha(\nu)d\nu \quad + \quad \left[\frac{4mc^2\varepsilon_o\nu_{max}}{n_o e^2(n-1)}\right]\alpha(\nu_{max}) \tag{2.12}$$

In the calculation of the sum rule integral, $\nu_{max}$ was $2\times10^7$ $cm^{-1}$. The value of $n$ was determined from the National Bureau of Standards data to be 2.6257. The numerical integration was done using Simpson's rule. As were all calculations for this research, the computation was done in a Fortran program with an AMDAHL 470 computer.

The first attempt yielded Z = 8.99086. Raising the experimental data of Heller *et al.* to their maximum within the stated error, except at the end points of the interval used, gave Z = 10.26559. A feature included in the data at $2.016\times10^5$ $cm^{-1}$ had been easily smoothed over within the experimental error, and was therefore ignored for the above two calculations. The curve had been made to follow the power law relation from $1.667\times10^5$ $cm^{-1}$ to the K-edge. For subsequent calculations, however, the power law relationship was applied only from $2.083\times10^5$ $cm^{-1}$ to the K-edge, and the previously ignored feature was included. This had the effect of shifting the curve above its previous position for the entire region of the data calculated from the power law relation. It allowed the data below $2.083\times10^5$ $cm^{-1}$ to be kept much closer to the

median experimental values. This is reasonable because the error stated by Heller et al. for the vicinity of $2.083 \times 10^5$ $cm^{-1}$ is 20 percent, while it is 10 percent for the lower wave number regions.

After 16 adjustments, the spectrum yielded Z = 10.00000. Figures 1 and 2 illustrate the first and last curve in the region of adjustment. Figure 3 is a graph of the final absorption spectrum in full. For the above illustrations, $\log_{10}\alpha(\nu)$ is plotted against $\log_{10}\nu$. Further, a graph of the value of the sum rule integral, Z plotted against $\log_{10}\nu$, is included as Figure 4 to show where the significant contributions to the sum rule occur. It is clear that the region of the data of Heller et al. corresponds to the greatest slope of the curve, thereby indicating the most significant contribution to the sum.

With the completion of this compilation, the absorption spectrum was ready to be Fourier transformed to give $n(\nu)$.

Fig. 1. The absorption spectrum in the region of adjustment. The log of the Lambert absorption coefficient, from $7.079 \times 10^4$ to $4.467 \times 10^6$ $cm^{-1}$, is plotted against the log of the wave number. The dashed line is the final curve obtained, which caused the sum rule integral to yield 10.00000. The sharp feature on the right is the K-edge.

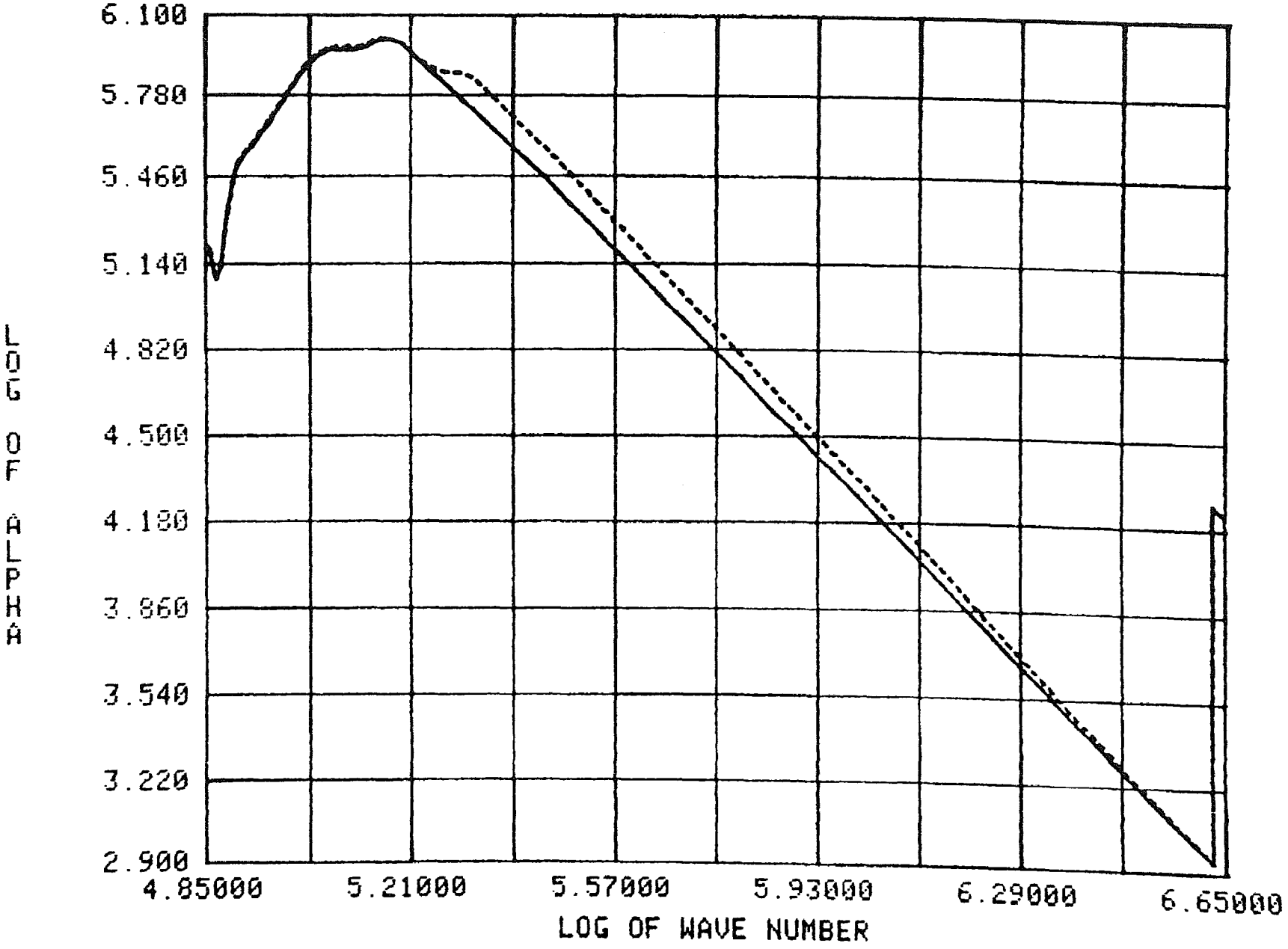
6.100
5.780
5.460
5.140
4.820
4.500
4.180
3.860
3.540
3.220
2.900
ALPHA OF GOF
4.85000
5.21000
5.57000
5.93000
6.29000
6.65000
LOG OF WAVE NUMBER

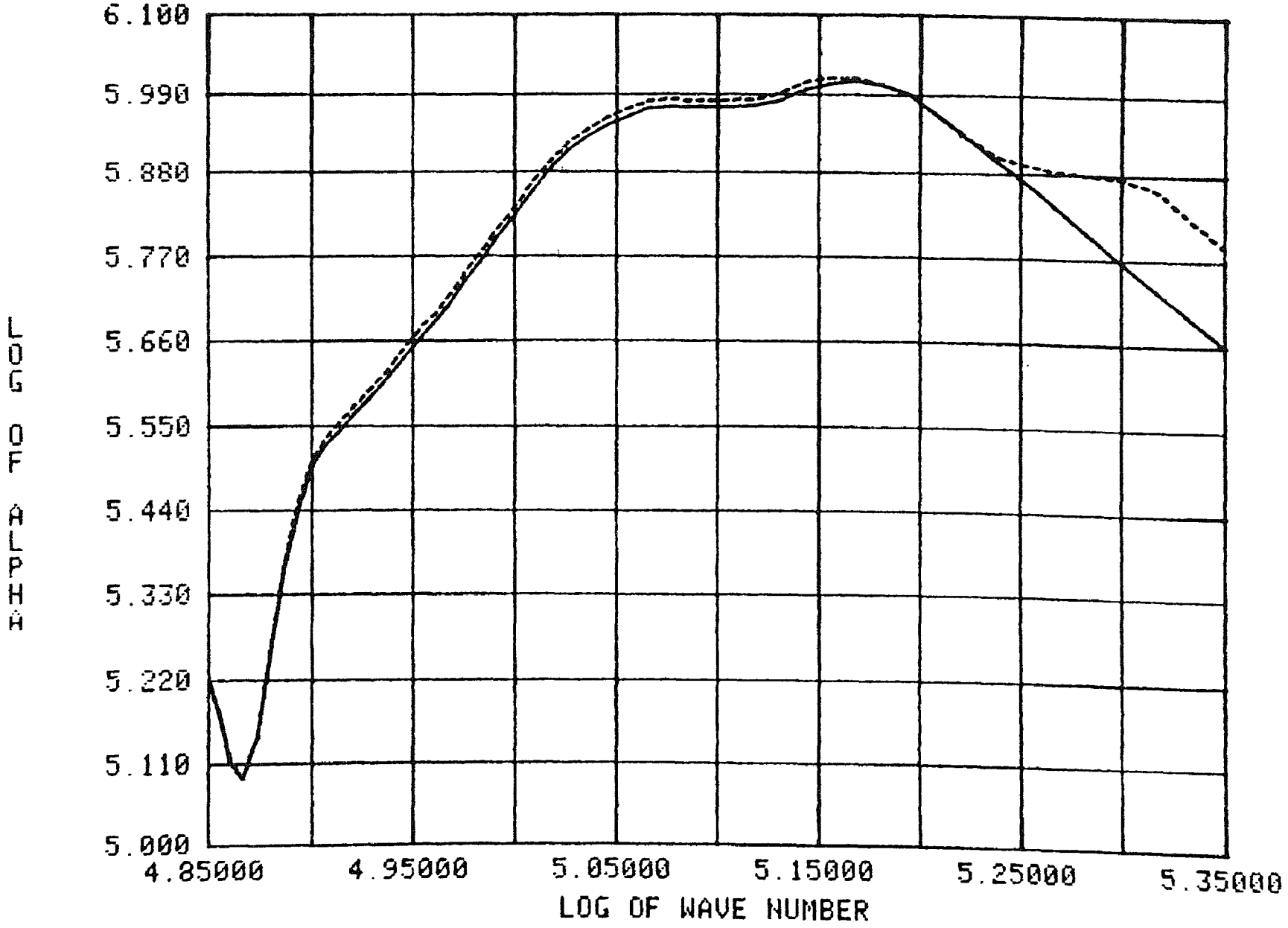
6.100
5.990
5.880
5.770
5.660
5.550
5.440
5.330
5.220
5.110
5.000
LOG OF ALPHA
4.85000
4.95000
5.05000
5.15000
5.25000
5.35000
LOG OF WAVE NUMBER

Fig. 3. The absorption spectrum in full as used in this work.

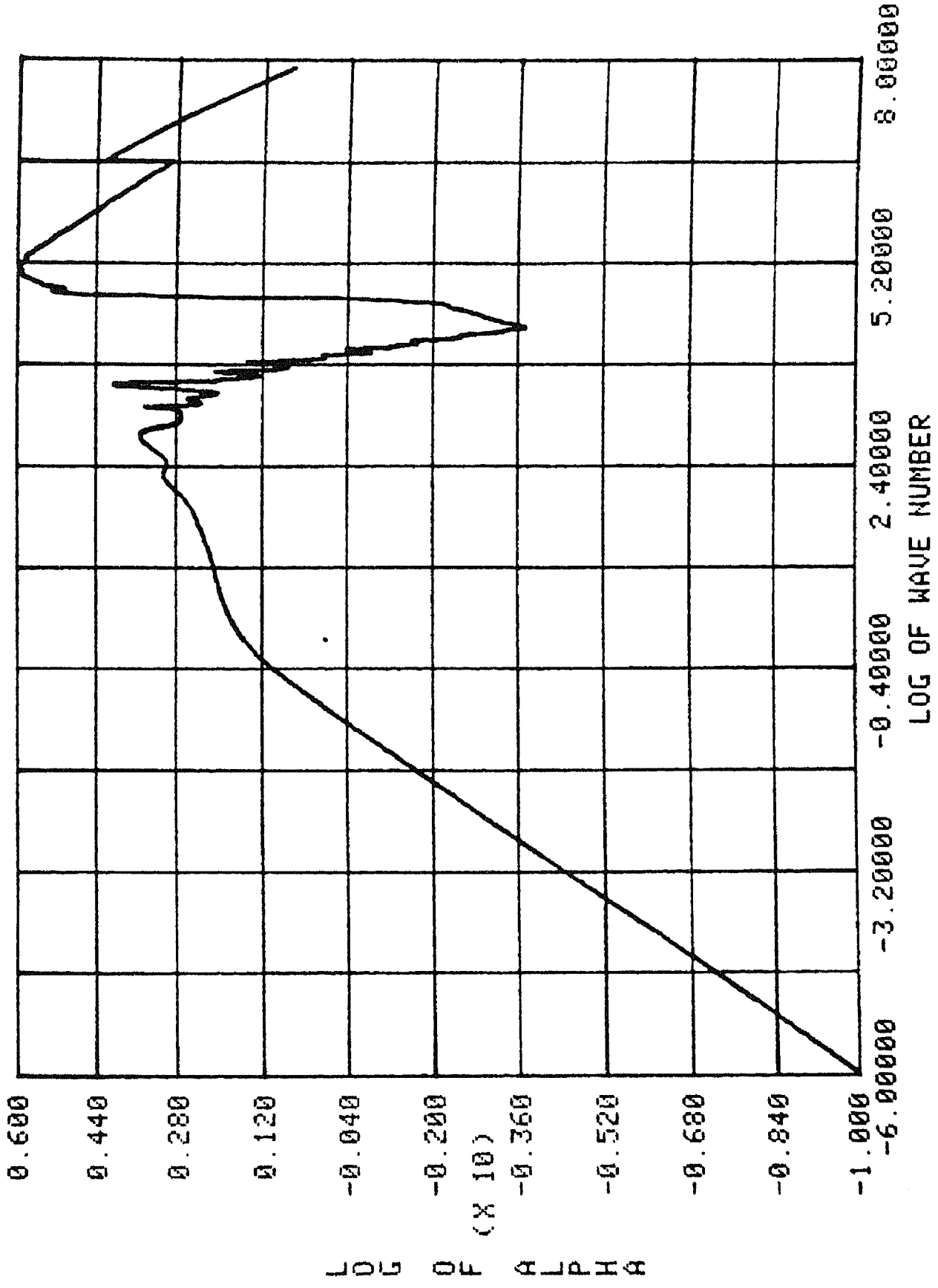
0.600
0.440
0.280
0.120
-0.040
-0.200
-0.360
-0.520
-0.680
-0.840
-1.000
(X 10)
LOG OF ALPHA
-6.00000
-3.20000
-0.40000
2.40000
5.20000
8.00000
LOG OF WAVE NUMBER

Fig. 4. The value of the sum rule integral plotted against the log of the value of the upper limit.

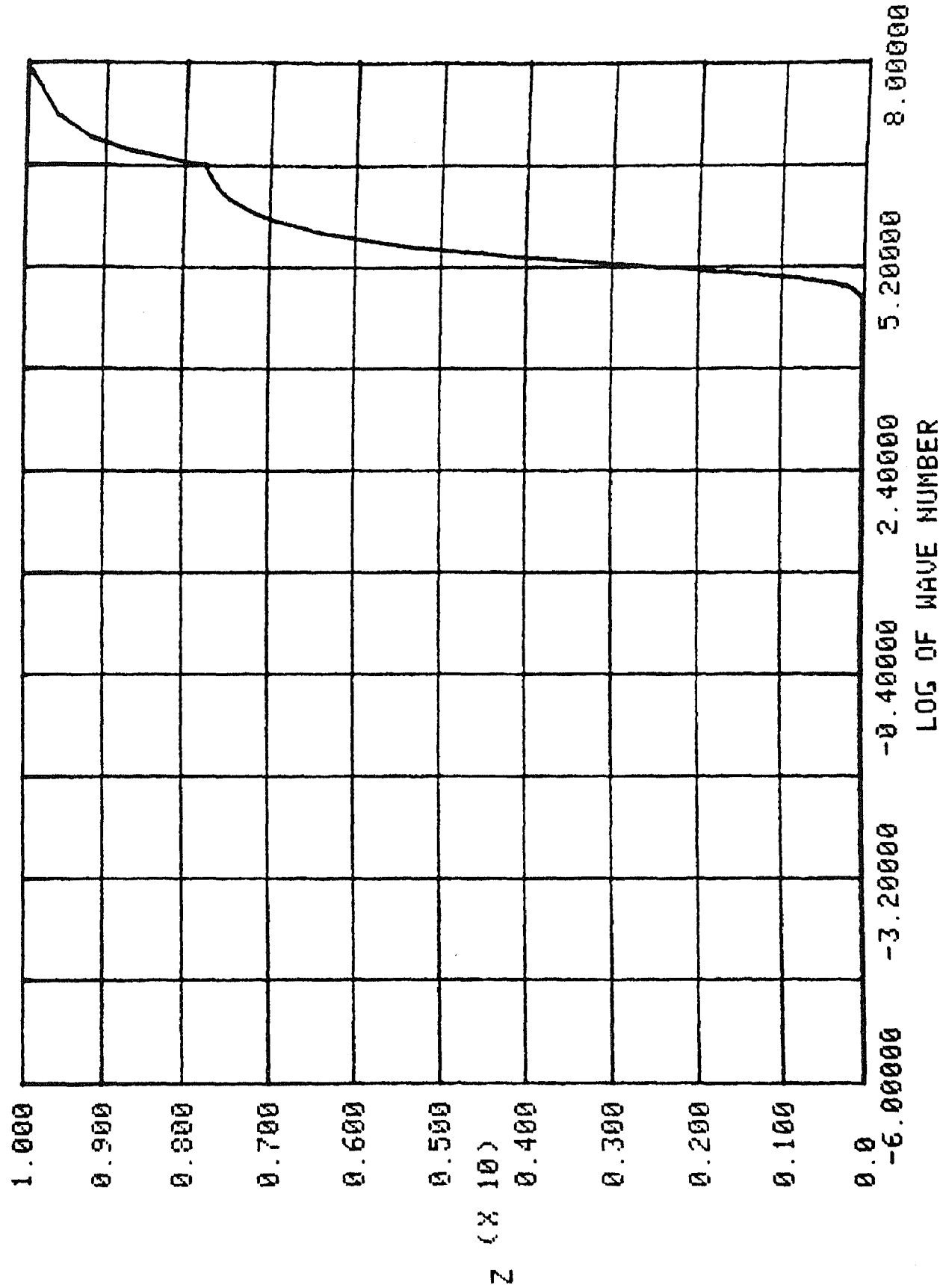
1.000
0.900
0.800
0.700
0.600
0.500
0.400
0.300
0.200
0.100
0.0
Z (X 10)
-6.00000
-3.20000
-0.40000
2.40000
5.20000
8.00000
LOG OF WAVE NUMBER

# CHAPTER III

## THEORETICAL METHODS

### The Complex Refractive Index

The laws governing the propagation of electric and magnetic fields are Maxwell's equations. We can find an expression for the fields in a medium which will yield the relationship between absorption and phase velocity, the time response and dielectric functions, dispersion relationships, and sum rules.

Maxwell's equations, in cgs units, are[21]

$$\nabla \cdot \vec{D} = 4\pi\rho \tag{3.1}$$

$$\nabla \cdot \vec{B} = 0 \tag{3.2}$$

$$\nabla \times \vec{E} + \frac{1}{c}\frac{\partial \vec{B}}{\partial t} = \vec{0} \tag{3.3}$$

$$\nabla \times \vec{H} - \frac{1}{c}\frac{\partial \vec{D}}{\partial t} = \frac{4\pi}{c}\vec{J} \tag{3.4}$$

The quantities in the equations are defined as follows:

$\vec{E} \equiv$ the electric field

$\vec{D} \equiv$ the electric displacement

$\vec{B} \equiv$ the magnetic induction

$\vec{H} \equiv$ the magnetic field

$\vec{J} \equiv$ the current density

$\rho \equiv$ the charge density

The constitutive relations for $\vec{D}$, $\vec{H}$, and $\vec{J}$ are

$$\vec{D} = \varepsilon\vec{E} \tag{3.5}$$

$$\vec{B} = \mu\vec{H} \tag{3.6}$$

$$\vec{J} = \sigma\vec{E} \tag{3.7}$$

where $\underline{\varepsilon}$ is the dielectric function, $\underline{\mu}$ is the magnetic permeability, and $\underline{\sigma}$ is the conductivity.

For an infinite medium which is charge free ($\rho=0$), homogeneous, isotropic, and linear ($\varepsilon$, $\mu$, and $\sigma$ do not depend on position or time), and conducting ($\sigma\neq 0$), the equations reduce to

$$\nabla \cdot \vec{E} = 0 \tag{3.8}$$

$$\nabla \cdot \vec{H} = 0 \tag{3.9}$$

$$\nabla \times \vec{E} + \frac{\mu}{c}\frac{\partial \vec{H}}{\partial t} = \vec{0} \tag{3.10}$$

$$\nabla \times \vec{H} - \frac{\varepsilon}{c}\frac{\partial \vec{E}}{\partial t} = \frac{4\pi\sigma}{c}\vec{E} \tag{3.11}$$

Taking the curl of Equation (3.10),

$$\nabla \times \left(\nabla \times \vec{E} + \frac{\mu}{c}\frac{\partial \vec{H}}{\partial t}\right) = \nabla \times \vec{0} = \vec{0}$$

$$\nabla \times \nabla \times \vec{E} + \frac{\mu}{c}\nabla \times \frac{\partial \vec{H}}{\partial t} = \vec{0} \tag{3.12}$$

Interchanging the order of differentiation,

$$\nabla \times \nabla \times \vec{E} + \frac{\mu}{c}\frac{\partial}{\partial t}(\nabla \times \vec{H}) = \vec{0} \tag{3.13}$$

Using the identity $\nabla \times \nabla \times \vec{E} = \nabla(\nabla \cdot \vec{E}) - \nabla^2 \vec{E}$, and noting from Equation (3.8) that the divergence of $\vec{E}$ vanishes, we may replace the first term of Equation (3.13) by $-\nabla^2 \vec{E}$ :

$$-\nabla^2 \vec{E} + \frac{\mu}{c} \frac{\partial}{\partial t}(\nabla \times \vec{H}) = \vec{0} \tag{3.14}$$

We obtain the curl of $\vec{H}$ from Equation (3.11):

$$-\nabla^2 \vec{E} + \frac{\mu}{c} \frac{\partial}{\partial t}\left( \frac{\varepsilon}{c} \frac{\partial \vec{E}}{\partial t} + \frac{4\pi\sigma}{c} \vec{E}\right) = \vec{0}$$

$$\nabla^2 \vec{E} - \frac{\mu\varepsilon}{c^2} \frac{\partial^2 \vec{E}}{\partial t^2} - \frac{4\pi\sigma\mu}{c^2} \frac{\partial \vec{E}}{\partial t} = \vec{0} \tag{3.15}$$

Similarly, taking the curl of Equation (3.11),

$$\nabla \times \left(\nabla \times \vec{H} - \frac{\varepsilon}{c} \frac{\partial \vec{E}}{\partial t} \right) = \nabla \times \left( \frac{4\pi\sigma}{c} \vec{E}\right)$$

$$\nabla \times \nabla \times \vec{H} - \frac{\varepsilon}{c} \frac{\partial}{\partial t}(\nabla \times \vec{E}) = \frac{4\pi\sigma}{c}(\nabla \times \vec{E}) \tag{3.16}$$

Obtaining the curl of $\vec{E}$ from Equation (3.10), and using the same identity for $\nabla \times \nabla \times \vec{H}$, with $\nabla \cdot \vec{H} = 0$ from Equation (3.9),

$$-\nabla^2 \vec{H} - \frac{\varepsilon}{c} \frac{\partial}{\partial t}\left(\frac{\mu}{c} \frac{\partial \vec{H}}{\partial t} \right) - \frac{4\pi\sigma}{c}\left(\frac{\mu}{c} \frac{\partial \vec{H}}{\partial t} \right) = \vec{0}$$

$$\nabla^2 \vec{H} - \frac{\mu\varepsilon}{c^2} \frac{\partial^2 \vec{H}}{\partial t^2} - \frac{4\pi\sigma\mu}{c^2} \frac{\partial \vec{H}}{\partial t} = \vec{0} \tag{3.17}$$

Thus, $\vec{E}$ and $\vec{H}$ both satisfy the same wave equation:

$$\left\{\nabla^2 - \frac{\mu\varepsilon}{c^2} \frac{\partial^2}{\partial t^2} - \frac{4\pi\sigma\mu}{c^2} \frac{\partial}{\partial t}\right\} \begin{Bmatrix} \vec{E} \\ \vec{H} \end{Bmatrix} = \vec{0} \tag{3.18}$$

We assume a solution of the form

$$\vec{E} = \vec{E}_o e^{i(\vec{\kappa}\cdot\vec{x}-\omega t)} \tag{3.19}$$

where $\underline{\vec{E}_o}$ is a constant vector. With $\kappa \equiv |\vec{\kappa}|$, we note the following:

$$\nabla^2 \vec{E} = \vec{E}_o (i\vec{\kappa})\cdot(i\vec{\kappa})\ e^{i(\vec{\kappa}\cdot\vec{x}-\omega t)} = -\kappa^2 \vec{E} \tag{3.20}$$

$$\frac{\partial \vec{E}}{\partial t} = -i\omega \vec{E} \tag{3.21}$$

$$\frac{\partial^2 \vec{E}}{\partial t^2} = (-i\omega)(-i\omega)\ \vec{E} = -\omega^2 \vec{E} \tag{3.22}$$

Then, substituting Equations (3.20), (3.21), and (3.22) into Equation (3.18),

$$\left\{\nabla^2 - \frac{\mu\varepsilon}{c^2}\frac{\partial^2}{\partial t^2} - \frac{4\pi\sigma\mu}{c^2}\frac{\partial}{\partial t}\right\}\vec{E} = \left[-\kappa^2 + \frac{\mu\varepsilon}{c^2}\omega^2 + i\left(\frac{4\pi\sigma\mu}{c^2}\right)\omega\right]\vec{E} \tag{3.23}$$

The coefficient of $\vec{E}$ must vanish. This requires that

$$\kappa^2 = \frac{\mu\varepsilon\omega^2}{c^2} + i\left(\frac{4\pi\sigma\mu\omega}{c^2}\right) \tag{3.24}$$

Assuming $\kappa$ is complex, we write $\kappa \equiv \alpha + i\beta$. Then,

$$\kappa^2 = (\alpha + i\beta)^2 = \alpha^2 - \beta^2 + 2i\alpha\beta \tag{3.25}$$

$$\mathrm{Re}(\kappa^2) = \alpha^2 - \beta^2 \tag{3.26}$$

$$\mathrm{Im}(\kappa^2) = 2\alpha\beta \tag{3.27}$$

To find the real and imaginary parts of $\kappa^2$, we assume that $\varepsilon$, $\mu$, and $\sigma$ are complex:

$$\varepsilon \equiv \varepsilon_r + i\varepsilon_i \tag{3.28}$$

$$\mu \equiv \mu_r + i\mu_i \tag{3.29}$$

$$\sigma \equiv \sigma_r + i\sigma_i \tag{3.30}$$

Then, substituting into Equation (3.24),

$$\kappa^2 = (\varepsilon_r + i\varepsilon_i)(\mu_r + i\mu_i)\frac{\omega^2}{c^2} + i4\pi(\sigma_r + i\sigma_i)(\mu_r + i\mu_i)\frac{\omega}{c^2} \tag{3.31}$$

$$\kappa^2 = \left[(\varepsilon_r\mu_r - \varepsilon_i\mu_i)\frac{\omega^2}{c^2} - 4\pi(\sigma_i\mu_r + \sigma_r\mu_i)\frac{\omega}{c^2}\right] + i\left[(\varepsilon_i\mu_r + \varepsilon_r\mu_i)\frac{\omega^2}{c^2} + 4\pi(\sigma_r\mu_r - \sigma_i\mu_i)\frac{\omega}{c^2}\right] \tag{3.32}$$

We then define

$$\gamma \equiv (\varepsilon_r\mu_r - \varepsilon_i\mu_i)\frac{\omega^2}{c^2} - 4\pi(\sigma_i\mu_r + \sigma_r\mu_i)\frac{\omega}{c^2} \tag{3.33}$$

$$\delta \equiv (\varepsilon_i\mu_r + \varepsilon_r\mu_i)\frac{\omega^2}{c^2} + 4\pi(\sigma_r\mu_r - \sigma_i\mu_i)\frac{\omega}{c^2} \tag{3.34}$$

Thus,

$$\kappa^2 = \gamma + i\delta \tag{3.35}$$

From Equations (3.26) and (3.27), we obtain

$$\gamma = \alpha^2 - \beta^2 \tag{3.36}$$

$$\delta = 2\alpha\beta \tag{3.37}$$

Using $\beta = \delta/2\alpha$ from Equation (3.37), the following quadratic results:

$$4\alpha^4 - \delta^2 = 4\gamma\alpha^2 \tag{3.38}$$

$$4(\alpha^2)^2 - 4\gamma(\alpha^2) - \delta^2 = 0 \tag{3.39}$$

The solutions are

$$\alpha^2 = \tfrac{1}{2}[\gamma \pm (\gamma^2 + \delta^2)^{\frac{1}{2}}] \tag{3.40}$$

Since $\alpha$ is real, $\alpha^2$ must be greater than zero. We must choose the plus sign. Therefore,

$$\alpha = \left[\frac{\gamma + (\gamma^2 + \delta^2)^{\frac{1}{2}}}{2}\right]^{\frac{1}{2}} \tag{3.41}$$

Similarly, $\alpha = \delta/2\beta$ yields the quadratic

$$4(\beta^2)^2 + 4\gamma(\beta^2) - \delta^2 = 0 \tag{3.42}$$

with solutions

$$\beta^2 = \tfrac{1}{2}[-\gamma \pm (\gamma^2 + \delta^2)^{\frac{1}{2}}] \tag{3.43}$$

Again we must choose the plus sign:

$$\beta = \left[\frac{-\gamma + (\gamma^2 + \delta^2)^{\frac{1}{2}}}{2}\right]^{\frac{1}{2}} \tag{3.44}$$

With the result $\vec{\kappa} = \kappa\hat{\kappa} = (\alpha + i\beta)\hat{\kappa}$, the complex phase velocity $\underline{\hat{v}_p}$ can be defined:

$$\vec{\kappa}\cdot\vec{x} - \omega t = \text{constant} \tag{3.45}$$

$$d(\vec{\kappa}\cdot\vec{x} - \omega t) = 0 \tag{3.46}$$

$$\vec{\kappa}\cdot d\vec{x} - \omega dt = 0 \tag{3.47}$$

$$(\alpha + i\beta)\hat{\kappa}\cdot d\vec{x} = \omega dt \tag{3.48}$$

$$\hat{\kappa}\cdot d\vec{x} = \left(\frac{\omega}{\alpha + i\beta}\right) dt \tag{3.49}$$

Measuring $\hat{v}_p$ in the direction of $\hat{\kappa}$, $\hat{\kappa}\cdot d\vec{x} = |\hat{\kappa}||d\vec{x}| = dx$, and

$$dx = \left(\frac{\omega}{\alpha + i\beta}\right) dt \tag{3.50}$$

$$\frac{dx}{dt} \equiv \hat{v}_p = \frac{\omega}{\alpha + i\beta} \tag{3.51}$$

If we define the complex refractive index $\underline{N}$ as

$$N \equiv \frac{c}{\hat{v}_p} \equiv n + ik \tag{3.52}$$

we finally obtain

$$N = \frac{c}{\omega}(\alpha + i\beta) \tag{3.53}$$

Thus, with $\underline{n}$ the real part of the refractive index, and $\underline{k}$ the imaginary part, the result is

$$n = \frac{c}{\omega}\alpha \tag{3.54}$$

$$k = \frac{c}{\omega}\beta \tag{3.55}$$

As an example of the relationship between $\varepsilon$ and N, consider a

non-conducting ($\sigma=0$), non-magnetic ($\mu=1$) material such as water. With these conditions,

$$\gamma = \varepsilon_r \frac{\omega^2}{c^2} \qquad \text{and} \qquad \delta = \varepsilon_i \frac{\omega^2}{c^2} \tag{3.56}$$

Then,

$$\alpha = \left[\frac{\gamma + (\gamma^2 + \delta^2)^{\frac{1}{2}}}{2}\right]^{\frac{1}{2}} = \frac{\omega}{c}\left[\frac{\varepsilon_r + (\varepsilon_r^2 + \varepsilon_i^2)^{\frac{1}{2}}}{2}\right]^{\frac{1}{2}} \tag{3.57}$$

$$\beta = \left[\frac{-\gamma + (\gamma^2 + \delta^2)^{\frac{1}{2}}}{2}\right]^{\frac{1}{2}} = \frac{\omega}{c}\left[\frac{-\varepsilon_r + (\varepsilon_r^2 + \varepsilon_i^2)^{\frac{1}{2}}}{2}\right]^{\frac{1}{2}} \tag{3.58}$$

Using Equation (3.53),

$$N = \frac{c}{\omega}\left\{\frac{\omega}{c}\left[\frac{\varepsilon_r + (\varepsilon_r^2 + \varepsilon_i^2)^{\frac{1}{2}}}{2}\right]^{\frac{1}{2}} + i\,\frac{\omega}{c}\left[\frac{-\varepsilon_r + (\varepsilon_r^2 + \varepsilon_i^2)^{\frac{1}{2}}}{2}\right]^{\frac{1}{2}}\right\} \tag{3.59}$$

$$N = [\tfrac{1}{2}(|\varepsilon| + \varepsilon_r)]^{\frac{1}{2}} + i[\tfrac{1}{2}(|\varepsilon| - \varepsilon_r)]^{\frac{1}{2}} \tag{3.60}$$

Squaring both sides,

$$N^2 = \tfrac{1}{2}(|\varepsilon| + \varepsilon_r) - \tfrac{1}{2}(|\varepsilon| - \varepsilon_r) + 2i[\tfrac{1}{2}(|\varepsilon| + \varepsilon_r)]^{\frac{1}{2}}[\tfrac{1}{2}(|\varepsilon| - \varepsilon_r)]^{\frac{1}{2}} \tag{3.61}$$

$$N^2 = \varepsilon_r + i\varepsilon_i = \varepsilon \tag{3.62}$$

The result is that, for water, the complex refractive index is the square of the dielectric function.

In general,

$$\kappa = \alpha + i\beta = \frac{\omega}{c}(n + ik) \tag{3.63}$$

Substituting into Equation (3.19),

$$\vec{E} = \vec{E}_o e^{i\frac{\omega}{c}(n+ik)\hat{\kappa}\cdot\vec{x}} e^{-i\omega t} \tag{3.64}$$

$$\vec{E} = \vec{E}_o e^{i\frac{\omega}{c}n(\hat{\kappa}\cdot\vec{x})} e^{-\frac{\omega}{c}k(\hat{\kappa}\cdot\vec{x})} e^{-i\omega t} \tag{3.65}$$

Clearly, $\underline{k}$ governs attenuation of the wave amplitude, and $\underline{n}$ governs the real phase velocity. Thus, the terms attenuation (or extinction) coefficient and real refractive index for $\underline{k}$ and $\underline{n}$ respectively.

The Lambert Absorption Coefficient

The Lambert absorption coefficient, $\underline{\alpha}$, is defined as the fractional decrease in intensity over distance:

$$\alpha \equiv -\frac{1}{I}\frac{dI}{dx} \tag{3.66}$$

We obtain an expression for the intensity by integrating:

$$-\alpha dx = \frac{dI}{I} \tag{3.67}$$

$$\int_0^x (-\alpha)dx' = \int_{I_o}^{I} \frac{dI'}{I'} \tag{3.68}$$

$$-\alpha x = \ln\left(\frac{I}{I_o}\right) \tag{3.69}$$

$$I = I_o e^{-\alpha x} \tag{3.70}$$

The intensity is proportional to the square of the magnitude of the electric field vector:

$$I \propto |\vec{E}|^2 = |\vec{E}_o|^2 \, e^{-2\frac{\omega}{c}k(\hat{\kappa}\cdot\vec{x})} \tag{3.71}$$

$$\frac{dI}{dx} \propto |\vec{E}_o|^2 (-\frac{2\omega k}{c}) \, |\hat{\kappa}| \, e^{-2\frac{\omega}{c}k(\hat{\kappa}\cdot\vec{x})} \tag{3.72}$$

$$-\frac{1}{I}\frac{dI}{dx} = \frac{2\omega k}{c} = \alpha \tag{3.73}$$

Writing $\omega = 2\pi f$ and $f = c/\lambda$, $\omega = 2\pi c/\lambda$. Then,

$$\alpha = \frac{2k}{c}\frac{2\pi c}{\lambda} = \frac{4\pi k}{\lambda} \tag{3.74}$$

With the definition of wave number, $\nu$, as $1/\lambda$,

$$\alpha = 4\pi k\nu \tag{3.75}$$

Absorption can also be written in terms of the formula

$$I = I_o e^{-\frac{\mu}{\rho}m} \tag{3.76}$$

where $\mu$ is defined as the linear absorption coefficient ($cm^{-1}$), $\rho$ is the density of the absorber ($gm/cm^3$), and $m$ is the mass per area of the absorber ($gm/cm^2$). Then, $\mu/\rho$ is the mass absorption coefficient ($cm^2/gm$).

It is easily shown that $\mu=\alpha$. From the definition of the Lambert coefficient, Equation (3.70), we require that

$$\alpha x = \frac{\mu}{\rho}m \tag{3.77}$$

Now, $x/m$ = volume/mass = $1/\rho$. Thus,

$$\alpha\frac{x}{m} = \alpha\frac{1}{\rho} = \mu\frac{1}{\rho} \tag{3.78}$$

The result is $\mu=\alpha$. The mass absorption coefficient, then, can be written as $\alpha/\rho$.

## The Kramers-Kronig Relations as Obtained From the Response Function

The real and imaginary parts of the dielectric function are related by a dispersion relation. This is a result of the frequency dependence of the quantities involved and our insistence on causality. The method was outlined by Peterson and Knight.[22] The relations will later be shown to apply also to the complex refractive index.

To be most general, the fields should be written as a Fourier superposition of the fields due to all frequencies. We begin by noting the definition of the electric displacement in cgs units:

$$\vec{D} = \vec{E} + 4\pi\vec{P} \tag{3.79}$$

With the assumption of linearity, the polarization can be written

$$\vec{P} = \chi_e(\omega)\ \vec{E} \tag{3.80}$$

$\chi_e(\omega)$ is the frequency-dependent electric susceptibility. Then,

$$\vec{D} = \vec{E} + 4\pi\chi_e(\omega)\ \vec{E} = [1 + 4\pi\chi_e(\omega)]\vec{E} \tag{3.81}$$

In general, the frequency-dependent dielectric function is defined by

$$\vec{D} = \varepsilon(\omega)\ \vec{E} \tag{3.82}$$

The result is

$$\varepsilon(\omega) = 1 + 4\pi\chi_e(\omega) \tag{3.83}$$

The frequency-dependent fields are written as

$$\vec{D}(\vec{x},\omega) = \varepsilon(\omega)\ \vec{E}(\vec{x},\omega) \tag{3.84}$$

where $\vec{D}(\vec{x},\omega)$ and $\vec{E}(\vec{x},\omega)$ are members of the Fourier-transform pairs

$$\vec{D}(\vec{x},t) = \frac{1}{\sqrt{2\pi}} \int_{-\infty}^{\infty} \vec{D}(\vec{x},\omega)\ e^{-i\omega t}\ d\omega \tag{3.85}$$

$$\vec{D}(\vec{x},\omega) = \frac{1}{\sqrt{2\pi}} \int_{-\infty}^{\infty} \vec{D}(\vec{x},t)\ e^{+i\omega t}\ dt \tag{3.86}$$

and

$$\vec{E}(\vec{x},t) = \frac{1}{\sqrt{2\pi}} \int_{-\infty}^{\infty} \vec{E}(\vec{x},\omega)\ e^{-i\omega t}\ d\omega \tag{3.87}$$

$$\vec{E}(\vec{x},\omega) = \frac{1}{\sqrt{2\pi}} \int_{-\infty}^{\infty} \vec{E}(\vec{x},t)\ e^{+i\omega t}\ dt \tag{3.88}$$

We proceed from Equation (3.85) as follows:

$$\vec{D}(\vec{x},t) = \frac{1}{\sqrt{2\pi}} \int_{-\infty}^{\infty} \varepsilon(\omega)\ \vec{E}(\vec{x},\omega)\ e^{-i\omega t}\ d\omega \tag{3.89}$$

$$\vec{D}(\vec{x},t) = \frac{1}{\sqrt{2\pi}} \int_{-\infty}^{\infty} [1+4\pi\chi_e(\omega)]\vec{E}(\vec{x},\omega)\ e^{-i\omega t}\ d\omega \tag{3.90}$$

$$\vec{D}(\vec{x},t) = \frac{1}{\sqrt{2\pi}}\int_{-\infty}^{\infty}\vec{E}(\vec{x},\omega)e^{-i\omega t}d\omega \; + \; \frac{1}{\sqrt{2\pi}}\int_{-\infty}^{\infty}4\pi\chi_e(\omega)\;\vec{E}(\vec{x},\omega)e^{-i\omega t}d\omega \tag{3.91}$$

$$\vec{D}(\vec{x},t) = \vec{E}(\vec{x},t) + \frac{1}{\sqrt{2\pi}}\int_{-\infty}^{\infty}4\pi\chi_e(\omega)\;\vec{E}(\vec{x},\omega)e^{-i\omega t}d\omega \tag{3.92}$$

We define the function $G(\tau)$ as

$$G(\tau) = \frac{1}{\sqrt{2\pi}}\int_{-\infty}^{\infty}4\pi\chi_e(\omega)\;e^{-i\omega\tau}d\omega \tag{3.93}$$

$G(\tau)$ is thus the Fourier transform of $4\pi\chi_e(\omega)$. Thus,

$$4\pi\chi_e(\omega) = \frac{1}{\sqrt{2\pi}}\int_{-\infty}^{\infty}G(\tau)\;e^{+i\omega\tau}d\tau \tag{3.94}$$

Substituting this into Equation (3.92) and interchanging the order of integration,

$$\vec{D}(\vec{x},t) = \vec{E}(\vec{x},t) + \frac{1}{\sqrt{2\pi}}\int_{-\infty}^{\infty}G(\tau)\left[\frac{1}{\sqrt{2\pi}}\int_{-\infty}^{\infty}\vec{E}(\vec{x},\omega)e^{-i\omega(t-\tau)}d\omega\right]d\tau \tag{3.95}$$

$$\vec{D}(\vec{x},t) = \vec{E}(\vec{x},t) + \frac{1}{\sqrt{2\pi}}\int_{-\infty}^{\infty}G(\tau)\;\vec{E}(\vec{x},t-\tau)\;d\tau \tag{3.96}$$

The fact that $\varepsilon(\omega)$ is a function of $\omega$ leads directly to this form for $\vec{D}(\vec{x},t)$, which has a non-local (temporally) contribution from

$\vec{E}(\vec{x},t)$. $G(\tau)$ is, evidently, the response function. Causality requires that there be no contribution tc $\vec{D}(\vec{x},t)$ from $\vec{E}(\vec{x},t-\tau)$ for $\tau<0$ (no contribution from the future). Then, $G(\tau)$ must be zero for $\tau<0$.

$\vec{D}(\vec{x},t)$ and $\vec{E}(\vec{x},t)$ must be real. Therefore, subtracting from Equation (3.96) its complex conjugate, we obtain the following:

$$\vec{D}(\vec{x},t) - \vec{D}^*(\vec{x},t) = \vec{E}(\vec{x},t) - \vec{E}^*(\vec{x},t) + \frac{1}{\sqrt{2\pi}}\int_{-\infty}^{\infty}[G(\tau)\vec{E}(\vec{x},t-\tau) - G^*(\tau)\vec{E}^*(\vec{x},t-\tau)]d\tau \tag{3.97}$$

$$0 = 0 + \frac{1}{\sqrt{2\pi}}\int_{-\infty}^{\infty}[G(\tau) - G^*(\tau)]\,\vec{E}(\vec{x},t-\tau)\,d\tau \tag{3.98}$$

This implies that $G(\tau) = G^*(\tau)$, or that $G(\tau)$ is real. We can, from this, deduce some properties of $4\pi\chi_e(\omega)$, and thus of $\varepsilon(\omega)$. Using the definition of $G(\tau)$ and Equation (3.83),

$$G(\tau) = \frac{1}{\sqrt{2\pi}}\int_{-\infty}^{\infty}[\varepsilon(\omega)-1]\,e^{-i\omega\tau}d\omega \tag{3.99}$$

The complex conjugate is

$$G^*(\tau) = \frac{1}{\sqrt{2\pi}}\int_{-\infty}^{\infty}[\varepsilon^*(\omega)-1]\,e^{+i\omega\tau}d\omega \tag{3.100}$$

In Equation (3.99) we substitute $-\omega$ for $\omega$ and obtain

$$G(\tau) = \frac{1}{\sqrt{2\pi}}\int_{-\infty}^{\infty}[\varepsilon(-\omega)-1]\,e^{+i\omega\tau}d\omega \tag{3.101}$$

Subtracting Equation (3.100) from Equation (3.101),

$$G(\tau) - G^*(\tau) = \frac{1}{\sqrt{2\pi}}\int_{-\infty}^{\infty}[\varepsilon(-\omega)-1]e^{i\omega\tau}d\omega - \frac{1}{\sqrt{2\pi}}\int_{-\infty}^{\infty}[\varepsilon^*(\omega)-1]e^{i\omega\tau}d\omega \tag{3.102}$$

$$0 = \frac{1}{\sqrt{2\pi}}\int_{-\infty}^{\infty}[\varepsilon(-\omega)-\varepsilon^*(\omega)]e^{i\omega\tau}d\omega \tag{3.103}$$

This implies that $\varepsilon(-\omega) = \varepsilon^*(\omega)$. Then

$$\mathrm{Re}[\varepsilon(-\omega)] + i\mathrm{Im}[\varepsilon(-\omega)] = \mathrm{Re}[\varepsilon(\omega)] - i\mathrm{Im}[\varepsilon(\omega)] \tag{3.104}$$

$$\mathrm{Re}[\varepsilon(-\omega)] = \mathrm{Re}[\varepsilon(\omega)] \tag{3.105}$$

Thus, $\mathrm{Re}[\varepsilon(\omega)]$ is an even function in $\omega$; further, the function $\mathrm{Re}[\varepsilon(\omega)-1] = \mathrm{Re}[4\pi\chi_e(\omega)]$ is even in $\omega$.

$$\mathrm{Im}[\varepsilon(-\omega)] = -\mathrm{Im}[\varepsilon(\omega)] \tag{3.106}$$

Thus, $\mathrm{Im}[\varepsilon(\omega)]$ is an odd function in $\omega$; further, the function $\mathrm{Im}[\varepsilon(\omega)-1] = \mathrm{Im}[4\pi\chi_e(\omega)]$ is odd in $\omega$.

Using the above results, we can separate $G(\tau)$ into a part symmetric in $\tau$, and a part anti-symmetric in $\tau$. Beginning with the definition of $G(\tau)$, separating the susceptibility and the exponential into real and imaginary parts, we find

$$G(\tau) = \frac{1}{\sqrt{2\pi}}\int_{-\infty}^{\infty}\left\{\mathrm{Re}[4\pi\chi_e(\omega)]\cos(\omega\tau) + \mathrm{Im}[4\pi\chi_e(\omega)]\sin(\omega\tau)\right\}d\omega + \frac{i}{\sqrt{2\pi}}\int_{-\infty}^{\infty}\left\{\mathrm{Im}[4\pi\chi_e(\omega)]\cos(\omega\tau) + \mathrm{Re}[4\pi\chi_e(\omega)]\sin(\omega\tau)\right\}d\omega \quad (3.107)$$

The integrand of the second integral is odd in $\omega$ and, therefore, vanishes. Thus,

$$G(\tau) = \frac{1}{\sqrt{2\pi}}\int_{-\infty}^{\infty}\mathrm{Re}[4\pi\chi_e(\omega)]\cos(\omega\tau)d\omega + \frac{1}{\sqrt{2\pi}}\int_{-\infty}^{\infty}\mathrm{Im}[4\pi\chi_e(\omega)]\sin(\omega\tau)d\omega \quad (3.108)$$

The first integral is even in $\tau$. We define it as $G_s(\tau)$ (where the subscript implies the symmetric property). Note that it can be written

$$G_s(\tau) = \frac{1}{\sqrt{2\pi}}\int_{-\infty}^{\infty}\mathrm{Re}[4\pi\chi_e(\omega)]e^{-i\omega\tau}d\omega \quad (3.109)$$

since the term containing the sine function is odd, causing that part of the integral to vanish. It is evident that $G_s(\tau)$ is the Fourier transform of $\mathrm{Re}[4\pi\chi_e(\omega)]$. Then,

$$\mathrm{Re}[4\pi\chi_e(\omega)] = \frac{1}{\sqrt{2\pi}}\int_{-\infty}^{\infty}G_s(\tau)e^{+i\omega\tau}d\tau \quad (3.110)$$

The second integral is odd in $\tau$. We define it as $G_a(\tau)$ (where the subscript implies the anti-symmetric property). Note that it can be written

$$G_a(\tau) = \frac{i}{\sqrt{2\pi}} \int_{-\infty}^{\infty} \mathrm{Im}[4\pi\chi_e(\omega)]e^{-i\omega\tau}d\omega \tag{3.111}$$

since the term containing the cosine function is odd, causing that part of the integral to vanish. It is evident that $G_a(\tau)$ is the Fourier transform of $i\mathrm{Im}[4\pi\chi_e(\omega)]$. Then,

$$\mathrm{Im}[4\pi\chi_e(\omega)] = -\frac{i}{\sqrt{2\pi}} \int_{-\infty}^{\infty} G_a(\tau)e^{+i\omega\tau}d\tau \tag{3.112}$$

We can relate the components of $G(\tau)$ by knowing that $G(\tau) = 0$ for $\tau < 0$, that $G_s(\tau)$ is even in $\tau$, and that $G_a(\tau)$ is odd in $\tau$. For $\tau < 0$,

$$G(\tau < 0) = G_s(\tau < 0) + G_a(\tau < 0) = 0 \tag{3.113}$$

$$G_s(\tau < 0) = -G_a(\tau < 0) \tag{3.114}$$

For $\tau > 0$ (and in general),

$$G_s(-\tau) = G_s(\tau) \tag{3.115}$$

$$G_a(-\tau) = -G_a(\tau) \tag{3.116}$$

Since $\tau > 0$ implies that $-\tau < 0$, Equations (3.114) and (3.116) give

$$G_s(-\tau) = -G_a(-\tau) = G_a(\tau) \tag{3.117}$$

Thus, for $\tau>0$,

$$G_s(-\tau) = G_s(\tau) = G_a(\tau) \tag{3.118}$$

The first result is from the symmetry property, and the last result is from Equation (3.117). Therefore,

$$G_s(\tau>0) = G_a(\tau>0) \tag{3.119}$$

Now we can relate the real and imaginary parts of $4\pi\chi_e(\omega)$. Separating the integral into one over negative $\tau$ and another over positive $\tau$,

$$\mathrm{Re}[4\pi\chi_e(\omega)] = \frac{1}{\sqrt{2\pi}}\int_{-\infty}^{0} G_s(\tau)e^{i\omega\tau}d\tau + \frac{1}{\sqrt{2\pi}}\int_{0}^{\infty} G_s(\tau)e^{i\omega\tau}d\tau \tag{3.120}$$

Then, using Equations (3.114) and (3.119),

$$\mathrm{Re}[4\pi\chi_e(\omega)] = \frac{1}{\sqrt{2\pi}}\int_{-\infty}^{0} [-G_a(\tau)]e^{i\omega\tau}d\tau + \frac{1}{\sqrt{2\pi}}\int_{0}^{\infty} G_a(\tau)e^{i\omega\tau}d\tau \tag{3.121}$$

Substituting $\underline{-\tau}$ for $\underline{\tau}$ in the first integral, we can recombine the integrals into

$$\mathrm{Re}[4\pi\chi_e(\omega)] = \frac{1}{\sqrt{2\pi}}\int_{0}^{\infty} G_a(\tau)\ (e^{-i\omega\tau} + e^{i\omega\tau})d\tau \tag{3.122}$$

We now substitute for $G_a(\tau)$ from Equation (3.111):

$$\mathrm{Re}[4\pi\chi_e(\omega)] = \frac{1}{\sqrt{2\pi}}\int_0^\infty \left\{ \frac{i}{\sqrt{2\pi}}\int_{-\infty}^{\infty} \mathrm{Im}[4\pi\chi_e(\omega')]e^{-i\omega'\tau}d\omega' \right\} \times$$

$$\times\ (e^{-i\omega\tau} + e^{i\omega\tau})d\tau \qquad (3.123)$$

Interchanging the order of integration and performing the integral over $\tau$,

$$\mathrm{Re}[4\pi\chi_e(\omega)] = \frac{1}{2\pi}\int_{-\infty}^{\infty} \mathrm{Im}[4\pi\chi_e(\omega')]\left(\frac{1}{\omega'+\omega} + \frac{1}{\omega'-\omega}\right) d\omega' \qquad (3.124)$$

$$\mathrm{Re}[4\pi\chi_e(\omega)] = \frac{1}{2\pi}\int_{-\infty}^{\infty} \frac{\mathrm{Im}[4\pi\chi_e(\omega')]d\omega'}{(\omega'+\omega)} \quad +$$

$$\frac{1}{2\pi}\int_{-\infty}^{\infty} \frac{\mathrm{Im}[4\pi\chi_e(\omega')]d\omega'}{(\omega'-\omega)} \qquad (3.125)$$

Substituting $-\omega'$ for $\omega'$ in the first integral, and using the fact that $\mathrm{Im}[4\pi\chi_e(\omega)]$ is odd in $\omega$, we obtain

$$\mathrm{Re}[4\pi\chi_e(\omega)] = \frac{1}{\pi}\int_{-\infty}^{\infty} \frac{\mathrm{Im}[4\pi\chi_e(\omega')]d\omega'}{(\omega'-\omega)} \qquad (3.126)$$

Now, using

$$\mathrm{Re}[4\pi\chi_e(\omega)] = \mathrm{Re}[\varepsilon(\omega)-1] = \mathrm{Re}[\varepsilon(\omega)] - 1 \qquad (3.127)$$

$$\mathrm{Im}[4\pi\chi_e(\omega)] = \mathrm{Im}[\varepsilon(\omega)-1] = \mathrm{Im}[\varepsilon(\omega)] \qquad (3.128)$$

the result is

$$\mathrm{Re}[\varepsilon(\omega)] = 1 + \frac{1}{\pi}\int_{-\infty}^{\infty}\frac{\mathrm{Im}[\varepsilon(\omega')]d\omega'}{(\omega'-\omega)} \tag{3.129}$$

Similarly, separating Equation (3.112) into two integrals and using Equations (3.114) and (3.119),

$$\mathrm{Im}[4\pi\chi_e(\omega)] = \frac{i}{\sqrt{2\pi}}\int_{0}^{\infty} G_s(\tau)\ (e^{-i\omega\tau} - e^{i\omega\tau})\ d\tau \tag{3.130}$$

Substituting for $G_s(\tau)$ from Equation (3.109),

$$\mathrm{Im}[4\pi\chi_e(\omega)] = \frac{i}{\sqrt{2\pi}}\int_{0}^{\infty}\left\{\frac{1}{\sqrt{2\pi}}\int_{-\infty}^{\infty}\mathrm{Re}[4\pi\chi_e(\omega')]e^{-i\omega'\tau}d\omega'\right\} \times$$
$$\times\ (e^{-i\omega\tau} - e^{i\omega\tau})d\tau \tag{3.131}$$

Interchanging the order of integration and performing the integral over $\tau$, we find

$$\mathrm{Im}[4\pi\chi_e(\omega)] = \frac{1}{2\pi}\int_{-\infty}^{\infty}\mathrm{Re}[4\pi\chi_e(\omega')]\left(\frac{1}{\omega'+\omega} - \frac{1}{\omega'-\omega}\right)d\omega' \tag{3.132}$$

$$\mathrm{Im}[4\pi\chi_e(\omega)] = \frac{1}{2\pi}\int_{-\infty}^{\infty}\frac{\mathrm{Re}[4\pi\chi_e(\omega')]d\omega'}{(\omega'+\omega)} -$$
$$\frac{1}{2\pi}\int_{-\infty}^{\infty}\frac{\mathrm{Re}[4\pi\chi_e(\omega')]d\omega'}{(\omega'-\omega)} \tag{3.133}$$

Substituting $-\omega'$ for $\omega'$ in the first integral and using the symmetry of $\mathrm{Re}[4\pi\chi_e(\omega)]$, these integrals become

$$\mathrm{Im}[4\pi\chi_e(\omega)] = -\frac{1}{\pi}\int_{-\infty}^{\infty}\frac{\mathrm{Re}[4\pi\chi_e(\omega')]d\omega'}{(\omega'-\omega)} \tag{3.134}$$

Thus, we obtain

$$\mathrm{Im}[\varepsilon(\omega)] = -\frac{1}{\pi}\int_{-\infty}^{\infty}\frac{\mathrm{Re}[\varepsilon(\omega')] - 1\, d\omega'}{(\omega'-\omega)} \tag{3.135}$$

These relations can be expressed slightly differently. Beginning with Equation (3.124), we combine the two terms in parentheses to form

$$\mathrm{Re}[4\pi\chi_e(\omega)] = \frac{1}{\pi}\int_{-\infty}^{\infty}\frac{\omega'\mathrm{Im}[4\pi\chi_e(\omega')]d\omega'}{(\omega'^2-\omega^2)} \tag{3.136}$$

Relying on the evenness of the integrand,

$$\mathrm{Re}[4\pi\chi_e(\omega)] = \frac{2}{\pi}\int_{0}^{\infty}\frac{\omega'\mathrm{Im}[4\pi\chi_e(\omega')]d\omega'}{(\omega'^2-\omega^2)} \tag{3.137}$$

$$\mathrm{Re}[\varepsilon(\omega)] = 1 + \frac{2}{\pi}\int_{0}^{\infty}\frac{\omega'\mathrm{Im}[\varepsilon(\omega')]d\omega'}{(\omega'^2-\omega^2)} \tag{3.138}$$

Similarly, beginning with Equation (3.132),

$$\mathrm{Im}[4\pi\chi_e(\omega)] = -\frac{\omega}{\pi}\int_{-\infty}^{\infty}\frac{\mathrm{Re}[4\pi\chi_e(\omega')]d\omega'}{(\omega'^2-\omega^2)} \tag{3.139}$$

$$\mathrm{Im}[4\pi\chi_e(\omega)] = -\frac{2\omega}{\pi}\int_{0}^{\infty}\frac{\mathrm{Re}[4\pi\chi_e(\omega')]d\omega'}{(\omega'^2-\omega^2)} \tag{3.140}$$

$$\mathrm{Im}[\varepsilon(\omega)] = -\frac{2\omega}{\pi}\int_0^\infty \frac{\mathrm{Re}[\varepsilon(\omega')] - 1\, d\omega'}{(\omega'^2-\omega^2)} \tag{3.141}$$

Equations (3.129) and (3.135), or alternatively (3.138) and (3.141), are the Kramers-Kronig relations.

The Lorentz Oscillator Model

Derivation of the dispersion relations for the complex refractive index requires some knowledge of the analytic properties of the function $N(\omega)$. Since, for water, $N^2(\omega)=\varepsilon(\omega)$, it is clear that a knowledge of the properties of $\varepsilon(\omega)$ will prove helpful in investigating the properties of $N(\omega)$. We begin with the Lorentz model of the dielectric function.

Consider the motion of an electron in an applied electric field. The electron is bound to the nucleus with a force constant $k$, and it experiences a damping force, proportional to its velocity, $-m\gamma v$. The equation of motion is

$$\vec{F} = m\frac{d^2\vec{x}}{dt^2} = -k\vec{x} - m\gamma\vec{v} + (-e)\vec{E} \tag{3.142}$$

$$m\frac{d^2\vec{x}}{dt^2} + m\gamma\frac{d\vec{x}}{dt} + k\vec{x} = -e\vec{E} \tag{3.143}$$

We assume an oscillating field vector with angular frequency $\omega$:

$$\vec{E} = \vec{E}_o e^{-i\omega t} \tag{3.144}$$

Then, substituting for $\vec{E}$ in Equation (3.143),

$$m\frac{d^2\vec{x}}{dt^2} + m\gamma\frac{d\vec{x}}{dt} + k\vec{x} = -e\vec{E}_o e^{-i\omega t} \tag{3.145}$$

We assume a solution of the form

$$\vec{x} = \vec{x}_o e^{-i\omega t} \tag{3.146}$$

Then, taking derivatives,

$$\frac{d\vec{x}}{dt} = -i\omega\vec{x}_o e^{-i\omega t} \tag{3.147}$$

$$\frac{d^2\vec{x}}{dt^2} = -\omega^2\vec{x}_o e^{-i\omega t} \tag{3.148}$$

The equation of motion becomes

$$-m\omega^2\vec{x}_o e^{-i\omega t} - i\gamma m\omega\vec{x}_o e^{-i\omega t} + k\vec{x}_o e^{-i\omega t} = -e\vec{E}_o e^{-i\omega t} \tag{3.149}$$

Dividing by $m$ and the exponential,

$$(-\omega^2 - i\gamma\omega + \frac{k}{m})\ \vec{x}_o = -\frac{e\vec{E}_o}{m} \tag{3.150}$$

Writing $\sqrt{k/m}$ as $\omega_o$, the natural oscillator frequency,

$$\vec{x}_o = -\frac{e\vec{E}_o}{m(\omega_o^2 - \omega^2 - i\gamma\omega)} \tag{3.151}$$

Then, writing $\vec{x}_o$ as in Equation (3.146), we obtain

$$\vec{x} = -\frac{e\vec{E}_o e^{-i\omega t}}{m(\omega_o^2-\omega^2-i\gamma\omega)} = -\frac{e\vec{E}}{m(\omega_o^2-\omega^2-i\gamma\omega)} \tag{3.152}$$

The dipole moment for this single oscillator is

$$\vec{p} = -e\vec{x} = \frac{e^2\vec{E}}{m(\omega_o^2-\omega^2-i\gamma\omega)} \tag{3.153}$$

If there are $\underline{N}$ such oscillators per unit volume, the polarization, $\vec{P}$, is given by

$$\vec{P} = N\vec{p} = \frac{Ne^2\vec{E}}{m(\omega_o^2-\omega^2-i\gamma\omega)} \tag{3.154}$$

Therefore, the electric susceptibility, $\chi_e$, is given by

$$\vec{P} = \chi_e\vec{E} = \left[\frac{Ne^2}{m(\omega_o^2-\omega^2-i\gamma\omega)}\right]\vec{E} \tag{3.155}$$

The dielectric function is related to $\chi_e$ as follows:

$$\varepsilon = 1 + 4\pi\chi_e = 1 + \frac{4\pi Ne^2}{m(\omega_o^2-\omega^2-i\gamma\omega)} \tag{3.156}$$

The term $\underline{4\pi Ne^2/m}$ is frequently written $\underline{\omega_p^2}$, where $\underline{\omega_p}$ is called the plasma frequency.

$$\varepsilon = 1 + \frac{\omega_p^2}{(\omega_o^2-\omega^2-i\gamma\omega)} \tag{3.157}$$

This single oscillator model can be extended to account for multiple oscillators. For $\underline{N}$ total electrons per unit volume, there are $\underline{N_j}$ with natural frequency $\underline{\omega_{oj}}$ and damping constant $\underline{\gamma_j}$. The obvious constraint is

$$\sum_j N_j = N \tag{3.158}$$

Then, adding up contributions from all types of electrons (oscillators),

$$\varepsilon = 1 + \frac{4\pi e^2}{m} \sum_j \frac{N_j}{(\omega_{oj}^2 - \omega^2 - i\gamma_j\omega)} \tag{3.159}$$

This can be separated into real and imaginary parts:

$$\varepsilon = 1 + \frac{4\pi e^2}{m} \sum_j \frac{N_j \left[(\omega_{oj}^2 - \omega^2) + i\gamma_j\omega\right]}{(\omega_{oj}^2 - \omega^2)^2 + \gamma_j^2\omega^2} \tag{3.160}$$

$$= \left[1 + \frac{4\pi e^2}{m} \sum_j \frac{N_j(\omega_{oj}^2 - \omega^2)}{(\omega_{oj}^2 - \omega^2)^2 + \gamma_j^2\omega^2}\right] + i\left[\frac{4\pi e^2}{m} \sum_j \frac{N_j\gamma_j\omega}{(\omega_{oj}^2 - \omega^2)^2 + \gamma_j^2\omega^2}\right] \tag{3.161}$$

Analytic Properties of $N(\omega)$

For water, $\varepsilon(\omega) = N^2(\omega)$. Then, Equation (3.157) gives

$$N^2(\omega) = 1 + \frac{\omega_p^2}{\omega_o^2 - \omega^2 - i\gamma\omega} \tag{3.162}$$

The zeroes of $N^2(\omega)$ are $\underline{\omega_a}$ and $\underline{\omega_b}$, obtained as follows:

$$0 = 1 + \frac{\omega_p^2}{\omega_o^2 - \omega^2 - i\gamma\omega} \tag{3.163}$$

$$\omega_p^2 = -\omega_o^2 + \omega^2 + i\gamma\omega \tag{3.164}$$

$$\omega^2 + (i\gamma)\omega - (\omega_p^2 + \omega_o^2) = 0 \tag{3.165}$$

$$\omega = -i\left(\frac{\gamma}{2}\right) \pm \left(\omega_o^2 + \omega_p^2 - \frac{\gamma^2}{4}\right)^{\frac{1}{2}} \tag{3.166}$$

With the following definition

$$\omega_1^2 \equiv \omega_o^2 + \omega_p^2 - \frac{\gamma^2}{4} \tag{3.167}$$

($\omega_1$ is real), the zeroes are

$$\omega_a = \omega_1 - i\left(\frac{\gamma}{2}\right) \tag{3.168}$$

$$\omega_b = -\omega_1 - i\left(\frac{\gamma}{2}\right) \tag{3.169}$$

The poles of $N^2(\omega)$ are $\underline{\omega_c}$ and $\underline{\omega_d}$, obtained as follows:

$$\omega_o^2 - \omega^2 - i\gamma\omega = 0 \tag{3.170}$$

$$\omega = -i\left(\frac{\gamma}{2}\right) \pm \left(\omega_o^2 - \frac{\gamma^2}{4}\right)^{\frac{1}{2}} \tag{3.171}$$

With the following definition

$$\omega_2^2 \equiv \omega_o^2 - \frac{\gamma^2}{4} \tag{3.172}$$

($\omega_2$ is real), the poles are

$$\omega_c = \omega_2 - i\left(\frac{\gamma}{2}\right) \tag{3.173}$$

$$\omega_d = -\omega_2 - i\left(\frac{\gamma}{2}\right) \tag{3.174}$$

We can write[23]

$$N^2(\omega) = \frac{(\omega-\omega_a)(\omega-\omega_b)}{(\omega-\omega_c)(\omega-\omega_d)} \tag{3.175}$$

This can be verified by direct substitution from Equations (3.168), (3.169), (3.173), and (3.174). The result is

$$N(\omega) = \left[\frac{(\omega-\omega_a)(\omega-\omega_b)}{(\omega-\omega_c)(\omega-\omega_d)}\right]^{\frac{1}{2}} \tag{3.176}$$

Since the function $N(\omega)$ is multi-valued, its branch line structure must be found in order to determine where it is analytic. The procedure was outlined by Churchill.[24]

Consider the functions

$$f_a(\omega) = \omega - \omega_a \tag{3.177}$$

$$f_b(\omega) = \omega - \omega_b \tag{3.178}$$

both of which are entire in the complex plane. Using Equation (3.168),

$$f_a(\omega) = \omega - \omega_1 + i\left(\frac{\gamma}{2}\right) \tag{3.179}$$

$\omega_1$ and $\gamma$ are real. We define

$$z \equiv \omega + i\left(\frac{\gamma}{2}\right) \tag{3.180}$$

Then, redefining $f_a(\omega)$ as $f_1^2(z)$,

$$\omega - \omega_a = z - \omega_1 \tag{3.181}$$

$$f_1(z) = (z-\omega_1)^{\frac{1}{2}} = \sqrt{r_1}\, e^{i\left(\frac{\theta_1}{2}\right)} \tag{3.182}$$

Similarly, using Equation (3.169),

$$f_b(\omega) = \omega + \omega_1 + i\left(\frac{\gamma}{2}\right) \tag{3.183}$$

With the corresponding definition of $f_b(\omega)$ as $f_2{}^2(z)$,

$$f_2(z) = (z+\omega_1)^{\frac{1}{2}} = \sqrt{r_2}\, e^{i\left(\frac{\theta_2}{2}\right)} \tag{3.184}$$

The polar coordinates for $f_1(z)$ and $f_2(z)$ are defined as in the following:

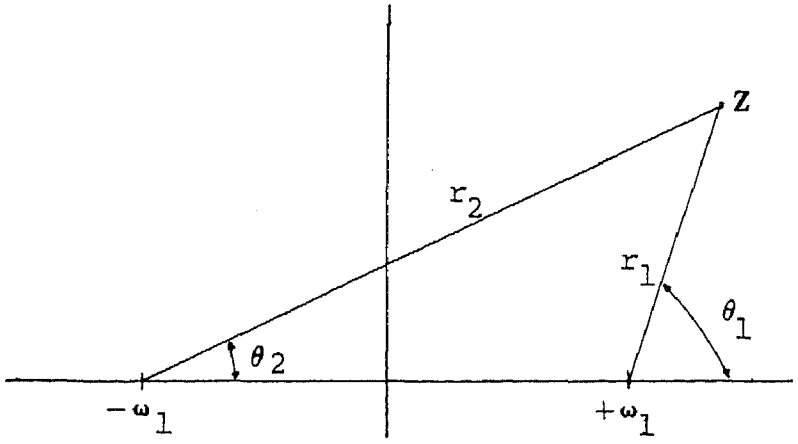


We define the function

$$f(z) \equiv \left[f_1(z)\right]\left[f_2(z)\right] \tag{3.185}$$

$$f(z) = (z-\omega_1)^{\frac{1}{2}}\,(z+\omega_1)^{\frac{1}{2}} = \sqrt{r_1 r_2}\, e^{i\left[\frac{(\theta_1+\theta_2)}{2}\right]} \tag{3.186}$$

We may define the domain of $f(z)$ as $\left\{0 \le \theta_1 < 2\pi,\ 0 \le \theta_2 < 2\pi,\ r_1 > 0,\ r_2 > 0, \text{ and } r_1+r_2 > 2\omega_1\right\}$. The last condition is imposed so that $f(z)$ is analytic in its domain. This result is equivalent to the statement that $f(z)$ is analytic everywhere except on the closed line segment connecting $-\omega_1$ and $+\omega_1$. This is shown as follows:

The branch cuts for $f_1(z)$ and $f_2(z)$ are the rays $\theta_1=0$ and $\theta_2=0$ respectively. Thus, $f(z)$ is analytic whenever $z\neq-\omega_1$ and $\theta_2\neq0$. The value of $f_1(z)$ is continuous (analytic) across $\theta_1=\pi$ ($f_1=i\sqrt{r_1}$), but the value of $f_2(z)$ jumps from $+\sqrt{r_2}$ to $-\sqrt{r_2}$ as z crosses from above to below this line segment connecting $-\omega_1$ and $+\omega_1$. Thus, $f(z)$ is not continuous (and not analytic) on that line segment.

Now, to investigate the behavior of $f(z)$ on the ray $\theta_1=0$, $r_1>0$, we define the function

$$F(z) \equiv \sqrt{r_1}\, e^{i\left(\frac{\phi_1}{2}\right)} \quad \sqrt{r_2}\, e^{i\left(\frac{\phi_2}{2}\right)} \tag{3.187}$$

in the domain $\{-\pi<\phi_1<\pi,\ -\pi<\phi_2<\pi,\ r_1>0,\ r_2>0\}$. $F(z)$ is continuous across the ray $\phi_1=0$ and is thus analytic there. (This is the same region of the real line as $\theta_1=0$, $r_1>0$.) If we can show that $f(z)=F(z)$ on, above, and below the ray $\theta_1=\phi_1=0$, then we will have shown $f(z)$ to be analytic on that ray. On the ray $\theta_1=\phi_1=0$, as well as above it, $\theta_1=\phi_1$ and $\theta_2=\phi_2$. Thus, $f(z)=F(z)$ for z on or above the ray $\theta_1=\phi_1=0$. For z below this ray, $\phi_1=\theta_1-2\pi$ and $\phi_2=\theta_2-2\pi$. Then,

$$F(z) = \sqrt{r_1}\, e^{i\left(\frac{\phi_1}{2}\right)} \quad \sqrt{r_2}\, e^{i\left(\frac{\phi_2}{2}\right)} \tag{3.188}$$

$$F(z) = \sqrt{r_1}\, e^{i\left[\frac{(\theta_1-2\pi)}{2}\right]} \quad \sqrt{r_2}\, e^{i\left[\frac{(\theta_2-2\pi)}{2}\right]} \tag{3.189}$$

$$F(z) = \sqrt{r_1 r_2}\, e^{i\left[\frac{(\theta_1+\theta_2)}{2}\right]} e^{-i2\pi} = \sqrt{r_1 r_2}\, e^{i\left[\frac{(\theta_1+\theta_2)}{2}\right]} = f(z) \tag{3.190}$$

Therefore, $f(z)$ is analytic on the ray $\theta_1=0$, $r_1>0$.

The branch line for f(z) is

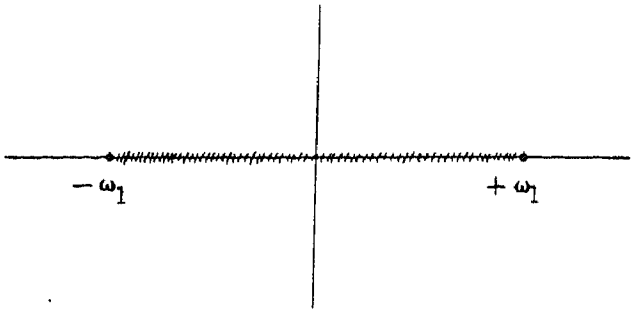


In crossing from above to below the branch line, the function shifts from

$$f_+ = \sqrt{r_1}\, e^{i\left(\frac{\pi}{2}\right)}\, e^{-i\delta}\, \sqrt{r_2}\, e^{i(0)}\, e^{+i\delta} = i\sqrt{r_1 r_2} \tag{3.191}$$

$(0<\delta<<1)$ to

$$f_- = \sqrt{r_1}\, e^{i\left(\frac{\pi}{2}\right)}\, e^{+i\delta}\, \sqrt{r_2}\, e^{i(\pi)}\, e^{-i\delta} = -i\sqrt{r_1 r_2} \tag{3.192}$$

Now consider the functions

$$f_c(\omega) \equiv (\omega - \omega_c) \tag{3.193}$$

$$f_d(\omega) \equiv (\omega - \omega_d) \tag{3.194}$$

both of which are entire in the complex plane. Using Equations (3.173), (3.174), and (3.180),

$$f_c(\omega) = \omega - \omega_2 + i\left(\frac{\gamma}{2}\right) = z - \omega_2 \tag{3.195}$$

$$f_d(\omega) = \omega + \omega_2 + i\left(\frac{\gamma}{2}\right) = z + \omega_2 \tag{3.196}$$

We now define the following functions:

$$g_1(z) \equiv (z-\omega_2)^{\frac{1}{2}} = \sqrt{r_3}\, e^{i\left(\frac{\theta_3}{2}\right)} \tag{3.197}$$

$$g_2(z) \equiv (z+\omega_2)^{\frac{1}{2}} = \sqrt{r_4}\, e^{i\left(\frac{\theta_4}{2}\right)} \tag{3.198}$$

The polar coordinates for $g_1(z)$ and $g_2(z)$ are defined as in the following:

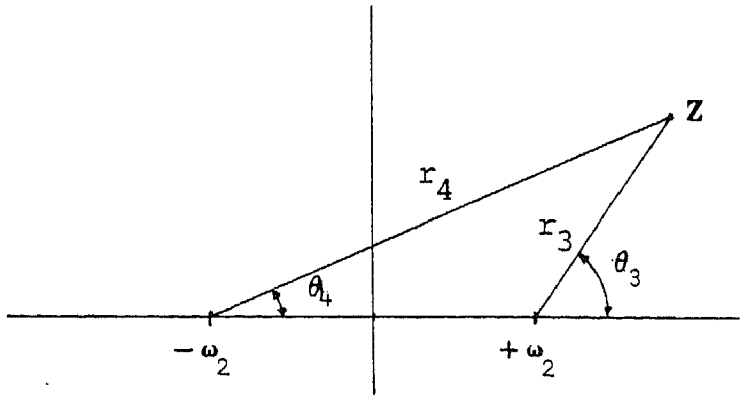


We may define

$$g(z) \equiv g_1(z)\; g_2(z) = \sqrt{r_3 r_4}\, e^{i\left[\frac{(\theta_3+\theta_4)}{2}\right]} \tag{3.199}$$

in the domain $\{0 \le \theta_3 < 2\pi,\ 0 \le \theta_4 < 2\pi,\ r_3 > 0,\ r_4 > 0,\ r_3 + r_4 > 2\omega_2\}$. As in the treatment for $f(z)$, the branch line for $g(z)$ is the closed line segment

connecting $-\omega_2$ and $+\omega_2$. Note that

$$|\omega_1| = |\mathrm{Re}(\omega_a)| = |\mathrm{Re}(\omega_b)| = |(\omega_o^2+\omega_p^2-\frac{\gamma}{4}^2)^{\frac{1}{2}}| \tag{3.200}$$

$$|\omega_2| = |\mathrm{Re}(\omega_c)| = |\mathrm{Re}(\omega_d)| = |(\omega_o^2-\frac{\gamma}{4}^2)^{\frac{1}{2}}| \tag{3.201}$$

Therefore,

$$|\omega_1| > |\omega_2| \tag{3.202}$$

The branch line for g(z) is

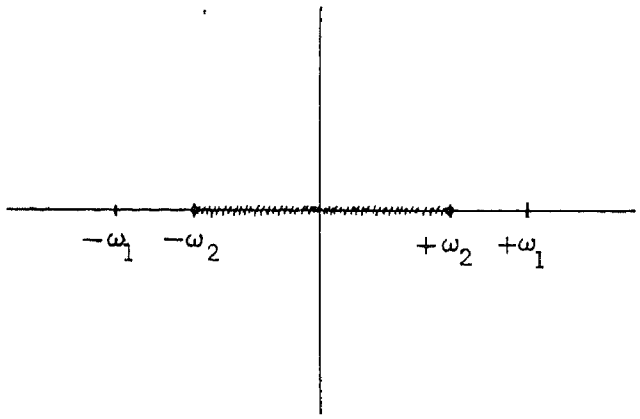


In crossing from above to below the branch line, g(z) shifts from $+i\sqrt{r_3r_4}$ to $-i\sqrt{r_3r_4}$. In crossing from above to below the ray $\theta_4=\pi$, g(z) varies continuously through $-\sqrt{r_3r_4}$. In crossing from above to below the ray $\theta_3=0$, g(z) varies continuously through $+\sqrt{r_3r_4}$.

Now, given the composite function

$$h(z) \equiv \frac{f(z)}{g(z)} \tag{3.203}$$

$h(z)$ is clearly continuous and analytic except perhaps on the closed line segment connecting $-\omega_1$ and $+\omega_1$. (This segment contains the segment connecting $-\omega_2$ and $+\omega_2$.)

First, consider the segment $-\omega_1$ to $-\omega_2$. For z crossing from above to below, $h(z)$ goes from

$$h_+ = \frac{f_+}{g_+} = \frac{i\sqrt{r_1 r_2}}{-\sqrt{r_3 r_4}} = -i\sqrt{\frac{r_1 r_2}{r_3 r_4}} \tag{3.204}$$

to

$$h_- = \frac{f_-}{g_-} = \frac{-i\sqrt{r_1 r_2}}{-\sqrt{r_3 r_4}} = +i\sqrt{\frac{r_1 r_2}{r_3 r_4}} \tag{3.205}$$

The function is discontinuous, and thus not analytic, on that segment.

Second, consider the segment $-\omega_2$ to $+\omega_2$. For z crossing from above to below, $h(z)$ goes from

$$h_+ = \frac{f_+}{g_+} = \frac{i\sqrt{r_1 r_2}}{i\sqrt{r_3 r_4}} = \sqrt{\frac{r_1 r_2}{r_3 r_4}} \tag{3.206}$$

to

$$h_- = \frac{f_-}{g_-} = \frac{-i\sqrt{r_1 r_2}}{-i\sqrt{r_3 r_4}} = \sqrt{\frac{r_1 r_2}{r_3 r_4}} \tag{3.207}$$

The function is continuous and analytic on that segment.

Third, consider the segment $+\omega_2$ to $+\omega_1$. For z crossing from above to below, $h(z)$ goes from

$$h_+ = \frac{f_+}{g_+} = \frac{i\sqrt{r_1 r_2}}{\sqrt{r_3 r_4}} = i\sqrt{\frac{r_1 r_2}{r_3 r_4}} \tag{3.208}$$

to

$$h_- = \frac{f_-}{g_-} = \frac{-i\sqrt{r_1 r_2}}{\sqrt{r_3 r_4}} = -i\sqrt{\frac{r_1 r_2}{r_3 r_4}} \tag{3.209}$$

The function is discontinuous, and thus not analytic, on that segment.

The branch line structure for h(z), therefore, is

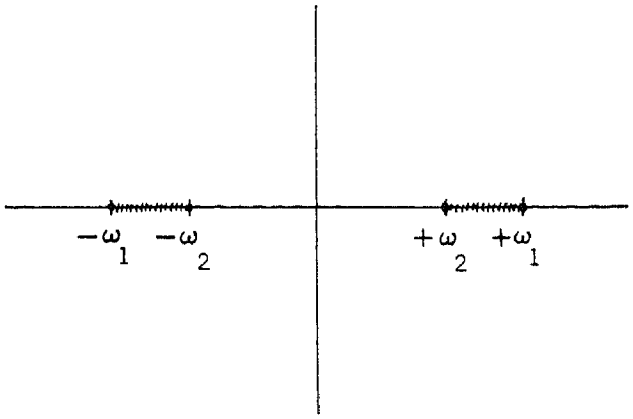


Substituting $z = \omega + i\left(\frac{\gamma}{2}\right)$, $\omega = z - i\left(\frac{\gamma}{2}\right)$, from Equation (3.180), we obtain $N(\omega)$ with branch lines as follows:

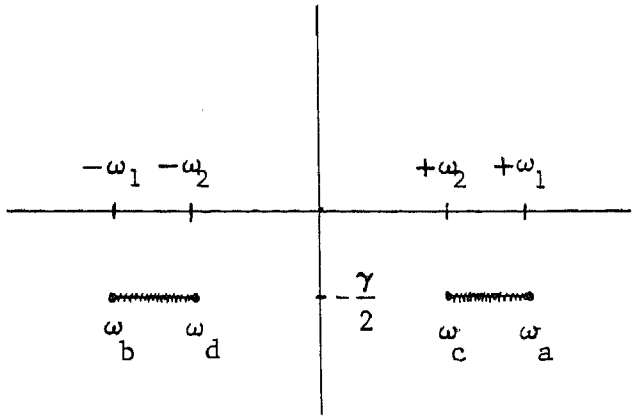

The result is that $N(\omega)$ is analytic on the real line and in the upper half plane.

We can find the high frequency limit for $N(\omega)$ as follows: For $|\omega| >> |\omega_o|$,

$$N^2(\omega) = 1 + \frac{\omega_p^2}{\omega_o^2 - \omega^2 - i\gamma\omega} \to 1 - \frac{\omega_p^2}{\omega^2} \tag{3.210}$$

$$N(\omega) \simeq \left(1 - \frac{\omega_p^2}{\omega^2}\right)^{\frac{1}{2}} = 1 - \frac{\omega_p^2}{2\omega^2} - \frac{\omega_p^4}{8\omega^4} - \ldots \simeq 1 - \frac{\omega_p^2}{2\omega^2} \tag{3.211}$$

As $\omega \to \infty$, $N(\omega) \to 1$.

This derivation is not invalidated by requiring a more complicated, or more realistic, model of $\varepsilon(\omega)$. Any model can be written in the form

$$\varepsilon(\omega) = \frac{\prod_{m=1}^{M} (\omega - Z_m)}{\prod_{n=1}^{N} (\omega - P_n)} \tag{3.212}$$

where $\underline{Z_m}$ are zeroes and $\underline{P_n}$ are poles of the function.[25] Causality implies that all the zeroes and poles lie below the real axis.[26] The result is the same analytical properties for $N(\omega)$.

The Kramers-Kronig Relations as Obtained From the Cauchy Integral Formula

With the above examination of the analytical properties of $\varepsilon(\omega)$ and $N(\omega)$, we can derive the dispersion relations for $N(\omega)$. We demonstrate the process first by obtaining the Kramers-Kronig relations for the dielectric function by contour integration.

We can show that the definition of $\varepsilon(\omega)$ via the time response function is consistent with the derived analytic properties. The definition of $G(\tau)$ yields

$$4\pi\chi_e(\omega) = \varepsilon(\omega) - 1 = \frac{1}{\sqrt{2\pi}} \int_{-\infty}^{\infty} G(\tau)\ e^{i\omega\tau} d\tau \tag{3.213}$$

Since $G(\tau)=0$ for $\tau<0$, we can write

$$\varepsilon(\omega) - 1 = \frac{1}{\sqrt{2\pi}} \int_{0}^{\infty} G(\tau)\ e^{i\omega\tau} d\tau \tag{3.214}$$

Separating $\omega$ into its real and imaginary parts,

$$\varepsilon(\omega) - 1 = \frac{1}{\sqrt{2\pi}} \int_{0}^{\infty} G(\tau)\ e^{i\omega_r\tau}\ e^{-\omega_i\tau} d\tau \tag{3.215}$$

It is clear that, for finite $G(\tau)$, the function $\varepsilon(\omega)-1$ exists, as does its derivative, for all $\omega$ such that $\omega_i \geq 0$. Therefore, the function $\varepsilon(\omega)-1$ is analytic on the real axis and in the upper half plane.

As a result, for any closed contour in the domain of analyticity of $\varepsilon(\omega)-1$, the Cauchy integral formula allows us to write

$$\varepsilon(\omega) - 1 = \frac{1}{2\pi i} \oint_C \frac{[\varepsilon(\omega')-1]d\omega'}{(\omega'-\omega)} \tag{3.216}$$

We will want to investigate the function for real, positive $\omega$. Therefore, placing $\omega$ on the positive real axis, we choose a contour $\underline{C}$ as follows:

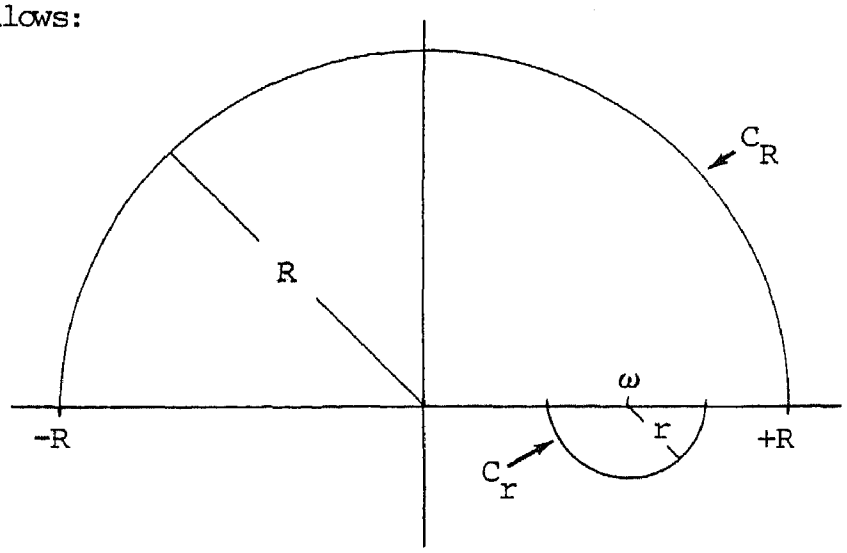


The integral around this contour can be written as the sum of four parts:

$$\oint_C \frac{[\varepsilon(\omega')-1]d\omega'}{(\omega'-\omega)} = \int_{-R}^{\omega-r} \frac{[\varepsilon(\omega')-1]d\omega'}{(\omega'-\omega)} + \int_{C_r} \frac{[\varepsilon(\omega')-1]d\omega'}{(\omega'-\omega)} +$$

$$\int_{\omega+r}^{R} \frac{[\varepsilon(\omega')-1]d\omega'}{(\omega'-\omega)} + \int_{C_R} \frac{[\varepsilon(\omega')-1]d\omega'}{(\omega'-\omega)} \tag{3.217}$$

Now, writing

$$\omega' \equiv \omega + re^{i\theta} \tag{3.218}$$

$$d\omega' = ire^{i\theta}d\theta \tag{3.219}$$

we can write the second integral as

$$\int_{-\pi}^{o} \frac{[\varepsilon(\omega')-1]ire^{i\theta}d\theta}{(\omega+re^{i\theta}-\omega)} = \int_{-\pi}^{o}[\varepsilon(\omega')-1]id\theta \tag{3.220}$$

Writing

$$\omega' \equiv Re^{i\phi} \tag{3.221}$$

$$d\omega' = ire^{i\phi}d\phi \tag{3.222}$$

we can write the last integral as

$$\int_{o}^{\pi} \frac{[\varepsilon(\omega')-1]iRe^{i\phi}d\phi}{(Re^{i\phi}-\omega)} \tag{3.223}$$

Then,

$$\oint_{C} \frac{[\varepsilon(\omega')-1]d\omega'}{(\omega'-\omega)} = \int_{-R}^{\omega-r} \frac{[\varepsilon(\omega')-1]d\omega'}{(\omega'-\omega)} + \int_{-\pi}^{o}[\varepsilon(\omega')-1]id\theta +$$

$$\int_{\omega+r}^{R} \frac{[\varepsilon(\omega')-1]d\omega'}{(\omega'-\omega)} + \int_{o}^{\pi} \frac{[\varepsilon(\omega')-1]iRe^{i\phi}d\phi}{(Re^{i\phi}-\omega)} \tag{3.224}$$

Now we apply a limiting process, allowing R to approach $\infty$ and r to approach zero. Since this includes and excludes no new poles, the

integral on the left of Equation (3.224) remains the same. The first and third integrals on the right become the Cauchy principal value (denoted P.V.) of the integral along the real line. In the second integral on the right, $\omega'$ becomes $\omega$ and the function $\varepsilon(\omega)-1$ can be moved outside the integral sign, the remainder yielding $\pi i$. The fourth integral on the right vanishes because $\varepsilon(\omega')$ approaches one as the magnitude of $\omega'$ increases without bound. Thus,

$$\oint_C \frac{[\varepsilon(\omega')-1]d\omega'}{(\omega'-\omega)} = \text{P.V.}\left\{\int_{-\infty}^{\infty} \frac{[\varepsilon(\omega')-1]d\omega'}{(\omega'-\omega)}\right\} + \pi i[\varepsilon(\omega)-1] \quad (3.225)$$

Now, using this in Equation (3.216) and rearranging, we obtain

$$\varepsilon(\omega) - 1 = \frac{1}{\pi i}\,\text{P.V.}\left\{\int_{-\infty}^{\infty} \frac{[\varepsilon(\omega')-1]d\omega'}{(\omega'-\omega)}\right\} \quad (3.226)$$

Separating the functions into real and imaginary parts yields the Kramers-Kronig relations.

One difficulty with the above derivation is the excursion into the lower half plane by the contour $C_r$. This path is of infinitesimal length; and with $\omega_i<\delta$ for all $\delta$, the function given by Equation (3.215) remains regular even with $\tau\to\infty$. Further, the physical constraints on $G(\tau)$ require that $G(\tau)\to 0$ as $\tau\to\infty$. However, this difficulty can be avoided by distorting the contour above, instead of below, the pole at $\omega$ on the real axis. Then, since no poles are enclosed, the integral must yield zero.

$$\oint_{C'} \frac{[\varepsilon(\omega')-1]d\omega'}{(\omega'-\omega)} = 0 \qquad (3.227)$$

As before, the integral is divided into four parts. The limit is taken allowing $R\to\infty$ and $r\to 0$. The only difference is the integration around the small semi-circular contour around $\omega$ which is counter-clockwise and yields $\underline{-\pi i[\varepsilon(\omega)-1]}$, the negative of the prior result. This, however, conspires with the zero on the right of Equation (3.227) to give the same answer as before, namely Equation (3.226) and the Kramers-Kronig relations.

The only requirements for the derivation of the Kramers-Kronig relations above were the analyticity of the function $\underline{\varepsilon(\omega)-1}$ in the upper half plane and on the real line, and the vanishing of the function for $|\omega|\to\infty$. We can, thus, derive similar relations for the complex index of refraction. We must use $\underline{N(\omega)-1}$, however, since $N(\omega)\to 1$ as $|\omega|\to\infty$. We write

$$N(\omega) - 1 = \frac{1}{2\pi i}\oint_{C} \frac{[N(\omega')-1]d\omega'}{(\omega'-\omega)} \qquad (3.228)$$

using a contour enclosing the pole at $\omega$ (real). If we wish to use a contour excluding that pole, the integral on the right of Equation (3.228) yields zero. In either case, the result is

$$N(\omega) - 1 = \frac{1}{\pi i}\,\text{P.V.}\left\{\int_{-\infty}^{\infty} \frac{[N(\omega')-1]d\omega'}{(\omega'-\omega)}\right\} \qquad (3.229)$$

Separating the functions into their real and imaginary parts,

$$n(\omega) = 1 + \frac{1}{\pi}\int_{-\infty}^{\infty}\frac{k(\omega')d\omega'}{(\omega'-\omega)} \tag{3.230}$$

$$k(\omega) = -\frac{1}{\pi}\int_{-\infty}^{\infty}\frac{[n(\omega')-1]d\omega'}{(\omega'-\omega)} \tag{3.231}$$

These are the Kramers-Kronig relations for the complex refractive index.

The Real Part of $N(\omega)$ as a Fourier Transform

We can obtain $n(\omega)$ as a series of two Fourier transforms. This will be the basis for the calculation described in Chapter IV. Beginning with Equation (3.230), we divide the integral into two equal parts.

$$n(\omega) - 1 = \frac{1}{2\pi}\int_{-\infty}^{\infty}\frac{k(\omega')d\omega'}{(\omega'-\omega)} + \frac{1}{2\pi}\int_{-\infty}^{\infty}\frac{k(\omega')d\omega'}{(\omega'-\omega)} \tag{3.232}$$

Substituting $-\omega'$ for $\omega'$ in the first integral, using the fact that $k(\omega')$ is odd, and reversing the limits, we can recombine the integrals.

$$n(\omega) - 1 = \frac{1}{2\pi}\int_{-\infty}^{\infty}k(\omega')\left[\frac{1}{(\omega'+\omega)} + \frac{1}{(\omega'-\omega)}\right]d\omega' \tag{3.233}$$

Now we rely on the value of the integral

$$i\int_{0}^{\infty}\left[e^{-i(\omega'+\omega)\tau} + e^{-i(\omega'-\omega)\tau}\right]d\tau = \frac{1}{(\omega'+\omega)} + \frac{1}{(\omega'-\omega)} \tag{3.234}$$

Substituting this integral over $\tau$ into Equation (3.233), we obtain

$$n(\omega)-1 = \frac{1}{2\pi}\int_{-\infty}^{\infty} k(\omega')\left\{ i\int_{0}^{\infty}\left[e^{-i(\omega'+\omega)\tau} + e^{-i(\omega'-\omega)\tau}\right]d\tau\right\}d\omega' \quad (3.235)$$

Since $k(\omega')$ is continuous, we can reverse the order of integration.

$$n(\omega)-1 = \frac{i}{2\pi}\int_{0}^{\infty}\left[\int_{-\infty}^{\infty} k(\omega')e^{-i\omega'\tau}d\omega'\right](e^{-i\omega\tau} + e^{i\omega\tau})d\tau \quad (3.236)$$

$$n(\omega)-1 = \frac{1}{\sqrt{2\pi}}\int_{0}^{\infty}\left\{\frac{1}{\sqrt{2\pi}}\int_{-\infty}^{\infty}[ik(\omega')]e^{-i\omega'\tau}d\omega'\right\}e^{-i\omega\tau}d\tau +$$

$$\frac{1}{\sqrt{2\pi}}\int_{0}^{\infty}\left\{\frac{1}{\sqrt{2\pi}}\int_{-\infty}^{\infty}[ik(\omega')]e^{-i\omega'\tau}d\omega'\right\}e^{+i\omega\tau}d\tau \quad (3.237)$$

Substituting $-\tau$ for $\tau$, the first integral in Equation (3.237) becomes

$$\frac{1}{\sqrt{2\pi}}\int_{-\infty}^{0}\left\{\frac{1}{\sqrt{2\pi}}\int_{-\infty}^{\infty}[ik(\omega')]e^{+i\omega'\tau}d\omega'\right\}e^{+i\omega\tau}d\tau \quad (3.238)$$

Now, substituting $-\omega'$ for $\omega'$, using the oddness of $k(\omega')$, and reversing the limits, the integral (3.238) becomes

$$\frac{1}{\sqrt{2\pi}}\int_{-\infty}^{0}\left\{-\frac{1}{\sqrt{2\pi}}\int_{-\infty}^{\infty}[ik(\omega')]e^{-i\omega'\tau}d\omega'\right\}e^{+i\omega\tau}d\tau \quad (3.239)$$

The result is

$$n(\omega)-1 = \frac{1}{\sqrt{2\pi}}\int_{-\infty}^{0}\left\{-\frac{1}{\sqrt{2\pi}}\int_{-\infty}^{\infty}[ik(\omega')]e^{-i\omega'\tau}d\omega'\right\}e^{+i\omega\tau}d\tau +$$

$$+ \frac{1}{\sqrt{2\pi}} \int_0^{\infty} \left\{ \frac{1}{\sqrt{2\pi}} \int_{-\infty}^{\infty} [ik(\omega')]\, e^{-i\omega'\tau} d\omega' \right\} e^{i\omega\tau} d\tau \tag{3.240}$$

If we define $f(\tau)$ as the Fourier transform of $ik(\omega')$,

$$f(\tau) \equiv \frac{1}{\sqrt{2\pi}} \int_{-\infty}^{\infty} [ik(\omega')]\, e^{-i\omega'\tau} d\omega' \tag{3.241}$$

the function $n(\omega)-1$ can be written

$$n(\omega)-1 = \frac{1}{\sqrt{2\pi}} \int_{-\infty}^{0} [-f(\tau)]\, e^{i\omega\tau} d\tau + \frac{1}{\sqrt{2\pi}} \int_0^{\infty} [f(\tau)] e^{i\omega\tau} d\tau \tag{3.242}$$

Now we define $g(\tau)$ as

$$g(\tau) \equiv \begin{cases} -f(\tau), & \tau \leq 0 \\ +f(\tau), & \tau > 0 \end{cases} \tag{3.243}$$

Then,

$$n(\omega)-1 = \frac{1}{\sqrt{2\pi}} \int_{-\infty}^{\infty} g(\tau) e^{i\omega\tau} d\tau \tag{3.244}$$

Thus, $n(\omega)-1$ is the Fourier transform of the $g(\tau)$ function.

## The Electronic Sum Rule

We are now in a position to derive the electronic sum rule. Beginning with the Kramers-Kronig relation for the real part of the refractive index, Equation (3.230), we express the integral over positive frequencies.

$$n(\omega)-1 = \frac{2}{\pi}\int_0^{\infty} \frac{\omega' k(\omega')\,d\omega'}{(\omega'^2-\omega^2)} \tag{3.245}$$

Now, we define $\omega_c$ as some cut-off frequency above which there is no absorption due to electronic oscillation. Then, that portion of the integral from $\omega_c$ to $\infty$ can be omitted.

$$n(\omega) = 1 + \frac{2}{\pi}\int_0^{\omega_c} \frac{\omega' k(\omega')\,d\omega'}{(\omega'^2-\omega^2)} \tag{3.246}$$

Choosing some $\omega>>\omega_c$, the $\omega^2$ term dominates the $\omega'^2$ in the denominator of the integrand. Ignoring $\omega'^2$ by comparison,

$$n(\omega) \simeq 1 + \frac{2}{\pi}\left(-\frac{1}{\omega^2}\right)\int_0^{\omega_c} \omega' k(\omega')\,d\omega' \tag{3.247}$$

This expression becomes more accurate as $\omega$ becomes larger. Also, for large $\omega$, Equation (3.211) gives

$$n(\omega) \simeq 1 - \frac{\omega_p^2}{2\omega^2} \tag{3.248}$$

This also becomes more accurate as $\omega$ becomes larger. We take the limiting case, $\omega\to\infty$. Then, equating the right sides of Equations (3.247) and (3.248),

$$1 - \frac{\omega_p^2}{2\omega^2} = 1 - \frac{2}{\pi\omega^2}\int_0^{\omega_c} \omega' k(\omega')\,d\omega' \tag{3.249}$$

$$\omega_p^2 = \frac{4}{\pi}\int_0^{\omega_c} \omega' k(\omega')\,d\omega' \tag{3.250}$$

We can extend the upper limit to ∞ since the integrand contributes nothing for $\omega > \omega_c$.

$$\omega_p^2 = \frac{4}{\pi}\int_0^{\infty} \omega' k(\omega') d\omega' \tag{3.251}$$

We substitute $4\pi Ne^2/m$ for $\omega_p^2$ and write N as $Zn_o$, where Z is the number of electrons in the molecule and $n_o$ is the number of water molecules per unit volume.

$$\frac{4\pi n_o Z e^2}{m} = \frac{4}{\pi}\int_0^{\infty} \omega' k(\omega') d\omega' \tag{3.252}$$

$$Z = \frac{m}{\pi^2 n_o e^2}\int_0^{\infty} \omega' k(\omega') d\omega' \tag{3.253}$$

Now, we write the angular frequency in terms of wave number.

$$\omega' = 2\pi c\nu \tag{3.254}$$

$$d\omega' = 2\pi c d\nu \tag{3.255}$$

Substituting Equations (3.254) and (3.255) into Equation (3.253), we obtain

$$Z = \frac{4mc^2}{n_o e^2}\int_0^{\infty} \nu k(\nu) d\nu \tag{3.256}$$

We substitute $\alpha(\nu)/4\pi\nu$ for $k(\nu)$.

$$Z = \frac{mc^2}{\pi n_o e^2} \int_0^\infty \alpha(\nu) d\nu \tag{3.257}$$

Transforming to mks units, we obtain the sum rule used in the calculations described in Chapter IV.

$$Z = \frac{4mc^2 \varepsilon_o}{n_o e^2} \int_0^\infty \alpha(\nu) d\nu \tag{3.258}$$

# CHAPTER IV

## NUMERICAL METHODS

### The Numerical Computation of $n(\omega)$ from $k(\omega)$

In Chapter III, we obtained Equation (3.230) expressing $n(\omega)$ in terms of an integral involving $k(\omega')$. For numerical calculation of $n(\omega)$, we must rely on numerical values of $k(\omega)$ known at discrete values of $\omega$ over a finite spectrum.

Assuming there is some $\omega_{max}$ above which $k(\omega)$ yields a negligible contribution to the integral, we can restrict our attention to those values of $|\omega| \leq \omega_{max}$. Since $k(\omega)$ is an odd function,

$$k(0) = 0 \tag{4.1}$$

Further, if we know $k(\omega)$ for $0 < \omega \leq \omega_{max}$, we automatically know $k(\omega)$ for $-\omega_{max} \leq \omega < 0$. We divide the interval $-\omega_{max} \leq \omega \leq \omega_{max}$ into N segments each of width $\Delta\omega$.

We begin by evaluating $f(\tau)$, the Fourier transform of $ik(\omega')$, as specified in Equation (3.241).

$$f(\tau) = \frac{1}{\sqrt{2\pi}} \int_{-\infty}^{\infty} ik(\omega') e^{-i\omega'\tau} d\omega' \tag{4.2}$$

This integral must be transformed into a discrete sum. For the N points

(including j=0) from j=-N/2 to j=(N/2)-1, with

$$\omega = j\Delta\omega \tag{4.3}$$

$$\tau = m\Delta\tau \tag{4.4}$$

(the index m to be summed over later), we find

$$f(\tau) = f(m) = \frac{i}{\sqrt{2\pi}} \sum_{j=-\frac{N}{2}}^{\frac{N}{2}-1} k(j)\ e^{-i(j\Delta\omega)(m\Delta\tau)}\ \Delta\omega \tag{4.5}$$

The summation is to (N/2)-1 since the function is presumed periodic (to be Fourier transformable) with period $N\Delta\omega$.[27] The value at j=N/2 is the first value of the next period of the function. ($N\to\infty$ in the Fourier integral.) We write $\omega$ and $\Delta\omega$ in terms of wave number.

$$\omega = 2\pi c\nu \tag{4.6}$$

$$\Delta\omega = 2\pi c\Delta\nu \tag{4.7}$$

$$f(m) = ic\Delta\nu\sqrt{2\pi} \sum_{j=-\frac{N}{2}}^{\frac{N}{2}-1} k(j)\ e^{-i2\pi jmc\Delta\nu\Delta\tau} \tag{4.8}$$

Now we impose the condition of periodicity by requiring that

$$f(m+qN) = f(m) \tag{4.9}$$

where q is any integer. Substituting m+qN for m in Equation (4.8) and

applying Equation (4.9) yields

$$e^{-i2\pi jqNc\Delta\nu\Delta\tau} = 1 \tag{4.10}$$

Therefore, $jqNc\Delta\nu\Delta\tau$ must be an integer. With $jq$ integral, we can require $Nc\Delta\nu\Delta\tau$ to be unity. Then,

$$\Delta\tau = \frac{1}{Nc\Delta\nu} \tag{4.11}$$

$$f(m) = ic\Delta\nu\sqrt{2\pi}\sum_{j=-\frac{N}{2}}^{\frac{N}{2}-1} k(j)\, e^{-i2\pi\left(\frac{m}{N}\right)j} \tag{4.12}$$

The only values of k(j) known from real data are those N/2 points for $0 < j \leq N/2$. Since k(j) is odd about zero, the values of k(j) in that part of the sum over negative integers must be replaced by $-k(-j)$.

$$f(m) = ic\Delta\nu\sqrt{2\pi}\left\{ \sum_{j=-\frac{N}{2}}^{-1} [-k(-j)]\, e^{-i2\pi\left(\frac{m}{N}\right)j} + \sum_{j=0}^{\frac{N}{2}-1} k(j)\, e^{-i2\pi\left(\frac{m}{N}\right)j} \right\} \tag{4.13}$$

This can be transformed into a sum over positive integers by defining a new index.

$$l \equiv N + j \tag{4.14}$$

We substitute $l$ for $j$ in the first sum in Equation (4.13), then change

the dummy index $l$ back to $j$.

$$f(m) = ic\Delta\nu\sqrt{2\pi}\left\{ \sum_{j=\frac{N}{2}}^{N-1} [-k(N-j)]\, e^{-i2\pi\left(\frac{m}{N}\right)j} + \sum_{j=0}^{\frac{N}{2}-1} k(j)\, e^{-i2\pi\left(\frac{m}{N}\right)j} \right\} \tag{4.15}$$

We define the function $k'(j)$ as follows:

$$k'(j) \equiv \begin{cases} -k(N-j), & \frac{N}{2} \le j < N \\ k(j), & 0 \le j < \frac{N}{2} \end{cases} \tag{4.16}$$

Then we can combine the sums in Equation (4.15).

$$f(m) = ic\Delta\nu\sqrt{2\pi} \sum_{j=0}^{N-1} k'(j)\, e^{-i2\pi\left(\frac{m}{N}\right)j} \tag{4.17}$$

We can calculate $n(\omega)-1$ with this function $f(m)$. The integral in Equation (3.242) can be transformed into a discrete sum. For a particular $\omega_o$,

$$\omega_o = l_o\Delta\omega \tag{4.18}$$

$$n(\omega_o)-1 = \frac{1}{\sqrt{2\pi}} \sum_{m=-\frac{N}{2}}^{-1} [-f(m)]\, e^{i(l_o\Delta\omega)(m\Delta\tau)}\Delta\tau + \cdots$$

$$+ \frac{1}{\sqrt{2\pi}} \sum_{m=0}^{\frac{N}{2}-1} f(m)\, e^{i(l_o \Delta\omega)(m\Delta\tau)} \Delta\tau \tag{4.19}$$

Now, using Equations (4.7) and (4.11), we obtain

$$n(\omega_o)-1 = \frac{1}{Nc\Delta\nu\sqrt{2\pi}} \left\{ \sum_{m=-\frac{N}{2}}^{-1} [-f(m)]\, e^{i2\pi\left(\frac{l_o}{N}\right)m} + \sum_{m=0}^{\frac{N}{2}-1} f(m)\, e^{i2\pi\left(\frac{l_o}{N}\right)m} \right\} \tag{4.20}$$

As before, this can be written as a sum over positive integers.

$$n(\omega_o)-1 = \frac{1}{Nc\Delta\nu\sqrt{2\pi}} \left\{ \sum_{m=\frac{N}{2}}^{N-1} [-f(m-N)]\, e^{i2\pi\left(\frac{l_o}{N}\right)m} + \sum_{m=0}^{\frac{N}{2}-1} f(m)\, e^{i2\pi\left(\frac{l_o}{N}\right)m} \right\} \tag{4.21}$$

We obtain $-f(m-N)$ and $f(m)$ from Equation (4.17) and substitute into Equation (4.21).

$$n(\omega_o)-1 = \left(\frac{i}{N}\right) \left\{ \sum_{m=\frac{N}{2}}^{N-1} \left[ -\sum_{j=0}^{N-1} k'(j)\, e^{-i2\pi\left(\frac{m}{N}\right)j} \right] e^{i2\pi\left(\frac{l_o}{N}\right)m} + \sum_{m=0}^{\frac{N}{2}-1} \left[ \sum_{j=0}^{N-1} k'(j)\, e^{-i2\pi\left(\frac{m}{N}\right)j} \right] e^{i2\pi\left(\frac{l_o}{N}\right)m} \right\} \tag{4.22}$$

Now we define the following function:

$$A(m) \equiv \begin{cases} -\sum_{j=0}^{N-1} k'(j)\, e^{-i2\pi\left(\frac{m}{N}\right)j}, & \frac{N}{2} \le m \le N-1 \\ +\sum_{j=0}^{N-1} k'(j)\, e^{-i2\pi\left(\frac{m}{N}\right)j}, & 0 \le m \le \frac{N}{2}-1 \end{cases} \tag{4.23}$$

The result is

$$n(\omega_o) = 1 + \left(\frac{i}{N}\right) \sum_{m=0}^{N-1} A(m)\, e^{i2\pi\left(\frac{l_o}{N}\right)m} \tag{4.24}$$

As one can see by tracing back from A(m) in Equation (4.23) through k'(j) in Equation (4.16), this enables the numerical calculation of $n(\omega)$ directly from the $k(\omega)$ spectrum.

Calculations

Each of these sums was computed by arranging appropriate arrays and using the FAST FOURIER TRANSFORM algorithm on the AMDAHL 470 computer. The wave number spectrum was divided into $2^{17}$ = 131,072 equal intervals. Since, for most k(j)'s, $j\Delta\nu$ fell between values of $\nu$ for which $k(\nu)$ data were available, the program interpolated to obtain the appropriate k(j). Then, the program calculated the $n(\nu)$ spectrum, yielding a value of $n(\nu)$ for each $\nu$ for which a $k(\nu)$ value had been input. Again, the program interpolated between the values of $n(m\Delta\nu)$, obtained for integral m, to arrive at $n(\nu)$ for the appropriate wave numbers.

The calculation was first done over the range 0 to $5\times10^6$ $cm^{-1}$. As is evident from the Kramers-Kronig integral, the greatest contribution

is obtained from those values of $k(\nu)$ for $\nu$ closest to the wave number for which $n(\nu)$ is being calculated. Thus, as long as the wave number being investigated is not near an end point of the range of calculation, it should yield a reasonable result. The result should be less reliable as one approaches an endpoint. This was found to be true.

The density of the data points input was much greater at low wave numbers than at high wave numbers. As a result, even with $2^{17}$ intervals, those intervals at the low end included, and glossed over, many data points. The resolution was, in effect, reduced at the low end. The phenomenon is illustrated by Figure 5, which shows the region 0 to 50 $cm^{-1}$. The jagged line was calculated by dividing the region of 0 to $5x10^5$ $cm^{-1}$ into $2^{17}$ intervals. The data, then, had influence every 3.8 $cm^{-1}$. The smooth line was calculated by dividing the region of 0 to $5x10^4$ $cm^{-1}$ into $2^{17}$ intervals, resulting in effective data every 0.38 $cm^{-1}$, and increased resolution.

In order to overcome the problem of resolution, it was necessary to choose a smaller range for the calculation. Division of the larger range into more and smaller intervals would have required more computer memory than was available. So long as the region of interest was kept some distance from the endpoints of the range, the results were good. With the intention of combining the results into a composite spectrum, calculations were made over the following regions, illustrated by the indicated figures: 0 to $5x10^6$ $cm^{-1}$, Figure 6; 0 to $5x10^5$ $cm^{-1}$, Figure 7; 0 to $5x10^4$ $cm^{-1}$, Figure 8; 0 to $5x10^3$ $cm^{-1}$, Figure 9; 0 to $5x10^2$ $cm^{-1}$, Figure 10; 0 to $5x10^1$ $cm^{-1}$, Figure 11; 0 to $5x10^0$ $cm^{-1}$, Figure 12; 0 to $5x10^{-1}$ $cm^{-1}$, Figure 13.

The phenomenon of deviation from good results as an endpoint is approached is illustrated by Figure 14. There, the values obtained from calculations over the two ranges 0 to $5x10^6$ and 0 to $5x10^5$ $cm^{-1}$ are superimposed. It is apparent that, as the vicinity of $1x10^5$ $cm^{-1}$ is passed, the calculation over the smaller range gives values which begin to differ from the other values, the latter being presumably more accurate since they are farther from an endpoint. This is characteristic of most of the calculations. The results seem accurate up to approximately $1x10^n$ $cm^{-1}$ for a calculation over the range of 0 to $5x10^n$ $cm^{-1}$. It seems reasonable, then, to use that part of each spectrum not limited by poor resolution or by proximity to an endpoint.

Since the Fourier transform technique is most accurate in defining the shape of the curve, but less accurate in defining its absolute position, it was deemed desirable to fix the height of the curve at an appropriate point. This was done by calculating the difference between the number obtained at a particular point by the program and a reasonably certain number for the same point obtained from experimental or other data. This difference was then added to (or subtracted from) the values obtained for the entire spectrum. The point used to fix the first calculated spectrum, from 0 to $5x10^6$ $cm^{-1}$, was $\nu = 1.580278x10^4$ $cm^{-1}$, for which the value assigned was n=1.33146.

This same point was similarly fixed in the calculations over the ranges 0 to $5x10^5$ and 0 to $5x10^4$ $cm^{-1}$. For calculations over the ranges 0 to $5x10^n$ for $n<4$, a point was chosen in the graph of the calculated spectrum for 0 to $5x10^{n+1}$ $cm^{-1}$ which seemed most likely to be

stable; that is, a point was chosen as far to the left (low wave number) as was reasonable, provided it was a region not undergoing violent oscillations, and hopefully provided it had a slope approximately zero. Accordingly, the following points were fixed for the ranges specified: for 0 to $5x10^3$ $cm^{-1}$, $\nu=2.103778x10^3$ $cm^{-1}$ was fixed at n=1.311148; for 0 to $5x10^2$ $cm^{-1}$, $\nu=1.064143x10^2$ $cm^{-1}$ was fixed at n=1.886343; for 0 to $5x10^1$, $\nu=8.332974$ $cm^{-1}$ was fixed at n=2.481153; for 0 to $5x10^0$, $\nu=9.090965x10^{-1}$ $cm^{-1}$ was fixed at n=6.094436; for 0 to $5x10^{-1}$ $cm^{-1}$, $\nu=1.204759x10^{-1}$ $cm^{-1}$ was fixed at n=8.676634.

The process of joining the parts into one complete spectrum was accomplished by matching slopes and applying a weighted average. The goal was to obtain a smooth transition from one curve to the next in the region where the greater accuracy was presumed to shift from the first to the second curve.

No adjustment was necessary in several cases. The curve calculated for the range 0 to $5x10^1$ $cm^{-1}$ was joined to the curve for the range 0 to $5x10^2$ $cm^{-1}$ at the point fixed as described above, at $\nu=8.332974$ $cm^{-1}$. This is illustrated in Figure 18. The curve for the range 0 to $5x10^2$ $cm^{-1}$ was joined to that for 0 to $5x10^3$ $cm^{-1}$ at the point $\nu=1.064143x10^2$ $cm^{-1}$, as illustrated in Figure 19. The curve for the range 0 to $5x10^3$ $cm^{-1}$ was joined to that for the range 0 to $5x10^4$ $cm^{-1}$ at $\nu=2.103778x10^3$ $cm^{-1}$, as illustrated in Figure 20. The curve for the range 0 to $5x10^5$ $cm^{-1}$ was joined to that for 0 to $5x10^6$ $cm^{-1}$ at $\nu=3.076097x10^4$ $cm^{-1}$, as shown in Figure 22.

Adjustments were necessary in four cases. For the low end, the

value for $n(\nu)$ calculated from the Cole-Cole equation was used to fix the single point $\nu=1x10^{-3}$ $cm^{-1}$. The curve there was assumed to have nearly zero slope. Then, a smooth transition was created up to the slope at $\nu=7.144963x10^{-2}$ $cm^{-1}$ as calculated from the curve for 0 to $5x10^{-1}$ $cm^{-1}$. A weighted average was applied to assure that the values of $n(\nu)$ were as required at the endpoints, $n=8.8486$ at $1x10^{-3}$ $cm^{-1}$ (from the Cole-Cole equation) and $n=8.7978$ at $7.144963x10^{-2}$ $cm^{-1}$ (from the calculation over the range 0 to $5x10^{-1}$ $cm^{-1}$). The result is illustrated by Figure 15. The curves for the ranges 0 to $5x10^{-1}$ and 0 to $5x10^{0}$ $cm^{-1}$ were connected by a similar procedure, the difference being that the slope at the lower end was calculated from the data just as was the slope at the higher end. The transition is illustrated by Figure 16. The curves for the ranges 0 to $5x10^{0}$ and 0 to $5x10^{1}$ $cm^{-1}$ were connected by the same process, as shown in Figure 17. The curves for the ranges 0 to $5x10^{4}$ and 0 to $5x10^{5}$ $cm^{-1}$ were connected by applying only a weighted average since this resulted in a smooth transition and left the fixed point, $\nu=1.580278x10^{4}$ $cm^{-1}$, intact. This is illustrated by Figure 21.

The final $n(\nu)$ spectrum is presented in Chapter V in both graphical and tabular form.

Fig. 5. An illustration of the increased resolution obtained by reducing the range of calculation. The solid line is the curve for $n(\nu)$ obtained by calculation over the range 0 to $5 \times 10^4$ $cm^{-1}$. The dashed line is the curve obtained by calculation over the range 0 to $5 \times 10^5$ $cm^{-1}$. The latter curve shows decreased resolution.

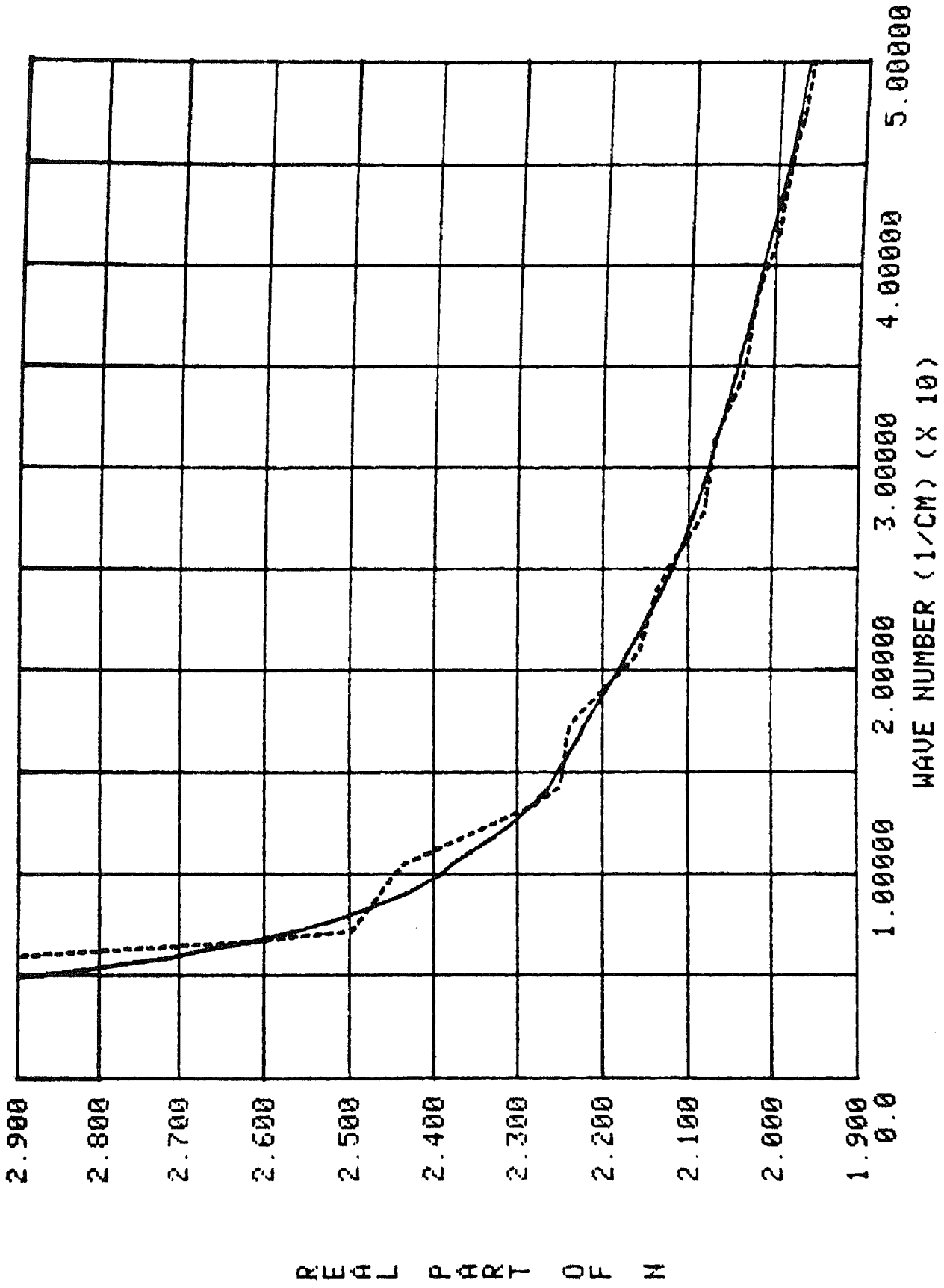
REAL PART OF N
2.900
2.800
2.700
2.600
2.500
2.400
2.300
2.200
2.100
2.000
1.900
0.0
1.00000
2.00000
3.00000
4.00000
5.00000
WAVE NUMBER (1/CM) (X 10)

Fig. 6. The spectrum calculated for the range 0 to $5 \times 10^6$ $cm^{-1}$. The inaccuracy at the right end of the curve (primarily due to the last datum point) is a result of proximity to the endpoint of the range of calculation. This is characteristic of the results illustrated in Figures 7 through 13 also. The phenomenon is discussed in the text.

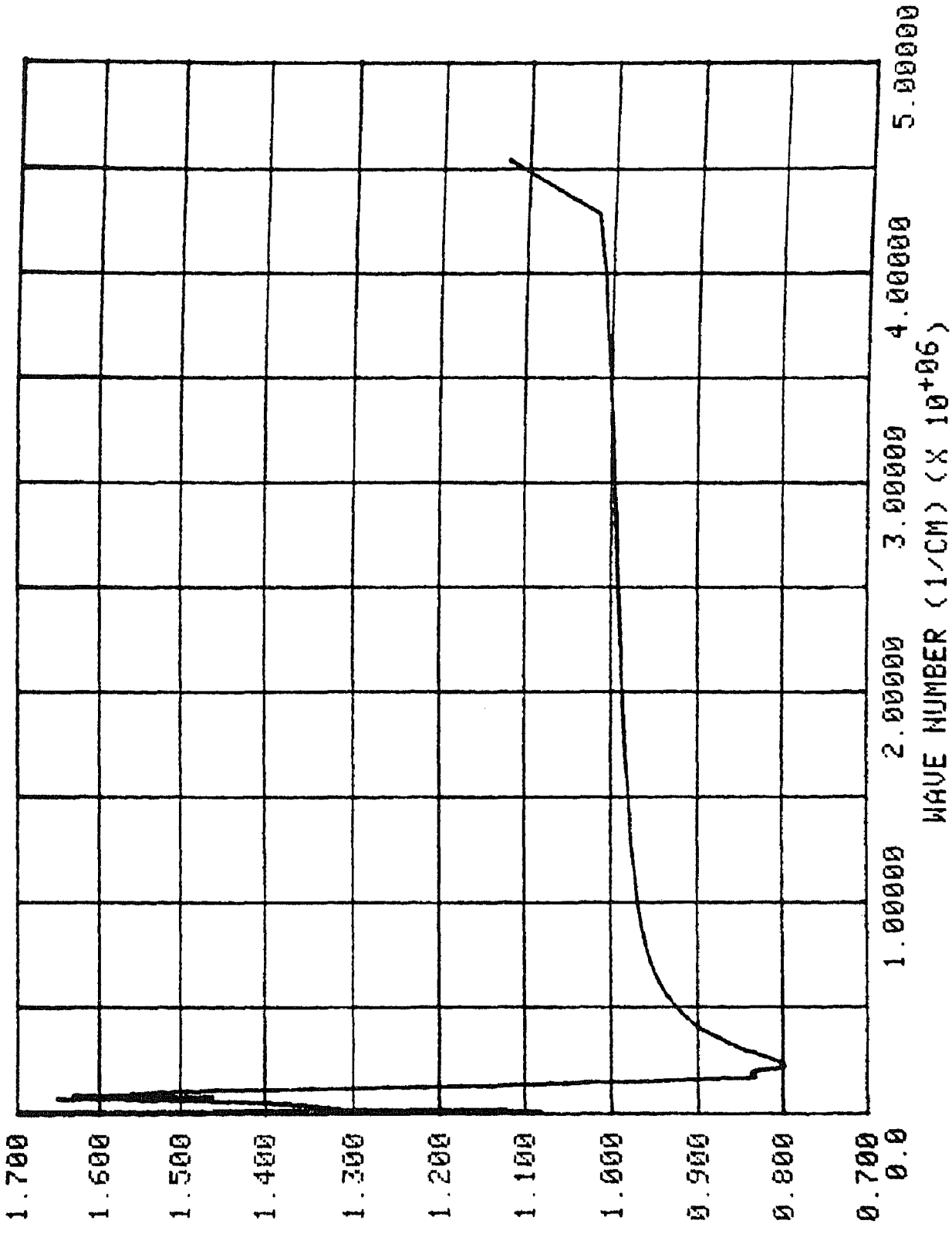
REAL PART OF N
1.700
1.600
1.500
1.400
1.300
1.200
1.100
1.000
0.900
0.800
0.700
0.0
1.00000
2.00000
3.00000
4.00000
5.00000
WAVE NUMBER (1/CM) (X 10+06)

Fig. 7. The spectrum calculated for the range 0 to $5 \times 10^5$ $cm^{-1}$.

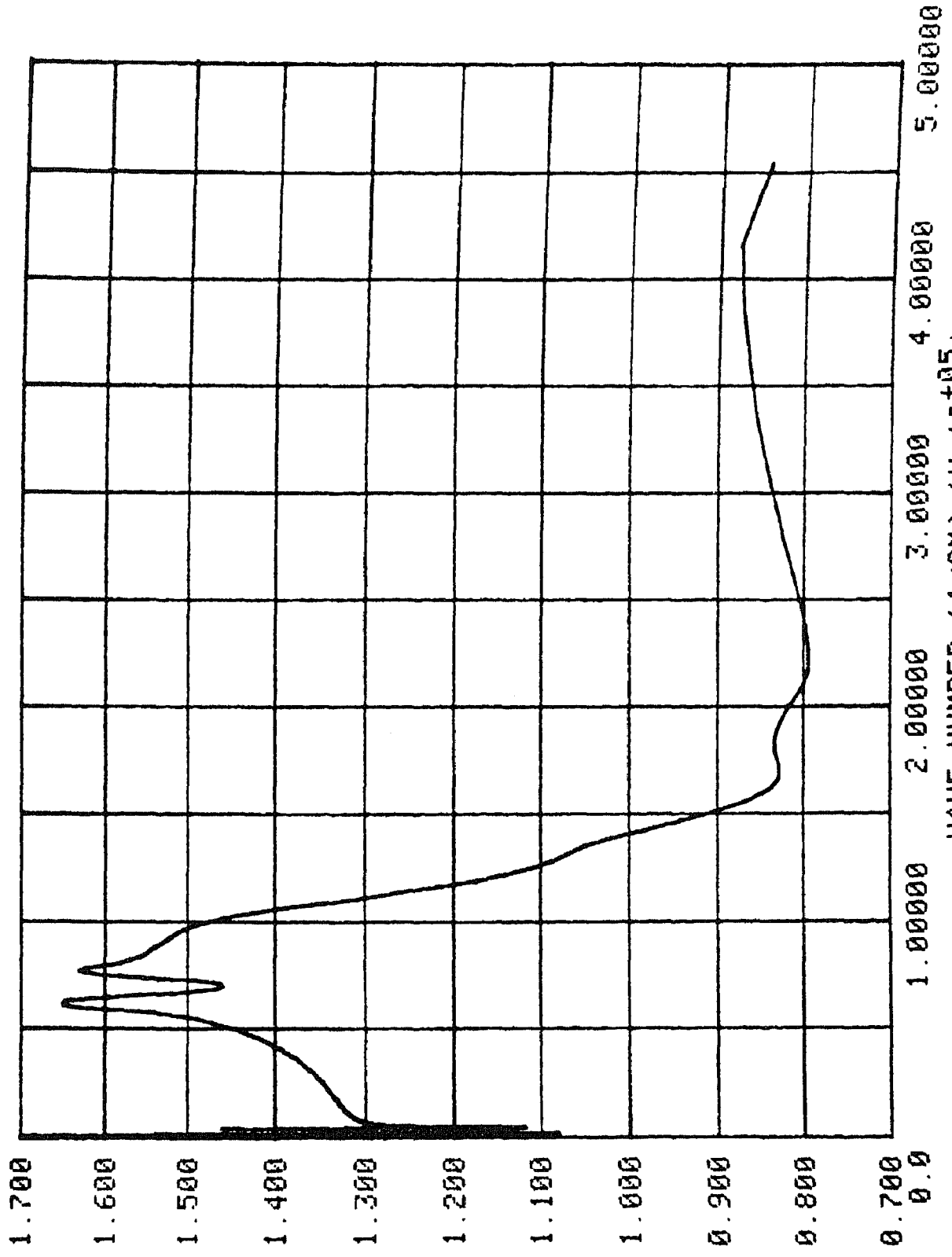
REAL PART OF H
1.700
1.600
1.500
1.400
1.300
1.200
1.100
1.000
0.900
0.800
0.700
0.0
1.00000
2.00000
3.00000
4.00000
5.00000
WAVE NUMBER (1/CM) (X 10+05)

Fig. 8. The spectrum calculated for the range 0 to $5 \times 10^4$ $cm^{-1}$.

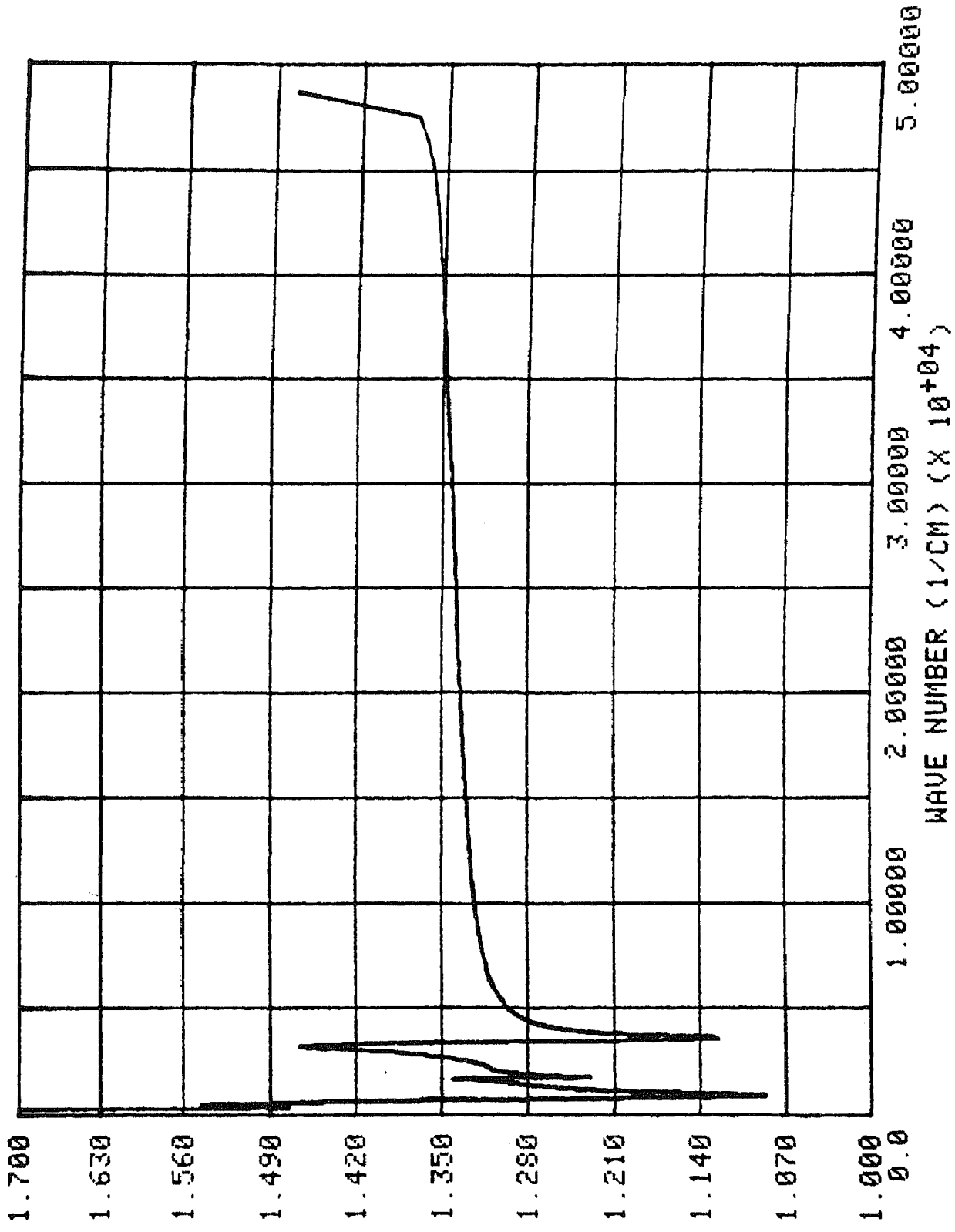
1.700
1.630
1.560
1.490
1.420
1.350
1.280
1.210
1.140
1.070
1.000
0.0
1.00000
2.00000
3.00000
4.00000
5.00000
WAVE NUMBER (1/CM) (X 10+04)
REAL PART OF N

Fig. 9. The spectrum calculated for the range 0 to $5 \times 10^3$ $cm^{-1}$.

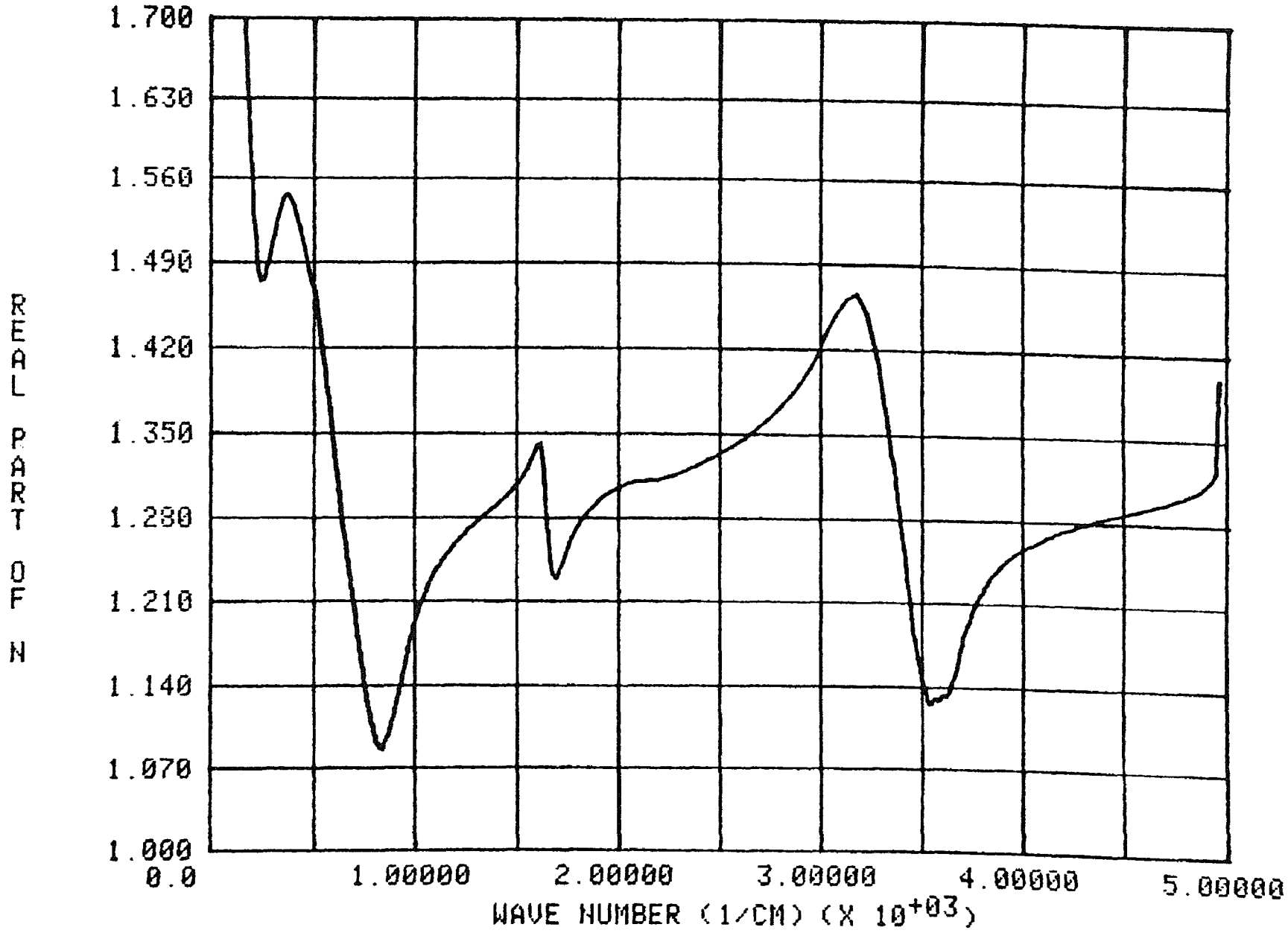
1.700
1.630
1.560
1.490
1.420
1.350
1.280
1.210
1.140
1.070
1.000
REAL PART OF N
0.0
1.00000
2.00000
3.00000
4.00000
5.00000
WAVE NUMBER (1/CM) (X 10+03)

Fig. 10. The spectrum calculated for the range 0 to $5 \times 10^2$ $cm^{-1}$.

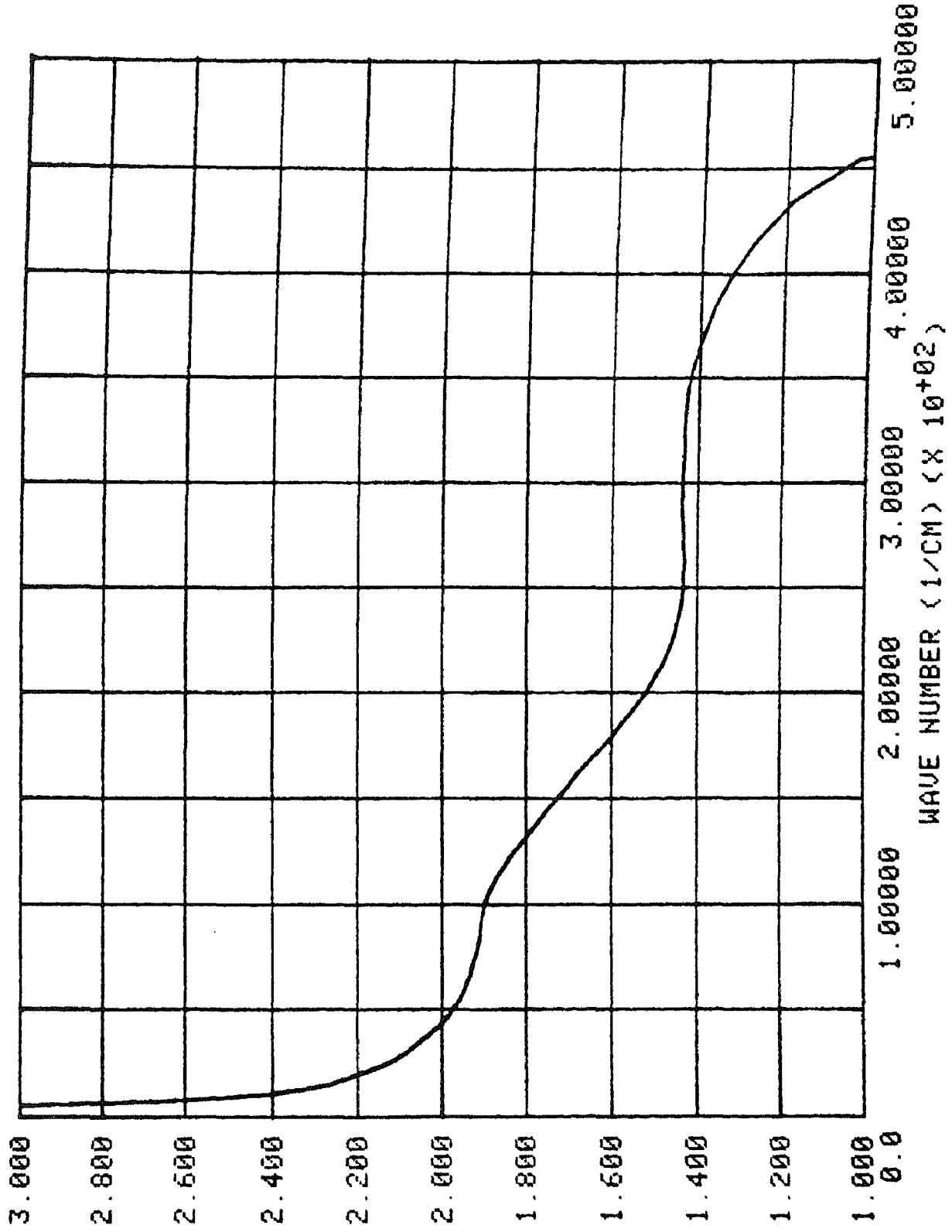
3.000
2.800
2.600
2.400
2.200
2.000
1.800
1.600
1.400
1.200
1.000
0.0
1.00000
2.00000
3.00000
4.00000
5.00000
WAVE NUMBER (1/CM) (X 10+02)
REAL PART OF N

Fig. 11. The spectrum calculated for the range 0 to $5 \times 10^{1}$ $cm^{-1}$.

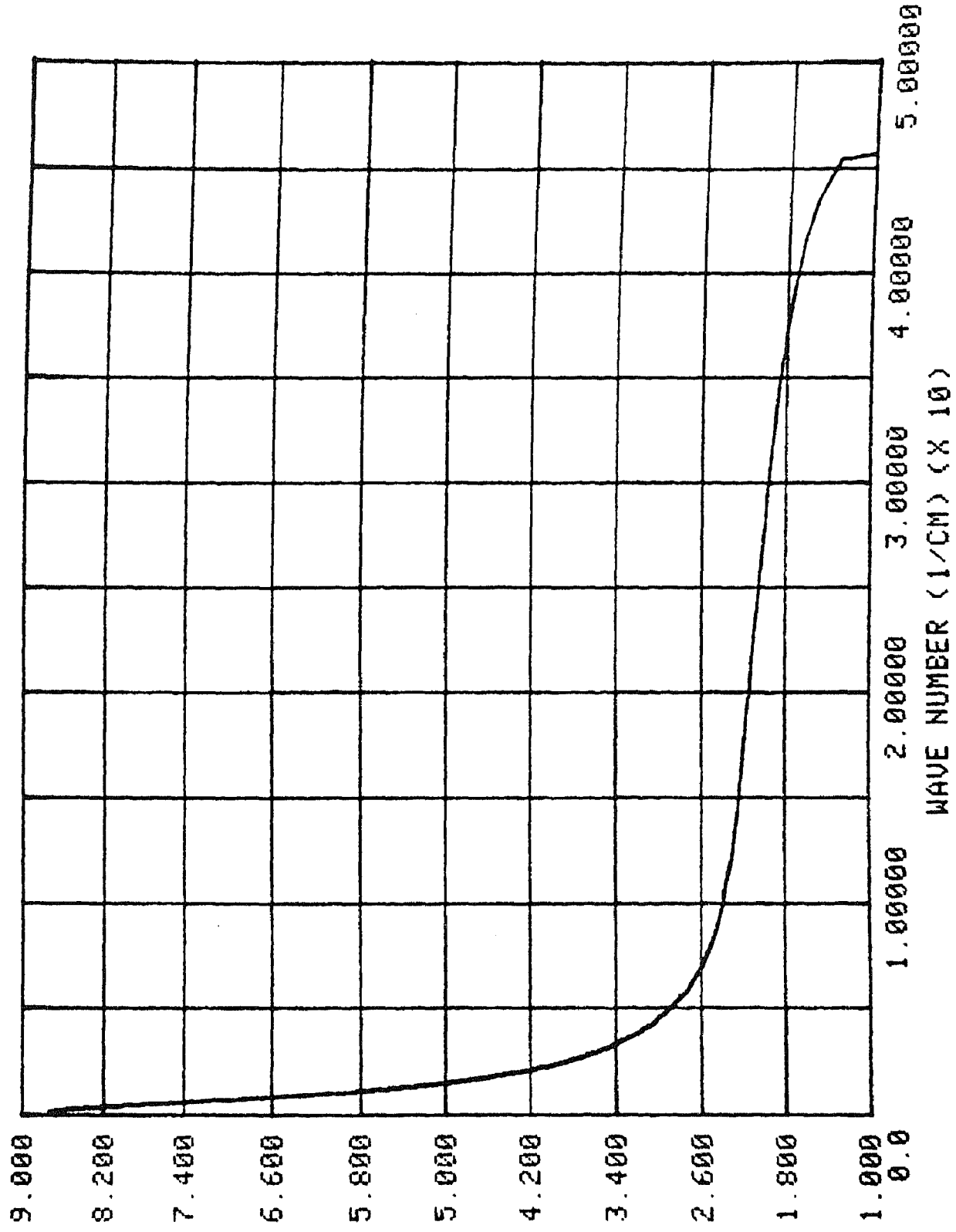
9.000
8.200
7.400
6.600
5.800
5.000
4.200
3.400
2.600
1.800
1.000
0.0
1.00000
2.00000
3.00000
4.00000
5.00000
WAVE NUMBER (1/CM) (X 10)
REAL PART OF N

Fig. 12. The spectrum calculated for the range 0 to 5 $cm^{-1}$.

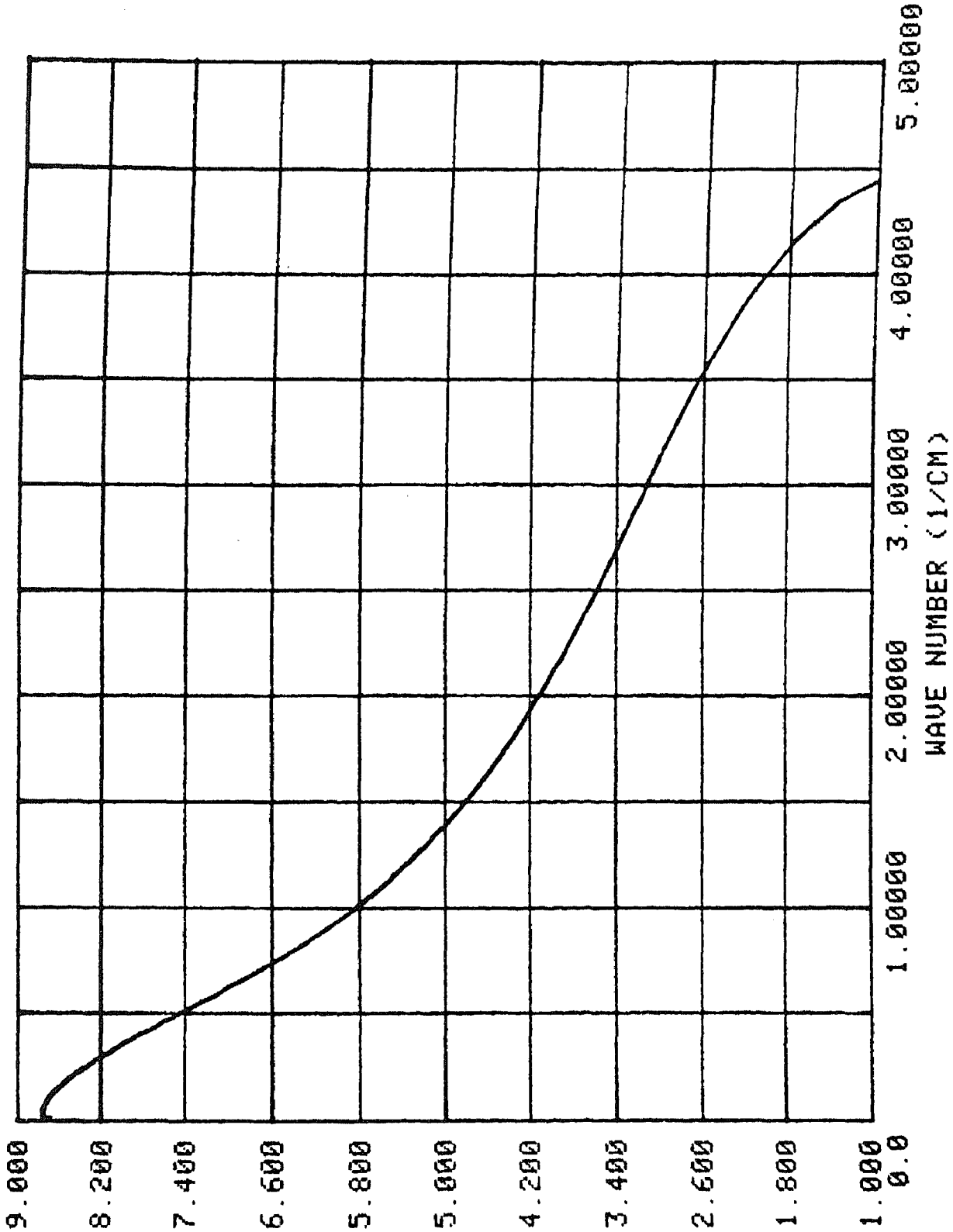
9.000
8.200
7.400
6.600
5.800
5.000
4.200
3.400
2.600
1.800
1.000
0.0
1.00000
2.00000
3.00000
4.00000
5.00000
WAVE NUMBER (1/CM)
REAL PART OF N

Fig. 13. The spectrum calculated for the range 0 to $5 \times 10^{-1}$ $cm^{-1}$.

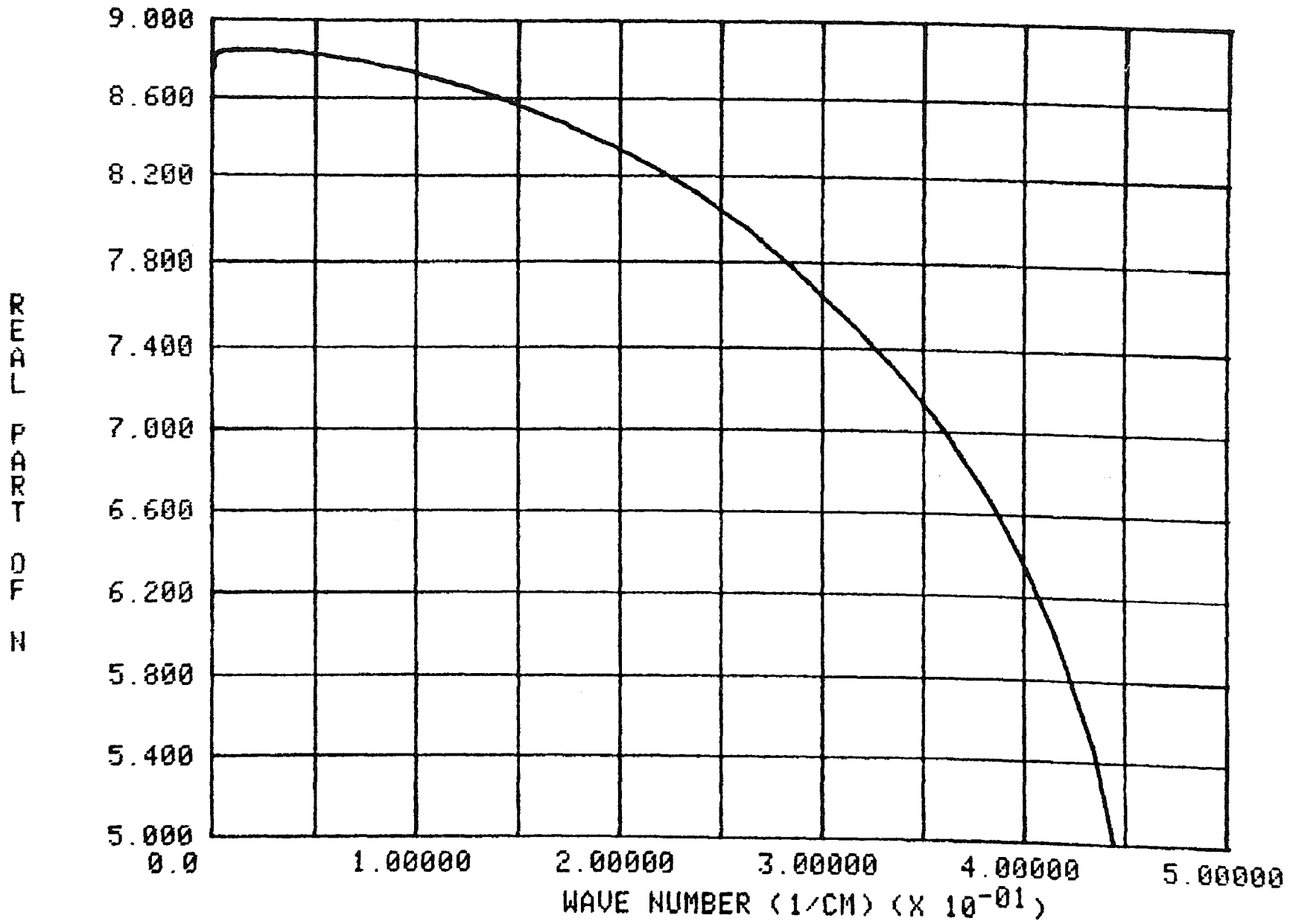
9.000
8.600
8.200
7.800
7.400
7.000
6.600
6.200
5.800
5.400
5.000
REAL PART OF N
0.0
1.00000
2.00000
3.00000
4.00000
5.00000
WAVE NUMBER (1/CM) (X 10^-01)

Fig. 14. An illustration of inaccuracy as an endpoint is approached. The dashed line is $n(\nu)$ as obtained by calculation over the range 0 to $5 \times 10^6$ $cm^{-1}$. The solid line was obtained by calculation over the smaller range 0 to $5 \times 10^5$ $cm^{-1}$. The latter deviates from the dashed line as it approaches the right endpoint of the range of calculation.

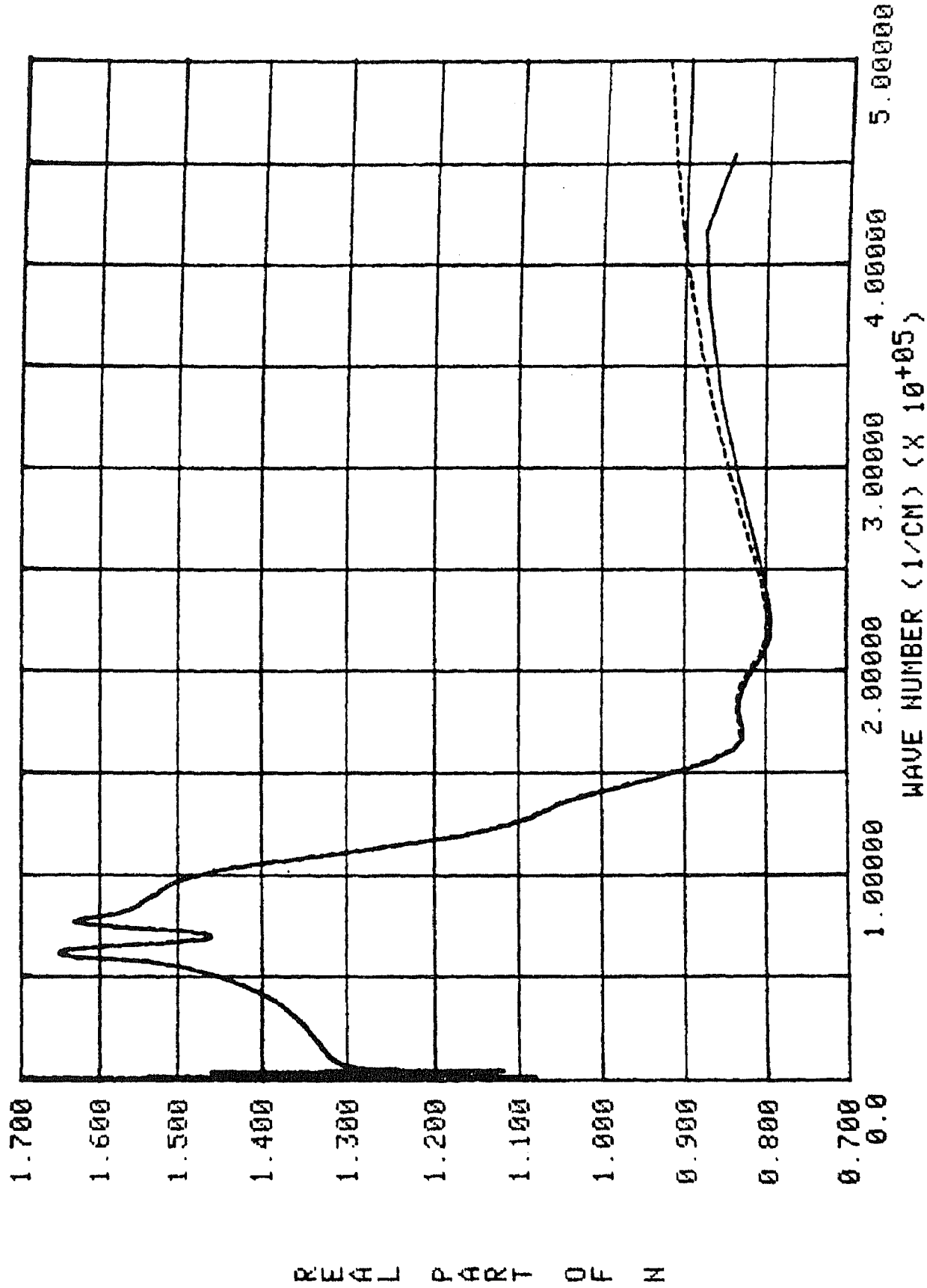
1.700
1.600
1.500
1.400
1.300
1.200
1.100
1.000
0.900
0.800
0.700
0.0
1.00000
2.00000
3.00000
4.00000
5.00000
WAVE NUMBER (1/CM) (X 10+05)
REAL PART OF N

Fig. 15. Fitting low frequency results. The dashed line is $n(\nu)$ as obtained by calculation over the range 0 to $5 \times 10^{-1}$ $cm^{-1}$. The solid line is that calculated to connect the value of $n(\nu)$ at $1 \times 10^{-3}$ $cm^{-1}$ (as obtained from the Cole-Cole equation) with the dashed curve in a smooth manner. The procedure is described in the text.

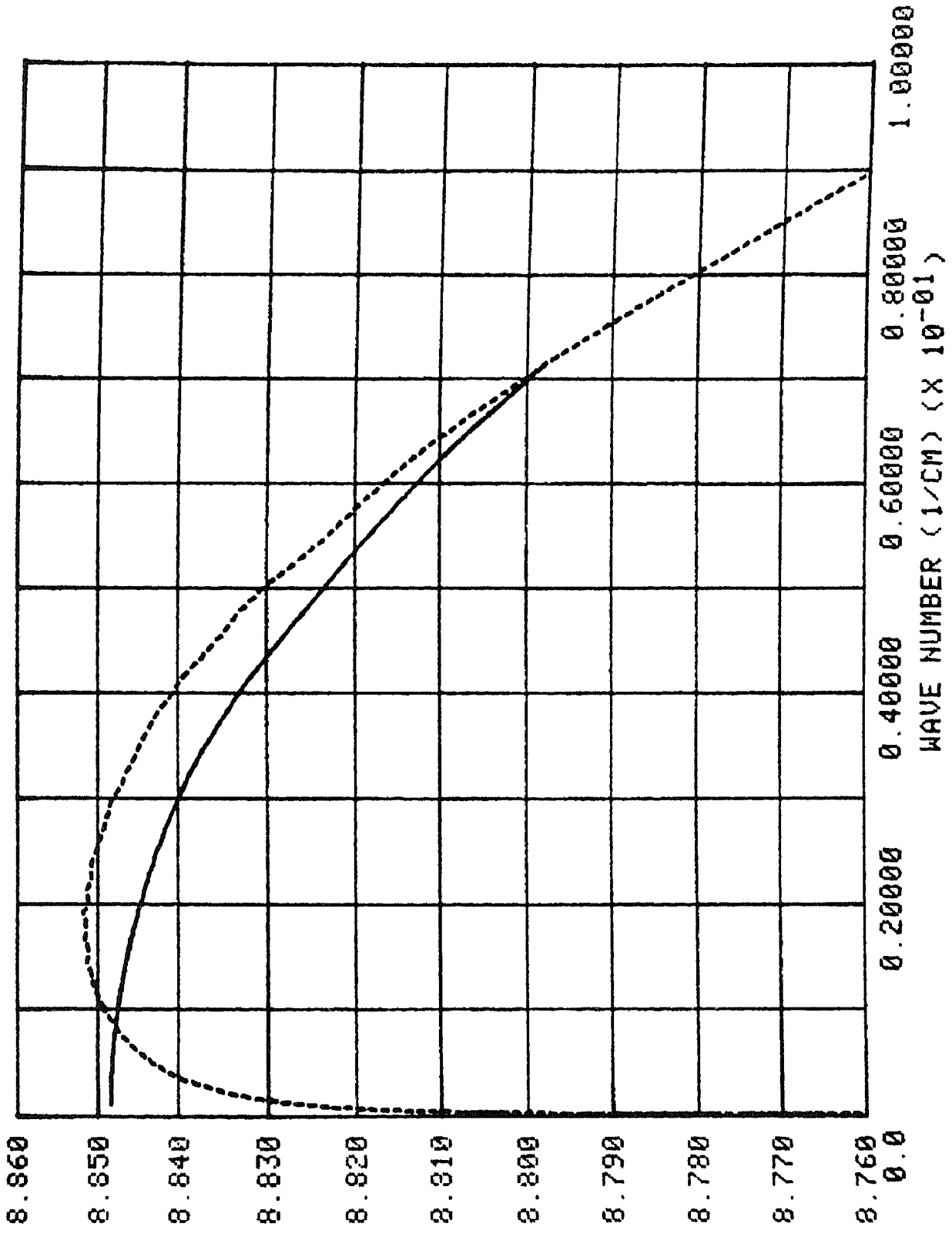
8.860
8.850
8.840
8.830
8.820
8.810
8.800
8.790
8.780
8.770
8.760
0.0
0.20000
0.40000
0.60000
0.80000
1.00000
WAVE NUMBER (1/CM) (X 10-01)
REAL PART OF N

Fig. 16. The transition in the region of $10^{-1}$ $cm^{-1}$. The short dashes are $n(\nu)$ as obtained by calculation over the range 0 to $5x10^{-1}$ $cm^{-1}$. The long dashes are $n(\nu)$ as calculated over the range 0 to 5 $cm^{-1}$. The solid curve is the calculated transition between the two.

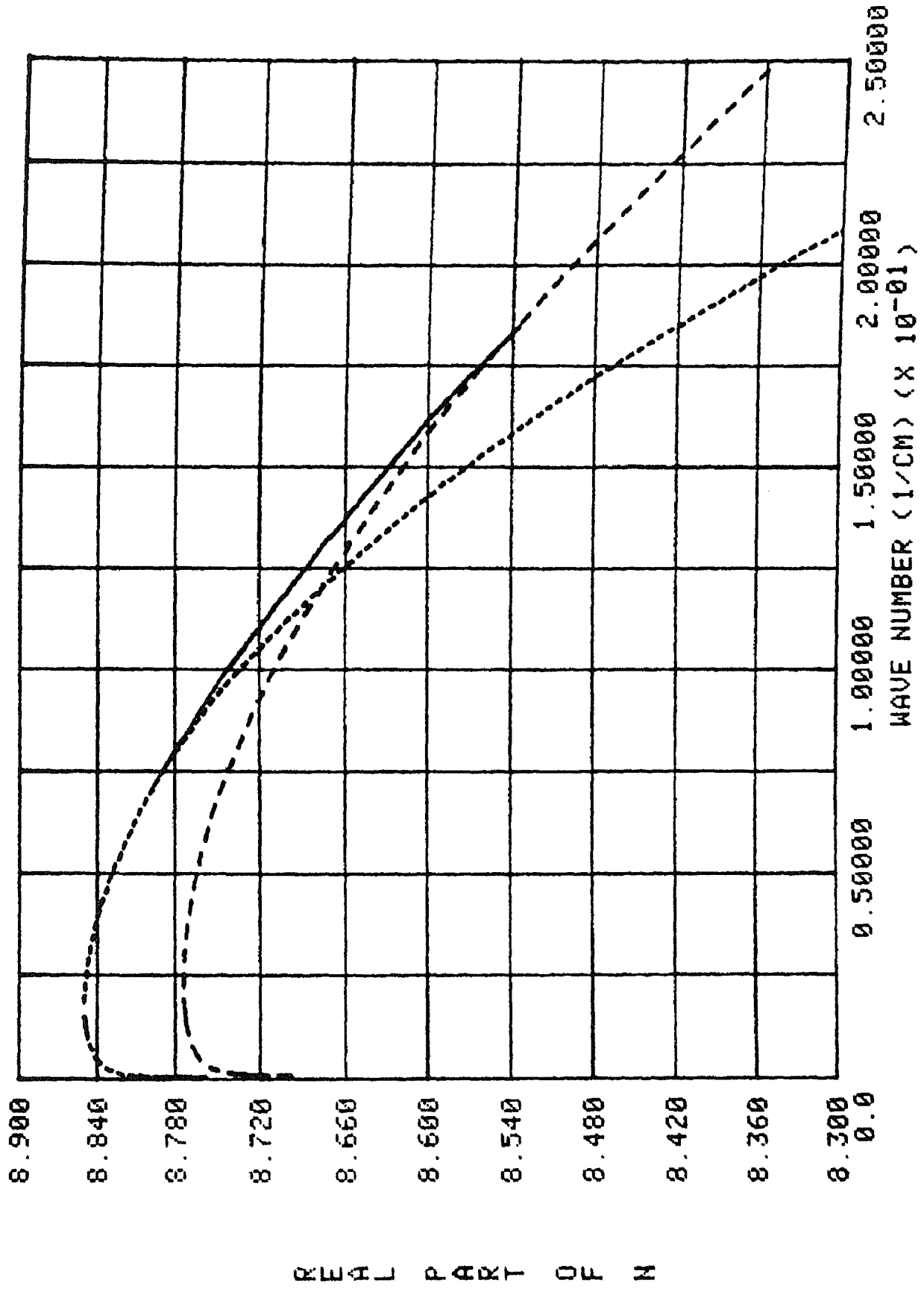
8.900
8.840
8.780
8.720
8.660
8.600
8.540
8.480
8.420
8.360
8.300
0.0
0.50000
1.00000
1.50000
2.00000
2.50000
WAVE NUMBER (1/CM) (X 10⁻⁰¹)
REAL PART OF N

Fig. 17. The transition in the region of 1 $cm^{-1}$. The short dashes are $n(\nu)$ as obtained by calculation over the range 0 to 5 $cm^{-1}$. The long dashes are $n(\nu)$ as calculated over the range 0 to $5x10^{1}$ $cm^{-1}$. The solid curve is the calculated transition between the two.

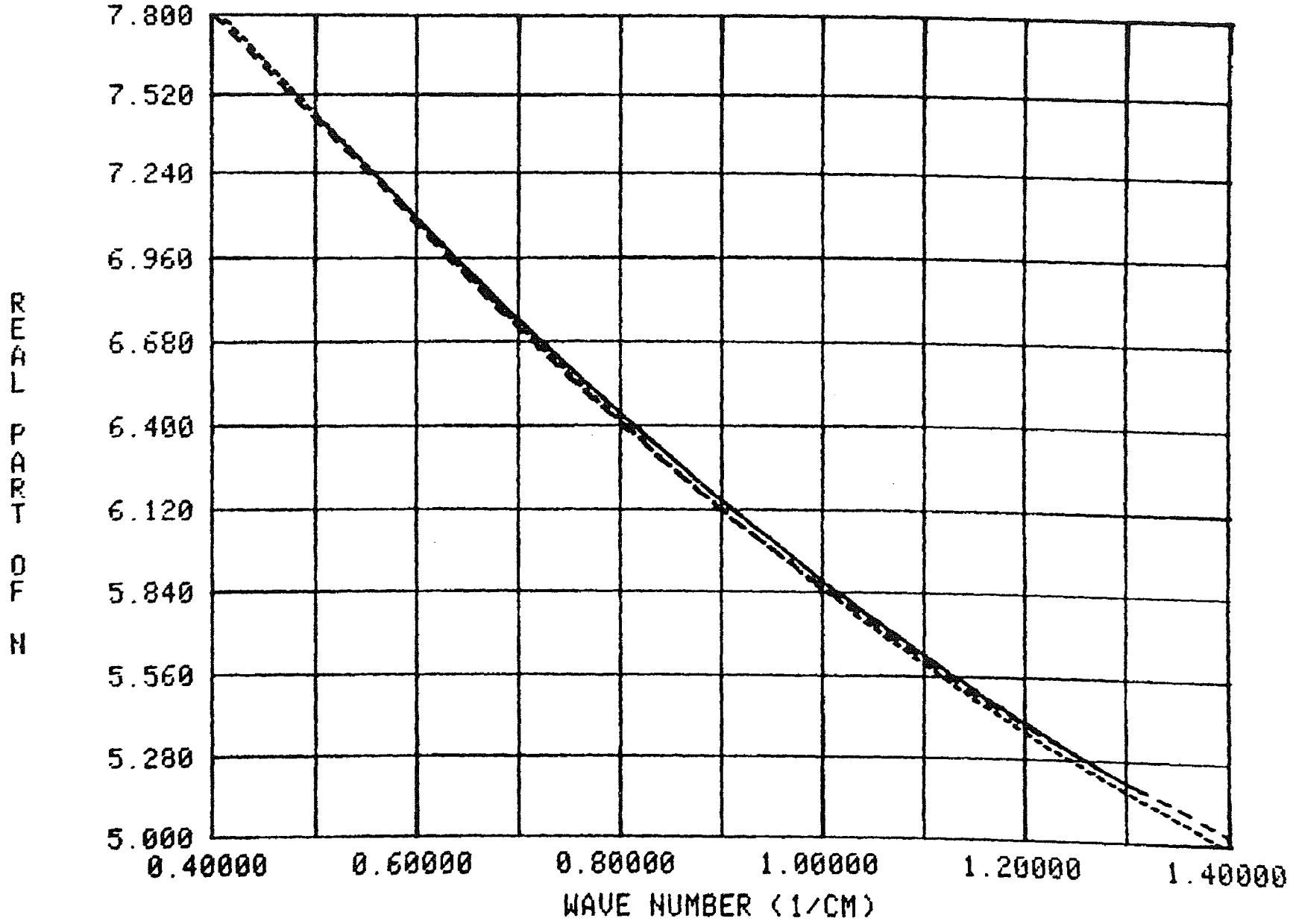
7.800
7.520
7.240
6.960
6.680
6.400
6.120
5.840
5.560
5.280
5.000
REAL PART OF N
0.40000
0.60000
0.80000
1.00000
1.20000
1.40000
WAVE NUMBER (1/CM)

Fig. 18. The transition in the region of 10 $cm^{-1}$. The solid line is $n(\nu)$ as obtained by calculation over the range 0 to $5x10^{1}$ $cm^{-1}$. The dashed line is $n(\nu)$ as calculated over the range 0 to $5x10^{2}$ $cm^{-1}$. The two curves were connected at their point of intersection.

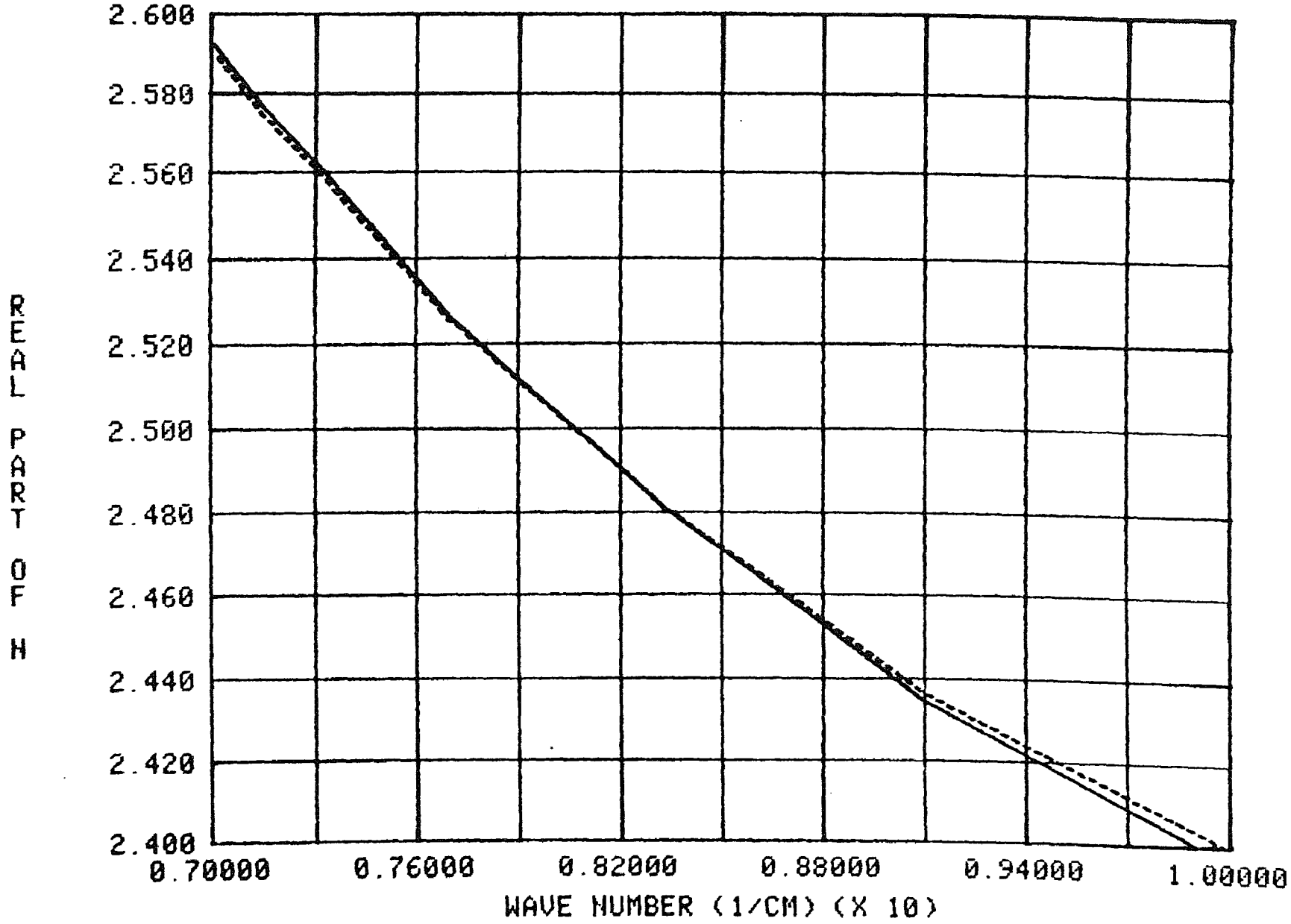
2.600
2.580
2.560
2.540
2.520
2.500
2.480
2.460
2.440
2.420
2.400
REAL PART OF H
0.70000
0.76000
0.82000
0.88000
0.94000
1.00000
WAVE NUMBER (1/CM) (X 10)

Fig. 19. The transition in the region of $10^2$ $cm^{-1}$. The solid line is $n(\nu)$ as obtained by calculation over the range 0 to $5x10^2$ $cm^{-1}$. The dashed line is $n(\nu)$ as calculated over the range 0 to $5x10^3$ $cm^{-1}$. The two curves were connected at their point of intersection

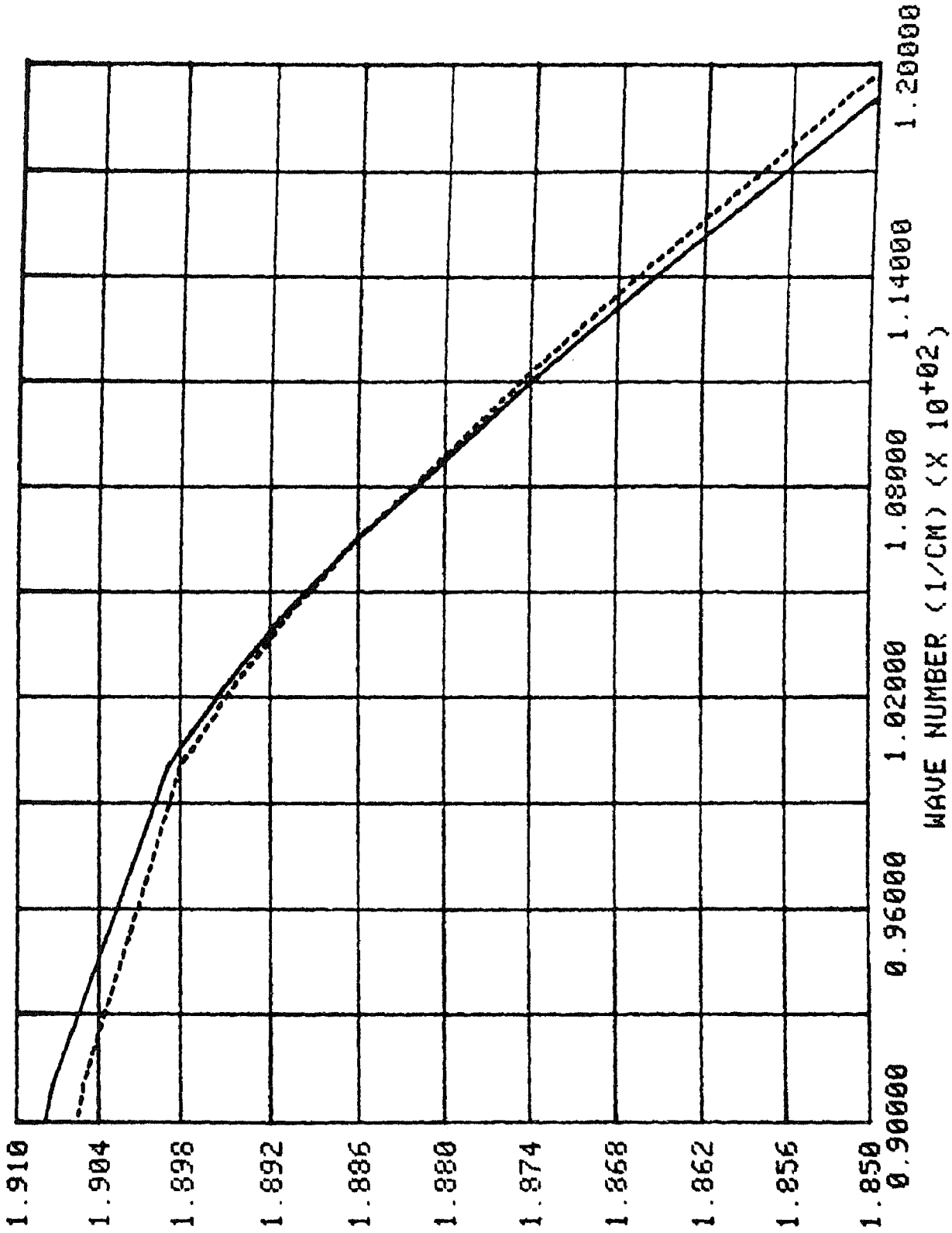
1.910
1.904
1.898
1.892
1.886
1.880
1.874
1.868
1.862
1.856
1.850
0.90000
0.96000
1.02000
1.08000
1.14000
1.20000
WAVE NUMBER (1/CM) (X 10+02)
REAL PART OF N

Fig. 20. The transition in the region of $10^3$ $cm^{-1}$. The solid line is $n(\nu)$ as obtained by calculation over the range 0 to $5x10^3$ $cm^{-1}$. The dashed line is $n(\nu)$ as calculated over the range 0 to $5x10^4$ $cm^{-1}$. The two curves were connected at their point of intersection. The curves are so close together in this region that they are difficult to distinguish.

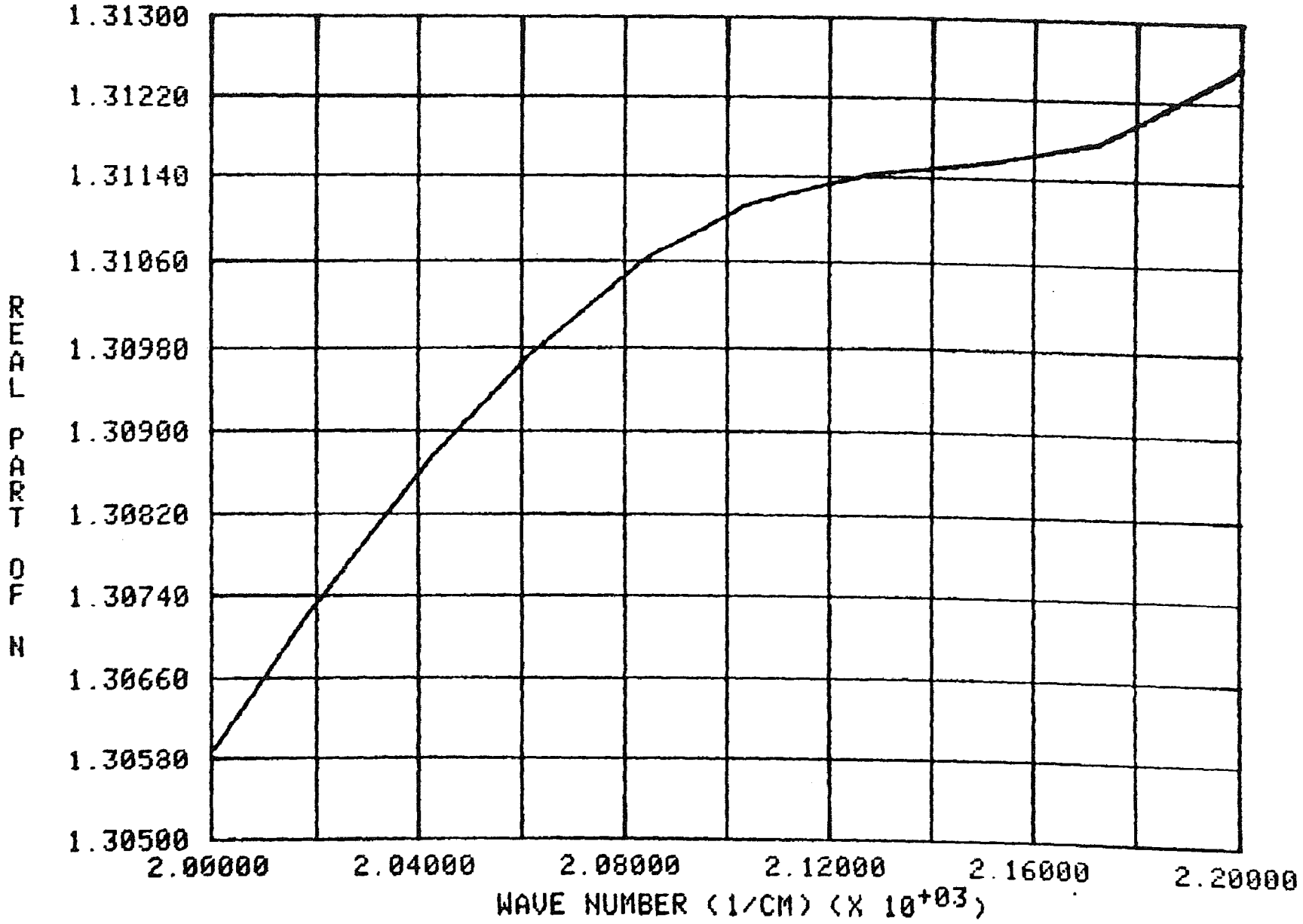
1.31300
1.31220
1.31140
1.31060
1.30980
1.30900
1.30820
1.30740
1.30660
1.30580
1.30500
REAL PART OF N
2.00000
2.04000
2.08000
2.12000
2.16000
2.20000
WAVE NUMBER (1/CM) (X 10+03)

Fig. 21. The transition in the region of $10^4$ $cm^{-1}$. The short dashes are $n(\nu)$ as obtained by calculation over the range 0 to $5x10^4$ $cm^{-1}$. The long dashes are $n(\nu)$ as calculated over the range 0 to $5x10^5$ $cm^{-1}$. The solid line is the calculated transition between the two.

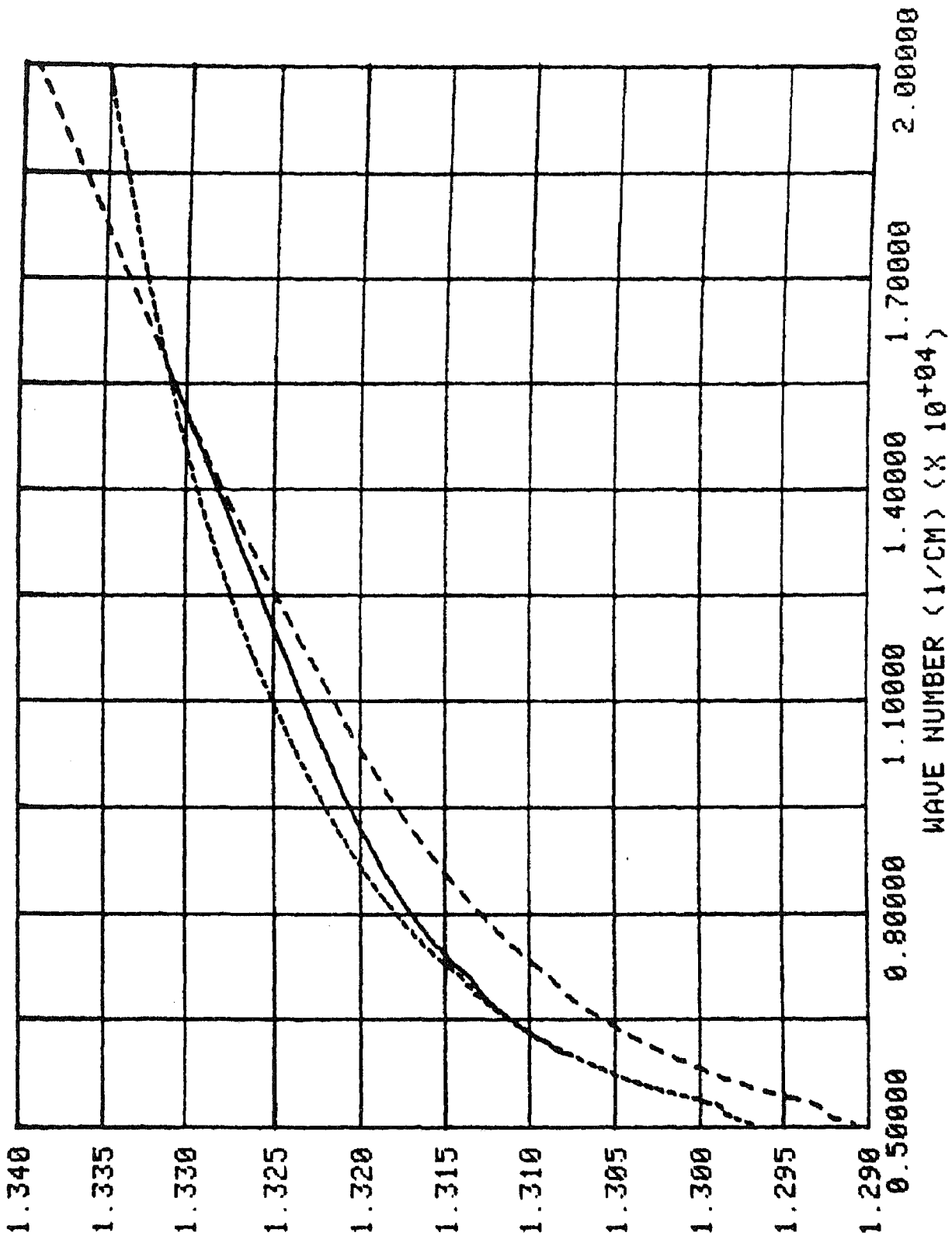
REAL PART OF N
1.340
1.335
1.330
1.325
1.320
1.315
1.310
1.305
1.300
1.295
1.290
0.50000
0.80000
1.10000
1.40000
1.70000
2.00000
WAVE NUMBER (1/CM) (X 10+04)

Fig. 22. The transition in the region of $10^5$ $cm^{-1}$. The solid line is $n(\nu)$ as obtained by calculation over the range 0 to $5x10^5$ $cm^{-1}$. The dashed line is $n(\nu)$ as calculated over the range 0 to $5x10^6$ $cm^{-1}$. The curves are so close together in this region that they are difficult to distinguish.

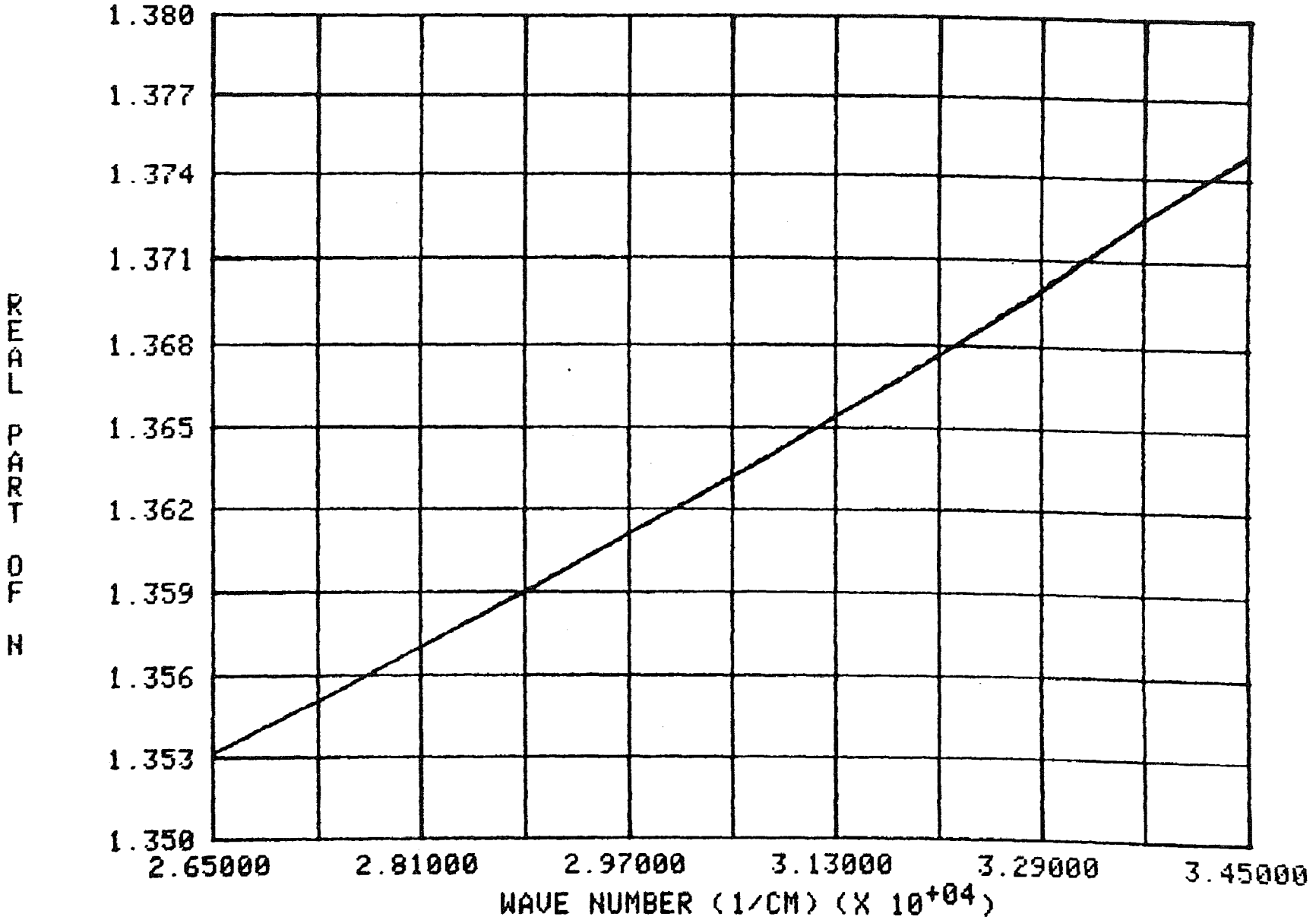
1.380
1.377
1.374
1.371
1.368
1.365
1.362
1.359
1.356
1.353
1.350
REAL PART OF N
2.65000
2.81000
2.97000
3.13000
3.29000
3.45000
WAVE NUMBER (1/CM) (X 10+04)

# CHAPTER V

## RESULTS

The final spectrum was obtained by combination of the several calculated curves as described in Chapter IV. To present only data of reasonably certain accuracy, values are not reported for the extreme endpoint regions of less than $1x10^{-3}$ $cm^{-1}$ and greater than $1x10^{6}$ $cm^{-1}$. The $n(\nu)$ spectrum is shown in Figures 23 through 30. The values of both the real and imaginary parts of $N(\nu)$ (n and k) are presented in Table 1, immediately below. These results are discussed in Chapter VI.

TABLE 1*

THE COMPLEX REFRACTIVE INDEX OF WATER

| Wave Number ($cm^{-1}$) | n | k |
|---|---|---|
| 1.0000000D-03 | 8.848600 | 6.9309081D-03 |
| 1.0092529D-03 | 8.848600 | 7.0111643D-03 |
| 1.0209395D-03 | 8.848600 | 7.0597634D-03 |
| 1.0303861D-03 | 8.848600 | 7.1415116D-03 |
| 1.0423174D-03 | 8.848600 | 7.2075912D-03 |
| 1.0519619D-03 | 8.848600 | 7.2910511D-03 |
| 1.0641430D-03 | 8.848600 | 7.3585144D-03 |
| 1.0764652D-03 | 8.848599 | 7.4437220D-03 |
| 1.0864256D-03 | 8.848599 | 7.5299162D-03 |
| 1.0990058D-03 | 8.848599 | 7.5995897D-03 |
| 1.1117317D-03 | 8.848599 | 7.6875888D-03 |
| 1.1246050D-03 | 8.848599 | 7.7587211D-03 |
| 1.1376273D-03 | 8.848599 | 7.8485629D-03 |
| 1.1481536D-03 | 8.848599 | 7.9577473D-03 |
| 1.1641260D-03 | 8.848599 | 8.0313794D-03 |

TABLE 1-Continued

| Wave Number ($cm^{-1}$) | n | k |
|---|---|---|
| 1.1776060D-03 | 8.848598 | 8.1243784D-03 |
| 1.1912420D-03 | 8.848598 | 8.2184543D-03 |
| 1.2050359D-03 | 8.848598 | 8.3327844D-03 |
| 1.2189896D-03 | 8.848598 | 8.4292735D-03 |
| 1.2359474D-03 | 8.848598 | 8.5268798D-03 |
| 1.2502590D-03 | 8.848598 | 8.6256165D-03 |
| 1.2647363D-03 | 8.848598 | 8.7456107D-03 |
| 1.2823306D-03 | 8.848597 | 8.8468801D-03 |
| 1.3001696D-03 | 8.848597 | 8.9493222D-03 |
| 1.3152248D-03 | 8.848597 | 9.0947370D-03 |
| 1.3335214D-03 | 8.848597 | 9.2000491D-03 |
| 1.3520726D-03 | 8.848596 | 9.3280345D-03 |
| 1.3708818D-03 | 8.848596 | 9.4578004D-03 |
| 1.3899526D-03 | 8.848596 | 9.5673165D-03 |
| 1.4092888D-03 | 8.848596 | 9.7004112D-03 |
| 1.4288940D-03 | 8.848595 | 9.8580302D-03 |
| 1.4487719D-03 | 8.848595 | 9.9951690D-03 |
| 1.4689263D-03 | 8.848595 | 1.0157577D-02 |
| 1.4927944D-03 | 8.848594 | 1.0298883D-02 |
| 1.5135612D-03 | 8.848594 | 1.0442155D-02 |
| 1.5381546D-03 | 8.848594 | 1.0611827D-02 |
| 1.5631476D-03 | 8.848593 | 1.0759452D-02 |
| 1.5885467D-03 | 8.848593 | 1.0909131D-02 |
| 1.6143586D-03 | 8.848592 | 1.1111947D-02 |
| 1.6405898D-03 | 8.848592 | 1.1292501D-02 |
| 1.6672472D-03 | 8.848591 | 1.1475990D-02 |
| 1.6943378D-03 | 8.848591 | 1.1662459D-02 |
| 1.7258379D-03 | 8.848590 | 1.1851959D-02 |
| 1.7538805D-03 | 8.848589 | 1.2072303D-02 |
| 1.7864876D-03 | 8.848589 | 1.2268463D-02 |
| 1.8197009D-03 | 8.848588 | 1.2496550D-02 |
| 1.8535316D-03 | 8.848587 | 1.2728879D-02 |
| 1.8879913D-03 | 8.848586 | 1.2965526D-02 |
| 1.9230917D-03 | 8.848585 | 1.3206573D-02 |
| 1.9588447D-03 | 8.848585 | 1.3483112D-02 |
| 1.9998619D-03 | 8.848584 | 1.3733782D-02 |
| 2.0417379D-03 | 8.848582 | 1.3989112D-02 |
| 2.0844909D-03 | 8.848581 | 1.4282037D-02 |
| 2.1281390D-03 | 8.848580 | 1.4581095D-02 |
| 2.1727012D-03 | 8.848579 | 1.4920732D-02 |
| 2.2233099D-03 | 8.848577 | 1.5233165D-02 |
| 2.2750974D-03 | 8.848576 | 1.5587991D-02 |
| 2.3280913D-03 | 8.848574 | 1.5914395D-02 |
| 2.3823195D-03 | 8.848572 | 1.6322630D-02 |

TABLE 1-Continued

| Wave Number ($cm^{-1}$) | n | k |
|---|---|---|
| 2.4378108D-03 | 8.848570 | 1.6702833D-02 |
| 2.5003454D-03 | 8.848568 | 1.7131293D-02 |
| 2.5644840D-03 | 8.848566 | 1.7570744D-02 |
| 2.6302680D-03 | 8.848563 | 1.8021467D-02 |
| 2.7039584D-03 | 8.848560 | 1.8483752D-02 |
| 2.7797133D-03 | 8.848557 | 1.9001599D-02 |
| 2.8575905D-03 | 8.848554 | 1.9533953D-02 |
| 2.9444216D-03 | 8.848550 | 2.0081222D-02 |
| 3.0269134D-03 | 8.848546 | 2.0739111D-02 |
| 3.1260794D-03 | 8.848541 | 2.1320144D-02 |
| 3.2284941D-03 | 8.848536 | 2.2018622D-02 |
| 3.3342641D-03 | 8.848531 | 2.2739983D-02 |
| 3.4514374D-03 | 8.848524 | 2.3484977D-02 |
| 3.5727284D-03 | 8.848518 | 2.4366331D-02 |
| 3.7068072D-03 | 8.848510 | 2.5222617D-02 |
| 3.8459178D-03 | 8.848501 | 2.6229508D-02 |
| 3.9994475D-03 | 8.848491 | 2.7213860D-02 |
| 4.1686938D-03 | 8.848480 | 2.8365480D-02 |
| 4.3451022D-03 | 8.848467 | 2.9565835D-02 |
| 4.5498806D-03 | 8.848452 | 3.0888025D-02 |
| 4.7643099D-03 | 8.848435 | 3.2343733D-02 |
| 5.0003453D-03 | 8.848415 | 3.3946120D-02 |
| 5.2601727D-03 | 8.848392 | 3.5710024D-02 |
| 5.5590426D-03 | 8.848364 | 3.7652181D-02 |
| 5.8884366D-03 | 8.848330 | 3.9791485D-02 |
| 6.2517269D-03 | 8.848291 | 4.2343831D-02 |
| 6.6680677D-03 | 8.848243 | 4.5059892D-02 |
| 7.1449633D-03 | 8.848183 | 4.8282544D-02 |
| 7.6913044D-03 | 8.848109 | 5.1974479D-02 |
| 8.3368118D-03 | 8.848013 | 5.6206966D-02 |
| 9.0991327D-03 | 8.847889 | 6.1205457D-02 |
| 1.0000000D-02 | 8.847727 | 6.7265154D-02 |
| 1.0092529D-02 | 8.847710 | 6.8044048D-02 |
| 1.0209395D-02 | 8.847688 | 6.8515707D-02 |
| 1.0303861D-02 | 8.847671 | 6.9309081D-02 |
| 1.0423174D-02 | 8.847648 | 6.9950391D-02 |
| 1.0519619D-02 | 8.847630 | 7.0760378D-02 |
| 1.0641430D-02 | 8.847606 | 7.1415116D-02 |
| 1.0764652D-02 | 8.847582 | 7.2242064D-02 |
| 1.0864256D-02 | 8.847563 | 7.3078587D-02 |
| 1.0990058D-02 | 8.847537 | 7.3754775D-02 |
| 1.1117317D-02 | 8.847512 | 7.4608815D-02 |
| 1.1246050D-02 | 8.847485 | 7.5472745D-02 |
| 1.1376273D-02 | 8.847459 | 7.6171085D-02 |

TABLE 1-Continued

| Wave Number ($cm^{-1}$) | n | k |
|---|---|---|
| 1.1481536D-02 | 8.847437 | 7.7230731D-02 |
| 1.1641260D-02 | 8.847403 | 7.7945338D-02 |
| 1.1776060D-02 | 8.847374 | 7.8847902D-02 |
| 1.1912420D-02 | 8.847344 | 7.9760918D-02 |
| 1.2050359D-02 | 8.847314 | 8.0870503D-02 |
| 1.2189896D-02 | 8.847283 | 8.1806939D-02 |
| 1.2359474D-02 | 8.847244 | 8.2754219D-02 |
| 1.2502590D-02 | 8.847212 | 8.3905445D-02 |
| 1.2647363D-02 | 8.847178 | 8.4877024D-02 |
| 1.2823306D-02 | 8.847137 | 8.5859854D-02 |
| 1.3001696D-02 | 8.847094 | 8.7054283D-02 |
| 1.3152248D-02 | 8.847058 | 8.8265329D-02 |
| 1.3335214D-02 | 8.847013 | 8.9287393D-02 |
| 1.3520726D-02 | 8.846967 | 9.0529505D-02 |
| 1.3708818D-02 | 8.846920 | 9.1788895D-02 |
| 1.3899526D-02 | 8.846871 | 9.2851761D-02 |
| 1.4092888D-02 | 8.846821 | 9.4360480D-02 |
| 1.4288940D-02 | 8.846769 | 9.5673165D-02 |
| 1.4487719D-02 | 8.846716 | 9.7004112D-02 |
| 1.4689263D-02 | 8.846662 | 9.8580302D-02 |
| 1.4927944D-02 | 8.846596 | 9.9951690D-02 |
| 1.5135612D-02 | 8.846538 | 1.0134216D-01 |
| 1.5381546D-02 | 8.846468 | 1.0298883D-01 |
| 1.5631476D-02 | 8.846396 | 1.0442155D-01 |
| 1.5885467D-02 | 8.846321 | 1.0611827D-01 |
| 1.6143586D-02 | 8.846244 | 1.0759452D-01 |
| 1.6405898D-02 | 8.846164 | 1.0934279D-01 |
| 1.6672472D-02 | 8.846082 | 1.1137562D-01 |
| 1.6943378D-02 | 8.845997 | 1.1318533D-01 |
| 1.7258379D-02 | 8.845896 | 1.1502444D-01 |
| 1.7538805D-02 | 8.845804 | 1.1716291D-01 |
| 1.7864876D-02 | 8.845696 | 1.1906665D-01 |
| 1.8197009D-02 | 8.845583 | 1.2128027D-01 |
| 1.8535316D-02 | 8.845467 | 1.2325091D-01 |
| 1.8879913D-02 | 8.845345 | 1.2583172D-01 |
| 1.9230917D-02 | 8.845220 | 1.2817111D-01 |
| 1.9588447D-02 | 8.845089 | 1.3085495D-01 |
| 1.9998619D-02 | 8.844936 | 1.3328772D-01 |
| 2.0417379D-02 | 8.844776 | 1.3576573D-01 |
| 2.0844909D-02 | 8.844609 | 1.3860859D-01 |
| 2.1281390D-02 | 8.844436 | 1.4151098D-01 |
| 2.1727012D-02 | 8.844254 | 1.4480720D-01 |
| 2.2233099D-02 | 8.844044 | 1.4783938D-01 |
| 2.2750974D-02 | 8.843823 | 1.5093506D-01 |

TABLE 1-Continued

| Wave Number ($cm^{-1}$) | n | k |
|---|---|---|
| 2.3280913D-02 | 8.843591 | 1.5445079D-01 |
| 2.3823195D-02 | 8.843349 | 1.5804841D-01 |
| 2.4378108D-02 | 8.843095 | 1.6210266D-01 |
| 2.5003454D-02 | 8.842801 | 1.6587852D-01 |
| 2.5644840D-02 | 8.842491 | 1.7013362D-01 |
| 2.6302680D-02 | 8.842166 | 1.7449788D-01 |
| 2.7039584D-02 | 8.841790 | 1.7897408D-01 |
| 2.7797133D-02 | 8.841394 | 1.8398827D-01 |
| 2.8575905D-02 | 8.840974 | 1.8914294D-01 |
| 2.9444216D-02 | 8.840491 | 1.9444203D-01 |
| 3.0269134D-02 | 8.840020 | 2.0081222D-01 |
| 3.1260794D-02 | 8.839434 | 2.0643824D-01 |
| 3.2284941D-02 | 8.838809 | 2.1320144D-01 |
| 3.3342641D-02 | 8.838141 | 2.2018622D-01 |
| 3.4514374D-02 | 8.837375 | 2.2739983D-01 |
| 3.5727284D-02 | 8.836475 | 2.3560806D-01 |
| 3.7068072D-02 | 8.835449 | 2.4411257D-01 |
| 3.8459178D-02 | 8.834348 | 2.5350711D-01 |
| 3.9994475D-02 | 8.833091 | 2.6344511D-01 |
| 4.1686938D-02 | 8.831656 | 2.7408808D-01 |
| 4.3451022D-02 | 8.830103 | 2.8595003D-01 |
| 4.5498806D-02 | 8.828230 | 2.9832534D-01 |
| 4.7643099D-02 | 8.826184 | 3.1231306D-01 |
| 5.0003453D-02 | 8.823834 | 3.2771034D-01 |
| 5.2601727D-02 | 8.821129 | 3.4481817D-01 |
| 5.5590426D-02 | 8.817867 | 3.6298622D-01 |
| 5.8884366D-02 | 8.814082 | 3.8369854D-01 |
| 6.2517269D-02 | 8.809677 | 4.0727724D-01 |
| 6.6680677D-02 | 8.804337 | 4.3370072D-01 |
| 7.1449633D-02 | 8.797836 | 4.6364987D-01 |
| 7.6913044D-02 | 8.788091 | 4.9829915D-01 |
| 8.3368118D-02 | 8.776133 | 5.3800975D-01 |
| 9.0991327D-02 | 8.761392 | 5.8450757D-01 |
| 1.0000000D-01 | 8.743107 | 6.4089981D-01 |
| 1.0101829D-01 | 8.741029 | 6.4705343D-01 |
| 1.0204694D-01 | 8.738919 | 6.5335639D-01 |
| 1.0308607D-01 | 8.736776 | 6.5984229D-01 |
| 1.0415977D-01 | 8.734549 | 6.6634653D-01 |
| 1.0526888D-01 | 8.732236 | 6.7296138D-01 |
| 1.0638980D-01 | 8.729884 | 6.7975145D-01 |
| 1.0752266D-01 | 8.727494 | 6.8672071D-01 |
| 1.0869261D-01 | 8.725011 | 6.9382532D-01 |
| 1.0990058D-01 | 8.722432 | 7.0093887D-01 |
| 1.1112199D-01 | 8.719808 | 7.0833083D-01 |

TABLE 1-Continued

| Wave Number ($cm^{-1}$) | n | k |
|---|---|---|
| 1.1235697D-01 | 8.717139 | 7.1591612D-01 |
| 1.1363183D-01 | 8.714366 | 7.2363597D-01 |
| 1.1494762D-01 | 8.711486 | 7.3137505D-01 |
| 1.1627866D-01 | 8.708553 | 7.3940119D-01 |
| 1.1765219D-01 | 8.705507 | 7.4756704D-01 |
| 1.1904194D-01 | 8.702404 | 7.5603194D-01 |
| 1.2047585D-01 | 8.699181 | 7.6453988D-01 |
| 1.2195511D-01 | 8.695941 | 7.7326819D-01 |
| 1.2345253D-01 | 8.692637 | 7.8222221D-01 |
| 1.2499712D-01 | 8.689204 | 7.9142569D-01 |
| 1.2659017D-01 | 8.685638 | 8.0073746D-01 |
| 1.2820353D-01 | 8.681999 | 8.1038267D-01 |
| 1.2986736D-01 | 8.678217 | 8.2014406D-01 |
| 1.3158307D-01 | 8.674287 | 8.3021417D-01 |
| 1.3332144D-01 | 8.670273 | 8.4060147D-01 |
| 1.3514501D-01 | 8.666029 | 8.5092277D-01 |
| 1.3699351D-01 | 8.661691 | 8.6176756D-01 |
| 1.3889928D-01 | 8.657181 | 8.7275057D-01 |
| 1.4083156D-01 | 8.652568 | 8.8448433D-01 |
| 1.4285650D-01 | 8.647693 | 8.9596314D-01 |
| 1.4494392D-01 | 8.642623 | 9.0779993D-01 |
| 1.4706184D-01 | 8.637431 | 9.2021677D-01 |
| 1.4924507D-01 | 8.632030 | 9.3280345D-01 |
| 1.5153048D-01 | 8.626323 | 9.4556229D-01 |
| 1.5385089D-01 | 8.620473 | 9.5893715D-01 |
| 1.5624280D-01 | 8.614382 | 9.7272515D-01 |
| 1.5874498D-01 | 8.607948 | 9.8671139D-01 |
| 1.6128724D-01 | 8.601342 | 1.0011292D+00 |
| 1.6394569D-01 | 8.594362 | 1.0159917D+00 |
| 1.6664796D-01 | 8.587191 | 1.0310747D+00 |
| 1.6947280D-01 | 8.579613 | 1.0471048D+00 |
| 1.7242491D-01 | 8.571605 | 1.0628945D+00 |
| 1.7542844D-01 | 8.563363 | 1.0801651D+00 |
| 1.7856651D-01 | 8.554652 | 1.0969584D+00 |
| 1.8180256D-01 | 8.545560 | 1.1150392D+00 |
| 1.8518252D-01 | 8.535947 | 1.1328963D+00 |
| 1.8866876D-01 | 8.526995 | 1.1520999D+00 |
| 1.9230917D-01 | 8.517490 | 1.1710897D+00 |
| 1.9606497D-01 | 8.507814 | 1.1912150D+00 |
| 1.9998619D-01 | 8.497290 | 1.2119652D+00 |
| 2.0407979D-01 | 8.486470 | 1.2330768D+00 |
| 2.0835312D-01 | 8.474673 | 1.2560015D+00 |
| 2.1276491D-01 | 8.462521 | 1.2778802D+00 |
| 2.1737020D-01 | 8.449912 | 1.3022373D+00 |

TABLE 1-Continued

| Wave Number ($cm^{-1}$) | n | k |
|---|---|---|
| 2.2222863D-01 | 8.435660 | 1.3270587D+00 |
| 2.2724796D-01 | 8.420858 | 1.3520419D+00 |
| 2.3254125D-01 | 8.405156 | 1.3781299D+00 |
| 2.3812226D-01 | 8.389151 | 1.4047212D+00 |
| 2.4389337D-01 | 8.371979 | 1.4341354D+00 |
| 2.4997697D-01 | 8.352700 | 1.4631544D+00 |
| 2.5638936D-01 | 8.332788 | 1.4931043D+00 |
| 2.6314796D-01 | 8.311297 | 1.5250713D+00 |
| 2.7027134D-01 | 8.288448 | 1.5570055D+00 |
| 2.7777938D-01 | 8.264599 | 1.5910731D+00 |
| 2.8569326D-01 | 8.238281 | 1.6270097D+00 |
| 2.9410337D-01 | 8.209818 | 1.6629919D+00 |
| 3.0304003D-01 | 8.179843 | 1.7009445D+00 |
| 3.1253596D-01 | 8.147128 | 1.7409654D+00 |
| 3.2255219D-01 | 8.112180 | 1.7811075D+00 |
| 3.3334965D-01 | 8.074469 | 1.8238543D+00 |
| 3.4482600D-01 | 8.033791 | 1.8680571D+00 |
| 3.5710835D-01 | 7.989355 | 1.9142125D+00 |
| 3.7033947D-01 | 7.941322 | 1.9610567D+00 |
| 3.8459178D-01 | 7.889643 | 2.0108985D+00 |
| 4.0003685D-01 | 7.831158 | 2.0639071D+00 |
| 4.1667745D-01 | 7.768902 | 2.1134411D+00 |
| 4.3481048D-01 | 7.701126 | 2.1701519D+00 |
| 4.5456919D-01 | 7.625553 | 2.2242835D+00 |
| 4.7621163D-01 | 7.544423 | 2.2802903D+00 |
| 5.0003453D-01 | 7.455943 | 2.3377074D+00 |
| 5.2625956D-01 | 7.358822 | 2.3965701D+00 |
| 5.5552038D-01 | 7.252419 | 2.4608783D+00 |
| 5.8830156D-01 | 7.135674 | 2.5187795D+00 |
| 6.2502876D-01 | 7.007965 | 2.5756695D+00 |
| 6.6665325D-01 | 6.867192 | 2.6296027D+00 |
| 7.1433183D-01 | 6.711149 | 2.6846653D+00 |
| 7.6930756D-01 | 6.538143 | 2.7333179D+00 |
| 8.3333572D-01 | 6.346035 | 2.7731295D+00 |
| 9.0909653D-01 | 6.131865 | 2.8065976D+00 |
| 1.0000000D+00 | 5.879378 | 2.8300242D+00 |
| 1.0101015D+00 | 5.853423 | 2.8276467D+00 |
| 1.0204083D+00 | 5.827179 | 2.8314972D+00 |
| 1.0309320D+00 | 5.800631 | 2.8350462D+00 |
| 1.0416696D+00 | 5.773802 | 2.8317841D+00 |
| 1.0526403D+00 | 5.746661 | 2.8347198D+00 |
| 1.0638245D+00 | 5.719272 | 2.8308714D+00 |
| 1.0752761D+00 | 5.691521 | 2.8331537D+00 |
| 1.0869511D+00 | 5.663535 | 2.8351768D+00 |

TABLE 1-Continued

| Wave Number ($cm^{-1}$) | n | k |
|---|---|---|
| 1.0989046D+00 | 5.635201 | 2.8302848D+00 |
| 1.1111175D+00 | 5.606586 | 2.8315885D+00 |
| 1.1235955D+00 | 5.577699 | 2.8325667D+00 |
| 1.1363706D+00 | 5.548489 | 2.8331537D+00 |
| 1.1494233D+00 | 5.519027 | 2.8268980D+00 |
| 1.1627866D+00 | 5.489262 | 2.8267679D+00 |
| 1.1764677D+00 | 5.459208 | 2.8262472D+00 |
| 1.1904742D+00 | 5.428878 | 2.8253363D+00 |
| 1.2048140D+00 | 5.398286 | 2.8240354D+00 |
| 1.2195230D+00 | 5.367389 | 2.8157892D+00 |
| 1.2345537D+00 | 5.336323 | 2.8137152D+00 |
| 1.2500000D+00 | 5.304929 | 2.8111249D+00 |
| 1.2659017D+00 | 5.273172 | 2.8079550D+00 |
| 1.2820353D+00 | 5.241539 | 2.8047241D+00 |
| 1.2986736D+00 | 5.209531 | 2.8008519D+00 |
| 1.3158307D+00 | 5.177179 | 2.7963411D+00 |
| 1.3332144D+00 | 5.146161 | 2.7918375D+00 |
| 1.3514501D+00 | 5.116001 | 2.7860579D+00 |
| 1.3699351D+00 | 5.083439 | 2.7866995D+00 |
| 1.3889928D+00 | 5.047771 | 2.7802903D+00 |
| 1.4083156D+00 | 5.013994 | 2.7738958D+00 |
| 1.4285650D+00 | 4.979800 | 2.7662418D+00 |
| 1.4494392D+00 | 4.946351 | 2.7579738D+00 |
| 1.4706184D+00 | 4.915201 | 2.7497306D+00 |
| 1.4924507D+00 | 4.881015 | 2.7471991D+00 |
| 1.5153048D+00 | 4.844068 | 2.7370967D+00 |
| 1.5385089D+00 | 4.811400 | 2.7270314D+00 |
| 1.5624280D+00 | 4.776470 | 2.7226395D+00 |
| 1.5874498D+00 | 4.740422 | 2.7107542D+00 |
| 1.6128724D+00 | 4.704528 | 2.7051425D+00 |
| 1.6394569D+00 | 4.667698 | 2.6920935D+00 |
| 1.6664796D+00 | 4.631138 | 2.6852835D+00 |
| 1.6947280D+00 | 4.593558 | 2.6711000D+00 |
| 1.7242491D+00 | 4.555811 | 2.6618902D+00 |
| 1.7542844D+00 | 4.518750 | 2.6466112D+00 |
| 1.7856651D+00 | 4.482558 | 2.6362716D+00 |
| 1.8180256D+00 | 4.442443 | 2.6253677D+00 |
| 1.8518252D+00 | 4.403706 | 2.6072948D+00 |
| 1.8866876D+00 | 4.367201 | 2.5947179D+00 |
| 1.9230917D+00 | 4.328263 | 2.5810127D+00 |
| 1.9606497D+00 | 4.288766 | 2.5667888D+00 |
| 1.9998619D+00 | 4.248425 | 2.5514681D+00 |
| 2.0407979D+00 | 4.207585 | 2.5350711D+00 |
| 2.0835312D+00 | 4.166540 | 2.5176198D+00 |

TABLE 1-Continued

| Wave Number ($cm^{-1}$) | n | k |
|---|---|---|
| 2.1276491D+00 | 4.125763 | 2.4997130D+00 |
| 2.1737020D+00 | 4.084851 | 2.4807908D+00 |
| 2.2222863D+00 | 4.045111 | 2.4603118D+00 |
| 2.2724796D+00 | 4.003601 | 2.4450635D+00 |
| 2.3254125D+00 | 3.960586 | 2.4226470D+00 |
| 2.3812226D+00 | 3.917021 | 2.4043082D+00 |
| 2.4389337D+00 | 3.873564 | 2.3800723D+00 |
| 2.4997697D+00 | 3.829496 | 2.3598812D+00 |
| 2.5638936D+00 | 3.785136 | 2.3328679D+00 |
| 2.6314796D+00 | 3.741930 | 2.3098839D+00 |
| 2.7027134D+00 | 3.695213 | 2.2855469D+00 |
| 2.7777938D+00 | 3.650102 | 2.2547072D+00 |
| 2.8569326D+00 | 3.607096 | 2.2278715D+00 |
| 2.9410337D+00 | 3.563346 | 2.1993287D+00 |
| 3.0304003D+00 | 3.516889 | 2.1741532D+00 |
| 3.1253596D+00 | 3.468221 | 2.1423486D+00 |
| 3.2255219D+00 | 3.422465 | 2.1095516D+00 |
| 3.3334965D+00 | 3.374610 | 2.0791707D+00 |
| 3.4482600D+00 | 3.326631 | 2.0426321D+00 |
| 3.5710835D+00 | 3.279470 | 2.0090472D+00 |
| 3.7033947D+00 | 3.228984 | 1.9732865D+00 |
| 3.8459178D+00 | 3.179887 | 1.9310350D+00 |
| 4.0003685D+00 | 3.133464 | 1.8909940D+00 |
| 4.1667745D+00 | 3.084049 | 1.8534896D+00 |
| 4.3481048D+00 | 3.032401 | 1.8092148D+00 |
| 4.5456919D+00 | 2.983258 | 1.7627476D+00 |
| 4.7621163D+00 | 2.933900 | 1.7178694D+00 |
| 5.0003453D+00 | 2.881863 | 1.6702833D+00 |
| 5.2625956D+00 | 2.831974 | 1.6165537D+00 |
| 5.5552038D+00 | 2.781861 | 1.5670763D+00 |
| 5.8830156D+00 | 2.729264 | 1.5107414D+00 |
| 6.2502876D+00 | 2.679108 | 1.4517443D+00 |
| 6.6665325D+00 | 2.629097 | 1.3928044D+00 |
| 7.1433183D+00 | 2.577344 | 1.3301179D+00 |
| 7.6930756D+00 | 2.527536 | 1.2609276D+00 |
| 8.3329735D+00 | 2.481153 | 1.1912150D+00 |
| 9.0907560D+00 | 2.436760 | 1.1199281D+00 |
| 1.0000000D+01 | 2.399111 | 1.0418139D+00 |
| 1.0519619D+01 | 2.385313 | 1.0110908D+00 |
| 1.1117317D+01 | 2.363856 | 9.8353573D-01 |
| 1.1776060D+01 | 2.337241 | 9.5014556D-01 |
| 1.2502590D+01 | 2.312599 | 9.1157025D-01 |
| 1.3335214D+01 | 2.290196 | 8.7254964D-01 |
| 1.4288940D+01 | 2.270109 | 8.3136195D-01 |

TABLE 1-Continued

| Wave Number ($cm^{-1}$) | n | k |
|---|---|---|
| 1.5381546D+01 | 2.254575 | 7.9211848D-01 |
| 1.6672472D+01 | 2.236685 | 7.6171085D-01 |
| 1.7258379D+01 | 2.228339 | 7.4780806D-01 |
| 1.7864876D+01 | 2.220374 | 7.3585144D-01 |
| 1.8535316D+01 | 2.210869 | 7.2408599D-01 |
| 1.9230917D+01 | 2.200349 | 7.1250865D-01 |
| 1.9998619D+01 | 2.188736 | 6.9950391D-01 |
| 2.0844909D+01 | 2.177335 | 6.8515707D-01 |
| 2.1727012D+01 | 2.166254 | 6.7265154D-01 |
| 2.2750974D+01 | 2.153213 | 6.5885545D-01 |
| 2.3823195D+01 | 2.139507 | 6.4534232D-01 |
| 2.5003454D+01 | 2.125742 | 6.2920207D-01 |
| 2.6302680D+01 | 2.112811 | 6.1346550D-01 |
| 2.7797133D+01 | 2.099543 | 5.9674686D-01 |
| 2.9444216D+01 | 2.086956 | 5.8048385D-01 |
| 3.1260794D+01 | 2.073976 | 5.6596574D-01 |
| 3.3342641D+01 | 2.059773 | 5.5054160D-01 |
| 3.4514374D+01 | 2.052476 | 5.4298789D-01 |
| 3.5727284D+01 | 2.045135 | 5.3553782D-01 |
| 3.7068072D+01 | 2.037243 | 5.2818996D-01 |
| 3.8459178D+01 | 2.029224 | 5.2094292D-01 |
| 3.9994475D+01 | 2.020318 | 5.1379532D-01 |
| 4.1686938D+01 | 2.010446 | 5.0558030D-01 |
| 4.3451022D+01 | 2.001418 | 4.9635242D-01 |
| 4.5498806D+01 | 1.992287 | 4.8729297D-01 |
| 4.7643099D+01 | 1.983438 | 4.7839887D-01 |
| 5.0003453D+01 | 1.974559 | 4.6966710D-01 |
| 5.2601727D+01 | 1.965156 | 4.6109471D-01 |
| 5.5590426D+01 | 1.955736 | 4.5059892D-01 |
| 5.8884366D+01 | 1.948419 | 4.4034203D-01 |
| 6.2517269D+01 | 1.941655 | 4.3330145D-01 |
| 6.6680677D+01 | 1.934154 | 4.2637344D-01 |
| 7.1449633D+01 | 1.927412 | 4.2052338D-01 |
| 7.6913044D+01 | 1.919973 | 4.1859125D-01 |
| 8.3368118D+01 | 1.911671 | 4.1666800D-01 |
| 9.0991327D+01 | 1.907505 | 4.1762851D-01 |
| 1.0000000D+02 | 1.899131 | 4.3831885D-01 |
| 1.0209395D+02 | 1.895435 | 4.4339434D-01 |
| 1.0423174D+02 | 1.891384 | 4.4852860D-01 |
| 1.0641430D+02 | 1.886330 | 4.5476826D-01 |
| 1.0864256D+02 | 1.880545 | 4.6003423D-01 |
| 1.1117317D+02 | 1.874242 | 4.6536117D-01 |
| 1.1376273D+02 | 1.867327 | 4.7183499D-01 |
| 1.1641260D+02 | 1.859854 | 4.7729858D-01 |

TABLE 1-Continued

| Wave Number ($cm^{-1}$) | n | k |
|---|---|---|
| 1.1912420D+02 | 1.851943 | 4.8393847D-01 |
| 1.2189896D+02 | 1.842330 | 4.9067072D-01 |
| 1.2502590D+02 | 1.830882 | 4.9635242D-01 |
| 1.2823306D+02 | 1.819110 | 5.0209991D-01 |
| 1.3152248D+02 | 1.805539 | 5.0791395D-01 |
| 1.3520726D+02 | 1.790800 | 5.1025838D-01 |
| 1.3899526D+02 | 1.777162 | 5.1379532D-01 |
| 1.4288940D+02 | 1.762824 | 5.1735678D-01 |
| 1.4689263D+02 | 1.747333 | 5.2094292D-01 |
| 1.5135612D+02 | 1.729441 | 5.2334749D-01 |
| 1.5631476D+02 | 1.709762 | 5.2455393D-01 |
| 1.6143586D+02 | 1.690223 | 5.2455393D-01 |
| 1.6672472D+02 | 1.669053 | 5.2576315D-01 |
| 1.7258379D+02 | 1.643739 | 5.2334749D-01 |
| 1.7864876D+02 | 1.619157 | 5.1616689D-01 |
| 1.8535316D+02 | 1.594131 | 5.0791395D-01 |
| 1.9230917D+02 | 1.567492 | 4.9749663D-01 |
| 1.9998619D+02 | 1.542270 | 4.7729858D-01 |
| 2.0417379D+02 | 1.531473 | 4.6750918D-01 |
| 2.0844909D+02 | 1.520272 | 4.5792056D-01 |
| 2.1281390D+02 | 1.508821 | 4.4646780D-01 |
| 2.1727012D+02 | 1.499424 | 4.3230489D-01 |
| 2.2233099D+02 | 1.491543 | 4.1762851D-01 |
| 2.2750974D+02 | 1.485266 | 4.0252248D-01 |
| 2.3280913D+02 | 1.480747 | 3.8796285D-01 |
| 2.3823195D+02 | 1.477194 | 3.7392986D-01 |
| 2.4378108D+02 | 1.475642 | 3.5874854D-01 |
| 2.5003454D+02 | 1.476571 | 3.4418358D-01 |
| 2.5644840D+02 | 1.478232 | 3.3173412D-01 |
| 2.6302680D+02 | 1.481006 | 3.1899960D-01 |
| 2.7039584D+02 | 1.486740 | 3.0675394D-01 |
| 2.7797133D+02 | 1.492960 | 2.9908191D-01 |
| 2.8575905D+02 | 1.498932 | 2.9160176D-01 |
| 2.9444216D+02 | 1.505906 | 2.8627943D-01 |
| 3.0269134D+02 | 1.511879 | 2.8300242D-01 |
| 3.1260794D+02 | 1.519076 | 2.7976291D-01 |
| 3.2284941D+02 | 1.527225 | 2.7911948D-01 |
| 3.3342641D+02 | 1.535500 | 2.8170214D-01 |
| 3.4514374D+02 | 1.542658 | 2.8892834D-01 |
| 3.5727284D+02 | 1.546272 | 2.9908191D-01 |
| 3.7068072D+02 | 1.546670 | 3.1030598D-01 |
| 3.8459178D+02 | 1.544080 | 3.2269344D-01 |
| 3.9994475D+02 | 1.537967 | 3.3557542D-01 |
| 4.1686938D+02 | 1.529309 | 3.4816903D-01 |

TABLE 1-Continued

| Wave Number ($cm^{-1}$) | n | k |
|---|---|---|
| 4.3451022D+02 | 1.516402 | 3.6290265D-01 |
| 4.5498806D+02 | 1.499422 | 3.7221181D-01 |
| 4.7643099D+02 | 1.483693 | 3.8175976D-01 |
| 5.0003453D+02 | 1.467642 | 3.9335995D-01 |
| 5.0118723D+02 | 1.467249 | 3.9426674D-01 |
| 5.0234259D+02 | 1.467000 | 3.9517562D-01 |
| 5.0350061D+02 | 1.466543 | 3.9699967D-01 |
| 5.0466130D+02 | 1.465400 | 3.9883214D-01 |
| 5.0582466D+02 | 1.463349 | 4.0067306D-01 |
| 5.0815944D+02 | 1.460391 | 4.0067306D-01 |
| 5.0933087D+02 | 1.459690 | 4.0159671D-01 |
| 5.1050500D+02 | 1.458719 | 4.0252248D-01 |
| 5.1168184D+02 | 1.457713 | 4.0345039D-01 |
| 5.1286138D+02 | 1.456898 | 4.0438044D-01 |
| 5.1404365D+02 | 1.455604 | 4.0624698D-01 |
| 5.1522864D+02 | 1.453825 | 4.0718347D-01 |
| 5.1641637D+02 | 1.452188 | 4.0812213D-01 |
| 5.1760683D+02 | 1.450255 | 4.0906295D-01 |
| 5.1999600D+02 | 1.447502 | 4.0906295D-01 |
| 5.2119471D+02 | 1.446666 | 4.1000594D-01 |
| 5.2239619D+02 | 1.445486 | 4.1095110D-01 |
| 5.2360044D+02 | 1.444197 | 4.1189844D-01 |
| 5.2480746D+02 | 1.442846 | 4.1284796D-01 |
| 5.2601727D+02 | 1.441618 | 4.1379967D-01 |
| 5.2722986D+02 | 1.439563 | 4.1570969D-01 |
| 5.2966344D+02 | 1.435881 | 4.1570969D-01 |
| 5.3088444D+02 | 1.434643 | 4.1666800D-01 |
| 5.3210826D+02 | 1.432797 | 4.1762851D-01 |
| 5.3333490D+02 | 1.431240 | 4.1762851D-01 |
| 5.3456436D+02 | 1.429982 | 4.1859125D-01 |
| 5.3579666D+02 | 1.428308 | 4.1955620D-01 |
| 5.3703180D+02 | 1.426178 | 4.2052338D-01 |
| 5.3951062D+02 | 1.422820 | 4.2052338D-01 |
| 5.4075432D+02 | 1.421557 | 4.2149278D-01 |
| 5.4200089D+02 | 1.419809 | 4.2246442D-01 |
| 5.4325033D+02 | 1.417548 | 4.2343831D-01 |
| 5.4450265D+02 | 1.415276 | 4.2343831D-01 |
| 5.4701596D+02 | 1.412092 | 4.2343831D-01 |
| 5.4827696D+02 | 1.410419 | 4.2441443D-01 |
| 5.4954087D+02 | 1.408657 | 4.2441443D-01 |
| 5.5080770D+02 | 1.406786 | 4.2539281D-01 |
| 5.5207744D+02 | 1.404604 | 4.2539281D-01 |
| 5.5462571D+02 | 1.401123 | 4.2539281D-01 |
| 5.5590426D+02 | 1.399826 | 4.2539281D-01 |

TABLE 1-Continued

| Wave Number ($cm^{-1}$) | n | k |
|---|---|---|
| 5.5718575D+02 | 1.398169 | 4.2637344D-01 |
| 5.5847019D+02 | 1.396377 | 4.2637344D-01 |
| 5.5975760D+02 | 1.394313 | 4.2735633D-01 |
| 5.6234133D+02 | 1.390838 | 4.2637344D-01 |
| 5.6363766D+02 | 1.389417 | 4.2735633D-01 |
| 5.6493697D+02 | 1.387734 | 4.2735633D-01 |
| 5.6623929D+02 | 1.385875 | 4.2834149D-01 |
| 5.6754461D+02 | 1.383660 | 4.2834149D-01 |
| 5.7016427D+02 | 1.380029 | 4.2834149D-01 |
| 5.7147864D+02 | 1.378598 | 4.2834149D-01 |
| 5.7279603D+02 | 1.376758 | 4.2932892D-01 |
| 5.7411646D+02 | 1.374519 | 4.2932892D-01 |
| 5.7676646D+02 | 1.370751 | 4.2932892D-01 |
| 5.7809605D+02 | 1.369211 | 4.2932892D-01 |
| 5.7942870D+02 | 1.367219 | 4.3031862D-01 |
| 5.8076442D+02 | 1.364655 | 4.3031862D-01 |
| 5.8344510D+02 | 1.361083 | 4.2932892D-01 |
| 5.8479008D+02 | 1.359301 | 4.3031862D-01 |
| 5.8613816D+02 | 1.356772 | 4.3031862D-01 |
| 5.8884366D+02 | 1.352834 | 4.2932892D-01 |
| 5.9020108D+02 | 1.351233 | 4.2932892D-01 |
| 5.9156163D+02 | 1.349696 | 4.2932892D-01 |
| 5.9292532D+02 | 1.347481 | 4.3031862D-01 |
| 5.9566214D+02 | 1.342949 | 4.2932892D-01 |
| 5.9703529D+02 | 1.341074 | 4.2932892D-01 |
| 5.9841160D+02 | 1.338869 | 4.2932892D-01 |
| 6.0117374D+02 | 1.334869 | 4.2834149D-01 |
| 6.0255959D+02 | 1.333056 | 4.2834149D-01 |
| 6.0394863D+02 | 1.330870 | 4.2834149D-01 |
| 6.0673633D+02 | 1.326773 | 4.2735633D-01 |
| 6.0813500D+02 | 1.324631 | 4.2735633D-01 |
| 6.0953690D+02 | 1.322675 | 4.2637344D-01 |
| 6.1094202D+02 | 1.320901 | 4.2637344D-01 |
| 6.1376201D+02 | 1.317122 | 4.2539281D-01 |
| 6.1517687D+02 | 1.315327 | 4.2539281D-01 |
| 6.1659500D+02 | 1.313112 | 4.2539281D-01 |
| 6.1944108D+02 | 1.308540 | 4.2441443D-01 |
| 6.2086903D+02 | 1.306556 | 4.2343831D-01 |
| 6.2373484D+02 | 1.303145 | 4.2246442D-01 |
| 6.2517269D+02 | 1.301310 | 4.2246442D-01 |
| 6.2661386D+02 | 1.298872 | 4.2246442D-01 |
| 6.2950618D+02 | 1.294706 | 4.2052338D-01 |
| 6.3095734D+02 | 1.292723 | 4.2052338D-01 |
| 6.3241185D+02 | 1.290576 | 4.1955620D-01 |

TABLE 1-Continued

| Wave Number ($cm^{-1}$) | n | k |
|---|---|---|
| 6.3533093D+02 | 1.286576 | 4.1859125D-01 |
| 6.3679552D+02 | 1.284709 | 4.1762851D-01 |
| 6.3826349D+02 | 1.282639 | 4.1762851D-01 |
| 6.4120958D+02 | 1.278233 | 4.1570969D-01 |
| 6.4268772D+02 | 1.276473 | 4.1475358D-01 |
| 6.4565423D+02 | 1.272559 | 4.1379967D-01 |
| 6.4714262D+02 | 1.270391 | 4.1284796D-01 |
| 6.4863443D+02 | 1.268440 | 4.1189844D-01 |
| 6.5162839D+02 | 1.265082 | 4.1000594D-01 |
| 6.5313055D+02 | 1.263173 | 4.1000594D-01 |
| 6.5614527D+02 | 1.258880 | 4.0812213D-01 |
| 6.5765784D+02 | 1.256977 | 4.0718347D-01 |
| 6.6069345D+02 | 1.253631 | 4.0531264D-01 |
| 6.6221650D+02 | 1.251704 | 4.0531264D-01 |
| 6.6374307D+02 | 1.249380 | 4.0438044D-01 |
| 6.6680677D+02 | 1.245318 | 4.0252248D-01 |
| 6.6834392D+02 | 1.243348 | 4.0159671D-01 |
| 6.7142885D+02 | 1.239445 | 3.9975154D-01 |
| 6.7297666D+02 | 1.237500 | 3.9883214D-01 |
| 6.7608298D+02 | 1.233597 | 3.9699967D-01 |
| 6.7764151D+02 | 1.231631 | 3.9608659D-01 |
| 6.8076936D+02 | 1.227627 | 3.9426674D-01 |
| 6.8233869D+02 | 1.225566 | 3.9335995D-01 |
| 6.8548823D+02 | 1.220973 | 3.9155263D-01 |
| 6.8706844D+02 | 1.218762 | 3.8975361D-01 |
| 6.9023980D+02 | 1.215328 | 3.8707056D-01 |
| 6.9183097D+02 | 1.213645 | 3.8618032D-01 |
| 6.9502432D+02 | 1.209428 | 3.8440599D-01 |
| 6.9662651D+02 | 1.207465 | 3.8263980D-01 |
| 6.9984200D+02 | 1.203552 | 3.8088173D-01 |
| 7.0145530D+02 | 1.201594 | 3.7913174D-01 |
| 7.0469307D+02 | 1.197623 | 3.7738979D-01 |
| 7.0631755D+02 | 1.195603 | 3.7565584D-01 |
| 7.0957777D+02 | 1.191399 | 3.7392986D-01 |
| 7.1121351D+02 | 1.189086 | 3.7221181D-01 |
| 7.1449633D+02 | 1.184740 | 3.6964952D-01 |
| 7.1614341D+02 | 1.182458 | 3.6795113D-01 |
| 7.1944898D+02 | 1.178513 | 3.6457774D-01 |
| 7.2276980D+02 | 1.174089 | 3.6206800D-01 |
| 7.2443596D+02 | 1.172049 | 3.5957554D-01 |
| 7.2777980D+02 | 1.167947 | 3.5710024D-01 |
| 7.2945751D+02 | 1.165763 | 3.5464198D-01 |
| 7.3282453D+02 | 1.161869 | 3.5139060D-01 |
| 7.3451387D+02 | 1.160150 | 3.4897165D-01 |

TABLE 1-Continued

| Wave Number ($cm^{-1}$) | n | k |
|---|---|---|
| 7.3790423D+02 | 1.156338 | 3.4656934D-01 |
| 7.4131024D+02 | 1.151643 | 3.4260220D-01 |
| 7.4301914D+02 | 1.149628 | 3.4024374D-01 |
| 7.4644876D+02 | 1.145850 | 3.3634900D-01 |
| 7.4989421D+02 | 1.141428 | 3.3249885D-01 |
| 7.5162289D+02 | 1.139515 | 3.2945048D-01 |
| 7.5509223D+02 | 1.135773 | 3.2567929D-01 |
| 7.5683290D+02 | 1.133825 | 3.2269344D-01 |
| 7.6032628D+02 | 1.130583 | 3.1826592D-01 |
| 7.6383578D+02 | 1.126485 | 3.1389915D-01 |
| 7.6559661D+02 | 1.124841 | 3.1030598D-01 |
| 7.6913044D+02 | 1.122067 | 3.0604842D-01 |
| 7.7268059D+02 | 1.118262 | 3.0115505D-01 |
| 7.7446180D+02 | 1.116753 | 2.9770775D-01 |
| 7.7803655D+02 | 1.114243 | 2.9294773D-01 |
| 7.8162780D+02 | 1.110319 | 2.8826382D-01 |
| 7.8342964D+02 | 1.108999 | 2.8365480D-01 |
| 7.8704579D+02 | 1.107403 | 2.7911948D-01 |
| 7.9067863D+02 | 1.104624 | 2.7402497D-01 |
| 7.9432823D+02 | 1.100816 | 2.6902345D-01 |
| 7.9615935D+02 | 1.099603 | 2.6411322D-01 |
| 7.9983426D+02 | 1.098011 | 2.5929261D-01 |
| 8.0352612D+02 | 1.095643 | 2.5280761D-01 |
| 8.0723503D+02 | 1.092375 | 2.4762252D-01 |
| 8.0909590D+02 | 1.091270 | 2.4198595D-01 |
| 8.1283052D+02 | 1.090913 | 2.3593379D-01 |
| 8.1658237D+02 | 1.089721 | 2.2950394D-01 |
| 8.2035154D+02 | 1.087212 | 2.2376396D-01 |
| 8.2224265D+02 | 1.086723 | 2.1766577D-01 |
| 8.2603795D+02 | 1.087993 | 2.1124680D-01 |
| 8.2985077D+02 | 1.087926 | 2.0548974D-01 |
| 8.3368118D+02 | 1.087480 | 1.9897117D-01 |
| 8.3752928D+02 | 1.086163 | 1.9265937D-01 |
| 8.3945999D+02 | 1.086474 | 1.8654781D-01 |
| 8.4333476D+02 | 1.089062 | 1.8021467D-01 |
| 8.4722741D+02 | 1.090622 | 1.7409654D-01 |
| 8.5113804D+02 | 1.092339 | 1.6779930D-01 |
| 8.5506671D+02 | 1.094339 | 1.6210266D-01 |
| 8.5901352D+02 | 1.096068 | 1.5696042D-01 |
| 8.6297855D+02 | 1.096584 | 1.5198130D-01 |
| 8.6496792D+02 | 1.097503 | 1.4716012D-01 |
| 8.6896043D+02 | 1.100705 | 1.4216417D-01 |
| 8.7297137D+02 | 1.103057 | 1.3702195D-01 |
| 8.7700082D+02 | 1.105361 | 1.3206573D-01 |

TABLE 1-Continued

| Wave Number ($cm^{-1}$) | n | k |
|---|---|---|
| 8.8104887D+02 | 1.107674 | 1.2699603D-01 |
| 8.8511561D+02 | 1.110334 | 1.2184007D-01 |
| 8.8920112D+02 | 1.113289 | 1.1716291D-01 |
| 8.9330548D+02 | 1.116059 | 1.1292501D-01 |
| 8.9742879D+02 | 1.118841 | 1.0834033D-01 |
| 9.0157114D+02 | 1.122010 | 1.0394178D-01 |
| 9.0573260D+02 | 1.125466 | 9.9951690D-02 |
| 9.0991327D+02 | 1.128640 | 9.6781009D-02 |
| 9.1411324D+02 | 1.131445 | 9.3280345D-02 |
| 9.1833260D+02 | 1.134419 | 8.9699525D-02 |
| 9.2257143D+02 | 1.137372 | 8.6455006D-02 |
| 9.2682982D+02 | 1.140345 | 8.2944987D-02 |
| 9.3110788D+02 | 1.143601 | 7.9577473D-02 |
| 9.3540567D+02 | 1.146959 | 7.6522675D-02 |
| 9.3972331D+02 | 1.150368 | 7.3585144D-02 |
| 9.4406088D+02 | 1.153843 | 7.0923497D-02 |
| 9.4841846D+02 | 1.157248 | 6.8515707D-02 |
| 9.5279616D+02 | 1.160584 | 6.6189659D-02 |
| 9.5719407D+02 | 1.163960 | 6.3942578D-02 |
| 9.6161228D+02 | 1.167354 | 6.1914183D-02 |
| 9.6605088D+02 | 1.170827 | 5.9950132D-02 |
| 9.7050997D+02 | 1.174182 | 5.8450757D-02 |
| 9.7498964D+02 | 1.178360 | 5.6336536D-02 |
| 9.7948999D+02 | 1.180893 | 5.8048385D-02 |
| 9.8627949D+02 | 1.183900 | 5.3800975D-02 |
| 9.9083194D+02 | 1.187365 | 5.2697516D-02 |
| 9.9540542D+02 | 1.190334 | 5.1735678D-02 |
| 1.0000000D+03 | 1.193164 | 5.0791395D-02 |
| 1.0046158D+03 | 1.195932 | 4.9979297D-02 |
| 1.0092529D+03 | 1.198600 | 4.9293555D-02 |
| 1.0162487D+03 | 1.202228 | 4.8505406D-02 |
| 1.0209395D+03 | 1.204471 | 4.7839887D-02 |
| 1.0256519D+03 | 1.206729 | 4.7183499D-02 |
| 1.0303861D+03 | 1.208909 | 4.6643394D-02 |
| 1.0351422D+03 | 1.211068 | 4.6003423D-02 |
| 1.0423174D+03 | 1.214136 | 4.5372232D-02 |
| 1.0471285D+03 | 1.216115 | 4.4749702D-02 |
| 1.0519619D+03 | 1.218113 | 4.4339434D-02 |
| 1.0592537D+03 | 1.220909 | 4.3731074D-02 |
| 1.0641430D+03 | 1.222699 | 4.3330145D-02 |
| 1.0690549D+03 | 1.224439 | 4.2932892D-02 |
| 1.0764652D+03 | 1.226967 | 4.2343831D-02 |
| 1.0814340D+03 | 1.228589 | 4.1955620D-02 |
| 1.0864256D+03 | 1.230259 | 4.1475358D-02 |

TABLE 1-Continued

| Wave Number ($cm^{-1}$) | n | k |
|---|---|---|
| 1.0939564D+03 | 1.232659 | 4.1095110D-02 |
| 1.0990058D+03 | 1.234142 | 4.0718347D-02 |
| 1.1040786D+03 | 1.235657 | 4.0345039D-02 |
| 1.1117317D+03 | 1.237862 | 3.9883214D-02 |
| 1.1168632D+03 | 1.239322 | 3.9517562D-02 |
| 1.1246050D+03 | 1.241424 | 3.9155263D-02 |
| 1.1297959D+03 | 1.242789 | 3.8796285D-02 |
| 1.1376273D+03 | 1.244791 | 3.8440599D-02 |
| 1.1428783D+03 | 1.246095 | 3.8088173D-02 |
| 1.1481536D+03 | 1.247433 | 3.7825976D-02 |
| 1.1561122D+03 | 1.249353 | 3.7479185D-02 |
| 1.1641260D+03 | 1.251193 | 3.7135574D-02 |
| 1.1694994D+03 | 1.252405 | 3.6879935D-02 |
| 1.1776060D+03 | 1.254220 | 3.6541817D-02 |
| 1.1830416D+03 | 1.255384 | 3.6373923D-02 |
| 1.1912420D+03 | 1.257072 | 3.6040445D-02 |
| 1.1967405D+03 | 1.258240 | 3.5792344D-02 |
| 1.2050359D+03 | 1.259903 | 3.5627893D-02 |
| 1.2133889D+03 | 1.261488 | 3.5301255D-02 |
| 1.2189896D+03 | 1.262564 | 3.5139060D-02 |
| 1.2274392D+03 | 1.264125 | 3.4897165D-02 |
| 1.2359474D+03 | 1.265652 | 3.4656934D-02 |
| 1.2416523D+03 | 1.266657 | 3.4497700D-02 |
| 1.2502590D+03 | 1.268163 | 3.4260220D-02 |
| 1.2589254D+03 | 1.269613 | 3.4102808D-02 |
| 1.2647363D+03 | 1.270543 | 3.3946120D-02 |
| 1.2735031D+03 | 1.271952 | 3.3712437D-02 |
| 1.2823306D+03 | 1.273363 | 3.3480362D-02 |
| 1.2912193D+03 | 1.274794 | 3.3249885D-02 |
| 1.3001696D+03 | 1.276220 | 3.3097115D-02 |
| 1.3061709D+03 | 1.277123 | 3.3020994D-02 |
| 1.3152248D+03 | 1.278508 | 3.2793679D-02 |
| 1.3243415D+03 | 1.279895 | 3.2718256D-02 |
| 1.3335214D+03 | 1.281248 | 3.2567929D-02 |
| 1.3427650D+03 | 1.282606 | 3.2493025D-02 |
| 1.3520726D+03 | 1.283912 | 3.2418293D-02 |
| 1.3614447D+03 | 1.285242 | 3.2269344D-02 |
| 1.3708818D+03 | 1.286624 | 3.2195127D-02 |
| 1.3803843D+03 | 1.287944 | 3.2195127D-02 |
| 1.3899526D+03 | 1.289296 | 3.2047204D-02 |
| 1.3995873D+03 | 1.290696 | 3.2047204D-02 |
| 1.4092888D+03 | 1.292093 | 3.1973497D-02 |
| 1.4190575D+03 | 1.293609 | 3.1899960D-02 |
| 1.4288940D+03 | 1.295193 | 3.1973497D-02 |

TABLE 1-Continued

| Wave Number ($cm^{-1}$) | n | k |
|---|---|---|
| 1.4387986D+03 | 1.296751 | 3.2121080D-02 |
| 1.4487719D+03 | 1.298382 | 3.2195127D-02 |
| 1.4588143D+03 | 1.300125 | 3.2418293D-02 |
| 1.4689263D+03 | 1.301901 | 3.2718256D-02 |
| 1.4825181D+03 | 1.304521 | 3.3097115D-02 |
| 1.4927944D+03 | 1.306716 | 3.3712437D-02 |
| 1.5031420D+03 | 1.309021 | 3.4497700D-02 |
| 1.5135612D+03 | 1.311404 | 3.5627893D-02 |
| 1.5275661D+03 | 1.314837 | 3.7306984D-02 |
| 1.5381546D+03 | 1.317726 | 3.9245525D-02 |
| 1.5488166D+03 | 1.320468 | 4.1762851D-02 |
| 1.5631476D+03 | 1.325038 | 4.4852860D-02 |
| 1.5739829D+03 | 1.329242 | 4.9521084D-02 |
| 1.5885467D+03 | 1.335754 | 5.6988883D-02 |
| 1.5995580D+03 | 1.339863 | 6.9468855D-02 |
| 1.6143586D+03 | 1.341605 | 8.7859786D-02 |
| 1.6255488D+03 | 1.330121 | 1.1716291D-01 |
| 1.6405898D+03 | 1.295314 | 1.3085495D-01 |
| 1.6519618D+03 | 1.268459 | 1.2496550D-01 |
| 1.6672472D+03 | 1.242862 | 1.0685384D-01 |
| 1.6788040D+03 | 1.231892 | 8.6455006D-02 |
| 1.6943378D+03 | 1.229289 | 6.2199965D-02 |
| 1.7100153D+03 | 1.234896 | 4.3230489D-02 |
| 1.7258379D+03 | 1.242239 | 3.2945048D-02 |
| 1.7378008D+03 | 1.248370 | 2.4819335D-02 |
| 1.7538805D+03 | 1.256584 | 2.0313752D-02 |
| 1.7701090D+03 | 1.262994 | 1.6587852D-02 |
| 1.7864876D+03 | 1.268802 | 1.4183720D-02 |
| 1.8030177D+03 | 1.273883 | 1.2583172D-02 |
| 1.8197009D+03 | 1.278291 | 1.1582176D-02 |
| 1.8365383D+03 | 1.282194 | 1.0784255D-02 |
| 1.8535316D+03 | 1.285729 | 1.0298883D-02 |
| 1.8706821D+03 | 1.289015 | 9.8807553D-03 |
| 1.8879913D+03 | 1.292117 | 9.7901680D-03 |
| 1.9054607D+03 | 1.294933 | 9.9035328D-03 |
| 1.9230917D+03 | 1.297550 | 1.0110908D-02 |
| 1.9408859D+03 | 1.299910 | 1.0611827D-02 |
| 1.9588447D+03 | 1.301965 | 1.1111947D-02 |
| 1.9815270D+03 | 1.304258 | 1.1797504D-02 |
| 1.9998619D+03 | 1.305885 | 1.2410525D-02 |
| 2.0183664D+03 | 1.307228 | 1.3115660D-02 |
| 2.0417379D+03 | 1.308720 | 1.3702195D-02 |
| 2.0606299D+03 | 1.309721 | 1.4414187D-02 |
| 2.0844909D+03 | 1.310657 | 1.4989603D-02 |

TABLE 1-Continued

| Wave Number ($cm^{-1}$) | n | k |
|---|---|---|
| 2.1037784D+03 | 1.311148 | 1.5516371D-02 |
| 2.1281390D+03 | 1.311451 | 1.5696042D-02 |
| 2.1527817D+03 | 1.311588 | 1.5480684D-02 |
| 2.1727012D+03 | 1.311785 | 1.4716012D-02 |
| 2.1978599D+03 | 1.312483 | 1.3607870D-02 |
| 2.2233099D+03 | 1.313587 | 1.2381981D-02 |
| 2.2490546D+03 | 1.314920 | 1.1396989D-02 |
| 2.2750974D+03 | 1.316398 | 1.0298883D-02 |
| 2.3014418D+03 | 1.318113 | 9.3065806D-03 |
| 2.3280913D+03 | 1.319948 | 8.4487049D-03 |
| 2.3550493D+03 | 1.321906 | 7.5995897D-03 |
| 2.3823195D+03 | 1.323997 | 6.8831961D-03 |
| 2.4099054D+03 | 1.326183 | 6.2199965D-03 |
| 2.4378108D+03 | 1.328504 | 5.6206966D-03 |
| 2.4717241D+03 | 1.331403 | 5.0674578D-03 |
| 2.5003454D+03 | 1.333929 | 4.6003423D-03 |
| 2.5292980D+03 | 1.336658 | 4.1570969D-03 |
| 2.5644840D+03 | 1.340174 | 3.8000573D-03 |
| 2.6001596D+03 | 1.343958 | 3.5301255D-03 |
| 2.6302680D+03 | 1.347393 | 3.4024374D-03 |
| 2.6668587D+03 | 1.351891 | 3.4024374D-03 |
| 2.7039584D+03 | 1.356937 | 3.5957554D-03 |
| 2.7415742D+03 | 1.362546 | 4.2343831D-03 |
| 2.7797133D+03 | 1.368863 | 5.1497974D-03 |
| 2.8183829D+03 | 1.376092 | 6.7887551D-03 |
| 2.8575905D+03 | 1.384213 | 9.3926933D-03 |
| 2.8973436D+03 | 1.393260 | 1.3206573D-02 |
| 2.9444216D+03 | 1.404875 | 1.9489026D-02 |
| 2.9853826D+03 | 1.417064 | 2.6108994D-02 |
| 3.0269134D+03 | 1.432585 | 3.6879935D-02 |
| 3.0760968D+03 | 1.449409 | 6.1064688D-02 |
| 3.1260794D+03 | 1.461522 | 9.2425146D-02 |
| 3.1768741D+03 | 1.466753 | 1.3483112D-01 |
| 3.2284941D+03 | 1.452013 | 1.9177418D-01 |
| 3.2809529D+03 | 1.411876 | 2.3976741D-01 |
| 3.3342641D+03 | 1.352917 | 2.7213860D-01 |
| 3.3496544D+03 | 1.334533 | 2.7213860D-01 |
| 3.3573761D+03 | 1.326310 | 2.7592442D-01 |
| 3.3728731D+03 | 1.307891 | 2.7847752D-01 |
| 3.3806484D+03 | 1.297762 | 2.8170214D-01 |
| 3.3884416D+03 | 1.285942 | 2.8235153D-01 |
| 3.4040819D+03 | 1.263935 | 2.8040783D-01 |
| 3.4119291D+03 | 1.252073 | 2.7976291D-01 |
| 3.4197944D+03 | 1.240033 | 2.7592442D-01 |

TABLE 1-Continued

| Wave Number ($cm^{-1}$) | n | k |
|---|---|---|
| 3.4276779D+03 | 1.229654 | 2.7151270D-01 |
| 3.4434993D+03 | 1.208002 | 2.6472207D-01 |
| 3.4514374D+03 | 1.195889 | 2.5810127D-01 |
| 3.4593938D+03 | 1.185419 | 2.4933896D-01 |
| 3.4673685D+03 | 1.178446 | 2.3921596D-01 |
| 3.4833732D+03 | 1.162372 | 2.2897609D-01 |
| 3.4914032D+03 | 1.152284 | 2.1816754D-01 |
| 3.4994517D+03 | 1.145545 | 2.0596344D-01 |
| 3.5075187D+03 | 1.142386 | 1.9399482D-01 |
| 3.5237087D+03 | 1.133346 | 1.7980019D-01 |
| 3.5318317D+03 | 1.127523 | 1.6702833D-01 |
| 3.5399734D+03 | 1.125351 | 1.5409557D-01 |
| 3.5481339D+03 | 1.125532 | 1.4216417D-01 |
| 3.5563132D+03 | 1.128413 | 1.3115660D-01 |
| 3.5727284D+03 | 1.129478 | 1.2100133D-01 |
| 3.5809644D+03 | 1.127558 | 1.1188971D-01 |
| 3.5892193D+03 | 1.127959 | 1.0204463D-01 |
| 3.5974934D+03 | 1.130913 | 9.2851761D-02 |
| 3.6140986D+03 | 1.132778 | 8.3519934D-02 |
| 3.6224300D+03 | 1.131711 | 7.4437220D-02 |
| 3.6307805D+03 | 1.132860 | 6.4832108D-02 |
| 3.6391504D+03 | 1.136183 | 5.4801209D-02 |
| 3.6475395D+03 | 1.142068 | 4.6215765D-02 |
| 3.6643757D+03 | 1.149520 | 3.8000573D-02 |
| 3.6728230D+03 | 1.152876 | 2.8170214D-02 |
| 3.6812897D+03 | 1.160993 | 2.0501713D-02 |
| 3.6897760D+03 | 1.168874 | 1.8611876D-02 |
| 3.6982818D+03 | 1.174582 | 1.6397972D-02 |
| 3.7068072D+03 | 1.179962 | 1.4514101D-02 |
| 3.7239171D+03 | 1.188087 | 1.2699603D-02 |
| 3.7325016D+03 | 1.191390 | 1.0490354D-02 |
| 3.7411059D+03 | 1.195340 | 8.5465363D-03 |
| 3.7497300D+03 | 1.199289 | 7.3247051D-03 |
| 3.7583740D+03 | 1.202951 | 6.2775495D-03 |
| 3.7670380D+03 | 1.206519 | 5.3677236D-03 |
| 3.7757219D+03 | 1.209954 | 4.8282544D-03 |
| 3.7931498D+03 | 1.215699 | 4.3630495D-03 |
| 3.8018940D+03 | 1.218078 | 4.0159671D-03 |
| 3.8106582D+03 | 1.220535 | 3.3020994D-03 |
| 3.8194427D+03 | 1.223082 | 2.9770775D-03 |
| 3.8282474D+03 | 1.225483 | 2.7026521D-03 |
| 3.8370725D+03 | 1.227769 | 2.5750765D-03 |
| 3.8547836D+03 | 1.231834 | 2.4762252D-03 |
| 3.8636698D+03 | 1.233679 | 2.4254378D-03 |

TABLE 1-Continued

| Wave Number ($cm^{-1}$) | n | k |
|---|---|---|
| 3.8725764D+03 | 1.235426 | 2.3866577D-03 |
| 3.8815037D+03 | 1.237089 | 2.3377074D-03 |
| 3.8904514D+03 | 1.238670 | 2.3109478D-03 |
| 3.8994199D+03 | 1.240167 | 2.2687683D-03 |
| 3.9174188D+03 | 1.243014 | 2.1418554D-03 |
| 3.9355008D+03 | 1.245672 | 2.0691413D-03 |
| 3.9536662D+03 | 1.248127 | 2.0173913D-03 |
| 3.9719155D+03 | 1.250383 | 1.9897117D-03 |
| 3.9810717D+03 | 1.251445 | 1.9533953D-03 |
| 3.9994475D+03 | 1.253465 | 1.9001599D-03 |
| 4.0179081D+03 | 1.255347 | 1.8104650D-03 |
| 4.0364539D+03 | 1.257102 | 1.7091892D-03 |
| 4.0457589D+03 | 1.257969 | 1.5804841D-03 |
| 4.0644333D+03 | 1.259683 | 1.4716012D-03 |
| 4.0831939D+03 | 1.261297 | 1.3483112D-03 |
| 4.1020410D+03 | 1.262824 | 1.2496550D-03 |
| 4.1114972D+03 | 1.263577 | 1.1502444D-03 |
| 4.1304750D+03 | 1.265059 | 1.0710017D-03 |
| 4.1495404D+03 | 1.266450 | 9.9035328D-04 |
| 4.1686938D+03 | 1.267787 | 9.0947370D-04 |
| 4.1879357D+03 | 1.269059 | 8.4877024D-04 |
| 4.1975898D+03 | 1.269682 | 7.9211848D-04 |
| 4.2169650D+03 | 1.270902 | 7.4266019D-04 |
| 4.2364297D+03 | 1.272062 | 6.8515707D-04 |
| 4.2559841D+03 | 1.273184 | 6.3648789D-04 |
| 4.2756289D+03 | 1.274257 | 5.9950132D-04 |
| 4.2953643D+03 | 1.275295 | 5.4298789D-04 |
| 4.3151908D+03 | 1.276305 | 5.1143464D-04 |
| 4.3251383D+03 | 1.276797 | 4.9180183D-04 |
| 4.3451022D+03 | 1.277755 | 4.6858690D-04 |
| 4.3651583D+03 | 1.278675 | 4.5059892D-04 |
| 4.3853070D+03 | 1.279561 | 4.2932892D-04 |
| 4.4055486D+03 | 1.280421 | 4.0812213D-04 |
| 4.4258837D+03 | 1.281256 | 3.8975361D-04 |
| 4.4463127D+03 | 1.282064 | 3.7392986D-04 |
| 4.4668359D+03 | 1.282852 | 3.5710024D-04 |
| 4.4874539D+03 | 1.283619 | 3.4577226D-04 |
| 4.5081670D+03 | 1.284365 | 3.4102808D-04 |
| 4.5289758D+03 | 1.285087 | 3.3868046D-04 |
| 4.5498806D+03 | 1.285790 | 3.3790152D-04 |
| 4.5708819D+03 | 1.286474 | 3.3946120D-04 |
| 4.5919801D+03 | 1.287139 | 3.4339198D-04 |
| 4.6131757D+03 | 1.287787 | 3.5058243D-04 |
| 4.6344692D+03 | 1.288418 | 3.5874854D-04 |

TABLE 1-Continued

| Wave Number ($cm^{-1}$) | n | k |
|---|---|---|
| 4.6558609D+03 | 1.289033 | 3.7050165D-04 |
| 4.6773514D+03 | 1.289634 | 3.8263980D-04 |
| 4.6989411D+03 | 1.290221 | 3.9699967D-04 |
| 4.7206304D+03 | 1.290795 | 4.1762851D-04 |
| 4.7424199D+03 | 1.291353 | 4.4034203D-04 |
| 4.7643099D+03 | 1.291899 | 4.6429087D-04 |
| 4.7863009D+03 | 1.292438 | 4.8841629D-04 |
| 4.8083935D+03 | 1.292966 | 5.2940757D-04 |
| 4.8305880D+03 | 1.293476 | 5.7251932D-04 |
| 4.8528850D+03 | 1.293973 | 6.2056909D-04 |
| 4.8752849D+03 | 1.294457 | 6.7420217D-04 |
| 4.8977882D+03 | 1.294919 | 7.3924797D-04 |
| 4.9317380D+03 | 1.295606 | 8.0498937D-04 |
| 4.9545019D+03 | 1.296066 | 8.8877155D-04 |
| 4.9773708D+03 | 1.296499 | 9.9035328D-04 |
| 5.0003453D+03 | 1.296913 | 1.1010072D-03 |
| 5.0234259D+03 | 1.297292 | 1.2496550D-03 |
| 5.0466130D+03 | 1.297607 | 1.4021360D-03 |
| 5.0815944D+03 | 1.298051 | 1.5480684D-03 |
| 5.1050500D+03 | 1.298308 | 1.7170785D-03 |
| 5.1286138D+03 | 1.298472 | 1.8483752D-03 |
| 5.1522864D+03 | 1.298590 | 1.9089306D-03 |
| 5.1760683D+03 | 1.298681 | 1.9221627D-03 |
| 5.2119471D+03 | 1.298793 | 1.8272171D-03 |
| 5.2360044D+03 | 1.298791 | 1.6779930D-03 |
| 5.2601727D+03 | 1.298998 | 1.1608875D-03 |
| 5.2966344D+03 | 1.299545 | 9.2212574D-04 |
| 5.3210826D+03 | 1.299860 | 7.2242064D-04 |
| 5.3456436D+03 | 1.300214 | 5.2094292D-04 |
| 5.3703180D+03 | 1.300633 | 3.2047204D-04 |
| 5.4075432D+03 | 1.301291 | 1.8611876D-04 |
| 5.4325033D+03 | 1.301709 | 1.5516371D-04 |
| 5.4701596D+03 | 1.302269 | 1.4183720D-04 |
| 5.4954087D+03 | 1.302616 | 1.3797174D-04 |
| 5.5207744D+03 | 1.302947 | 1.3711663D-04 |
| 5.5590426D+03 | 1.303418 | 1.3592212D-04 |
| 5.5847019D+03 | 1.303718 | 1.3304242D-04 |
| 5.6234133D+03 | 1.304155 | 1.2186813D-04 |
| 5.6493697D+03 | 1.304442 | 1.1201860D-04 |
| 5.6754461D+03 | 1.304727 | 1.0512116D-04 |
| 5.7147864D+03 | 1.305142 | 9.9997730D-05 |
| 5.7411646D+03 | 1.305413 | 9.5102108D-05 |
| 5.7809605D+03 | 1.305809 | 8.9000028D-05 |
| 5.8076442D+03 | 1.306070 | 8.4098867D-05 |

TABLE 1-Continued

| Wave Number ($cm^{-1}$) | n | k |
|---|---|---|
| 5.8479008D+03 | 1.306453 | 8.0498937D-05 |
| 5.8384366D+03 | 1.306829 | 7.7426592D-05 |
| 5.9156163D+03 | 1.307073 | 7.6013397D-05 |
| 5.9566214D+03 | 1.307435 | 7.4953194D-05 |
| 5.9841160D+03 | 1.307672 | 7.4044046D-05 |
| 6.0255959D+03 | 1.308021 | 7.3975881D-05 |
| 6.0673633D+03 | 1.308341 | 7.5908453D-05 |
| 6.0953690D+03 | 1.308548 | 7.9029665D-05 |
| 6.1376201D+03 | 1.308855 | 8.0963662D-05 |
| 6.1659500D+03 | 1.309055 | 8.3097918D-05 |
| 6.2086903D+03 | 1.309352 | 8.8042049D-05 |
| 6.2517269D+03 | 1.309642 | 9.3473853D-05 |
| 6.2950618D+03 | 1.309928 | 9.9400860D-05 |
| 6.3241185D+03 | 1.310114 | 1.0707551D-04 |
| 6.3679552D+03 | 1.310387 | 1.1402239D-04 |
| 6.4120958D+03 | 1.310659 | 1.2396245D-04 |
| 6.4565423D+03 | 1.310923 | 1.3483112D-04 |
| 6.4863443D+03 | 1.311097 | 1.4414187D-04 |
| 6.5313055D+03 | 1.311352 | 1.6024709D-04 |
| 6.5765784D+03 | 1.311604 | 1.7409654D-04 |
| 6.6221650D+03 | 1.311852 | 1.9578984D-04 |
| 6.6680677D+03 | 1.312093 | 2.2479681D-04 |
| 6.7142885D+03 | 1.312318 | 2.6594397D-04 |
| 6.7608298D+03 | 1.312525 | 3.0184928D-04 |
| 6.8076936D+03 | 1.312715 | 3.3868046D-04 |
| 6.8548823D+03 | 1.312888 | 3.6040445D-04 |
| 6.9023980D+03 | 1.313055 | 3.6373923D-04 |
| 6.9502432D+03 | 1.313220 | 3.6290265D-04 |
| 6.9984200D+03 | 1.313373 | 3.5382633D-04 |
| 7.0469307D+03 | 1.313518 | 3.1973497D-04 |
| 7.0957777D+03 | 1.313671 | 2.5397452D-04 |
| 7.1449633D+03 | 1.313871 | 1.5303478D-04 |
| 7.1944898D+03 | 1.314104 | 1.0599616D-04 |
| 7.2443596D+03 | 1.314329 | 7.8017161D-05 |
| 7.2945751D+03 | 1.314547 | 5.8035021D-05 |
| 7.3451387D+03 | 1.314760 | 4.5049517D-05 |
| 7.4131024D+03 | 1.315031 | 4.0465988D-05 |
| 7.4644876D+03 | 1.315228 | 2.8489849D-05 |
| 7.5162289D+03 | 1.315425 | 2.2505577D-05 |
| 7.5683290D+03 | 1.315618 | 1.9120099D-05 |
| 7.6383578D+03 | 1.315868 | 1.6390422D-05 |
| 7.6913044D+03 | 1.316052 | 1.4002002D-05 |
| 7.7446180D+03 | 1.316233 | 1.2211532D-05 |
| 7.8162780D+03 | 1.316470 | 1.1394365D-05 |

TABLE 1-Continued

| Wave Number ($cm^{-1}$) | n | k |
|---|---|---|
| 7.8704579D+03 | 1.316645 | 1.0904861D-05 |
| 7.9432823D+03 | 1.316873 | 1.0790713D-05 |
| 7.9983426D+03 | 1.317042 | 1.1002215D-05 |
| 8.0723503D+03 | 1.317263 | 1.1388857D-05 |
| 8.1283052D+03 | 1.317427 | 1.1602462D-05 |
| 8.2035154D+03 | 1.317641 | 1.1790172D-05 |
| 8.2603795D+03 | 1.317799 | 1.1905843D-05 |
| 8.3368118D+03 | 1.318008 | 1.1994997D-05 |
| 8.3945999D+03 | 1.318162 | 1.1812182D-05 |
| 8.4722741D+03 | 1.318366 | 1.1603263D-05 |
| 8.5506671D+03 | 1.318566 | 1.1195156D-05 |
| 8.6297855D+03 | 1.318763 | 1.0688829D-05 |
| 8.6896043D+03 | 1.318909 | 9.3064735D-06 |
| 8.7700082D+03 | 1.319103 | 5.9510026D-06 |
| 8.8511561D+03 | 1.319296 | 3.8689235D-06 |
| 8.9330548D+03 | 1.319488 | 2.6283920D-06 |
| 9.0157114D+03 | 1.319678 | 2.0384034D-06 |
| 9.0991327D+03 | 1.319865 | 1.7084023D-06 |
| 9.1833260D+03 | 1.320051 | 1.4986152D-06 |
| 9.2682982D+03 | 1.320233 | 1.3285874D-06 |
| 9.3540567D+03 | 1.320416 | 1.2588968D-06 |
| 9.4406088D+03 | 1.320596 | 1.2989431D-06 |
| 9.5279616D+03 | 1.320775 | 1.4193521D-06 |
| 9.6161228D+03 | 1.320952 | 1.6900134D-06 |
| 9.7050997D+03 | 1.321128 | 2.0007376D-06 |
| 9.7948999D+03 | 1.321303 | 2.3522861D-06 |
| 9.9083194D+03 | 1.321521 | 2.6877579D-06 |
| 1.0000000D+04 | 1.321695 | 2.9997851D-06 |
| 1.0046158D+04 | 1.321780 | 3.1310510D-06 |
| 1.0092529D+04 | 1.321866 | 3.2530455D-06 |
| 1.0162487D+04 | 1.321994 | 3.3364924D-06 |
| 1.0209395D+04 | 1.322080 | 3.4181423D-06 |
| 1.0256519D+04 | 1.322165 | 3.4800873D-06 |
| 1.0303861D+04 | 1.322249 | 3.5017904D-06 |
| 1.0351422D+04 | 1.322333 | 3.4640978D-06 |
| 1.0423174D+04 | 1.322462 | 3.3580731D-06 |
| 1.0471285D+04 | 1.322546 | 3.1899960D-06 |
| 1.0519619D+04 | 1.322630 | 2.9321767D-06 |
| 1.0592537D+04 | 1.322757 | 2.5573498D-06 |
| 1.0641430D+04 | 1.322842 | 2.1691528D-06 |
| 1.0690549D+04 | 1.322926 | 1.7708841D-06 |
| 1.0764652D+04 | 1.323054 | 1.3683278D-06 |
| 1.0814340D+04 | 1.323138 | 1.0597176D-06 |
| 1.0864256D+04 | 1.323222 | 8.3040536D-07 |

TABLE 1-Continued

| Wave Number ($cm^{-1}$) | n | k |
|---|---|---|
| 1.0939564D+04 | 1.323351 | 6.6956099D-07 |
| 1.0990058D+04 | 1.323434 | 5.6988883D-07 |
| 1.1040786D+04 | 1.323520 | 5.1497974D-07 |
| 1.1117317D+04 | 1.323648 | 4.8617222D-07 |
| 1.1168632D+04 | 1.323732 | 4.6215765D-07 |
| 1.1246050D+04 | 1.323859 | 4.4034203D-07 |
| 1.1297959D+04 | 1.323946 | 4.2343831D-07 |
| 1.1376273D+04 | 1.324074 | 4.0531264D-07 |
| 1.1428783D+04 | 1.324159 | 3.9065208D-07 |
| 1.1481536D+04 | 1.324244 | 3.7479185D-07 |
| 1.1561122D+04 | 1.324373 | 3.5464198D-07 |
| 1.1641260D+04 | 1.324502 | 3.3480362D-07 |
| 1.1694994D+04 | 1.324590 | 3.1534805D-07 |
| 1.1776060D+04 | 1.324718 | 2.9294773D-07 |
| 1.1830416D+04 | 1.324805 | 2.6902345D-07 |
| 1.1912420D+04 | 1.324937 | 2.4591790D-07 |
| 1.1967405D+04 | 1.325025 | 2.2427979D-07 |
| 1.2050359D+04 | 1.325157 | 2.0407516D-07 |
| 1.2133889D+04 | 1.325290 | 1.8188218D-07 |
| 1.2189896D+04 | 1.325379 | 1.6210266D-07 |
| 1.2274392D+04 | 1.325512 | 1.4480720D-07 |
| 1.2359474D+04 | 1.325648 | 1.3298117D-07 |
| 1.2416523D+04 | 1.325739 | 1.2699603D-07 |
| 1.2502590D+04 | 1.325874 | 1.2496550D-07 |
| 1.2589254D+04 | 1.326012 | 1.2583172D-07 |
| 1.2647363D+04 | 1.326104 | 1.2817111D-07 |
| 1.2735031D+04 | 1.326244 | 1.3390295D-07 |
| 1.2823306D+04 | 1.326382 | 1.4086080D-07 |
| 1.2912193D+04 | 1.326524 | 1.4783938D-07 |
| 1.3001696D+04 | 1.326667 | 1.5268281D-07 |
| 1.3061709D+04 | 1.326764 | 1.5696042D-07 |
| 1.3152248D+04 | 1.326909 | 1.5804841D-07 |
| 1.3243415D+04 | 1.327055 | 1.5804841D-07 |
| 1.3335214D+04 | 1.327201 | 1.5587991D-07 |
| 1.3427650D+04 | 1.327350 | 1.5303478D-07 |
| 1.3520726D+04 | 1.327502 | 1.4581095D-07 |
| 1.3614447D+04 | 1.327652 | 1.3483112D-07 |
| 1.3708818D+04 | 1.327808 | 1.1502444D-07 |
| 1.3803843D+04 | 1.327963 | 9.1367164D-08 |
| 1.3899526D+04 | 1.328120 | 7.2910511D-08 |
| 1.3995873D+04 | 1.328279 | 5.9950132D-08 |
| 1.4092888D+04 | 1.328440 | 4.9979297D-08 |
| 1.4190575D+04 | 1.328603 | 4.1000594D-08 |
| 1.4288940D+04 | 1.328769 | 3.3480362D-08 |

TABLE 1-Continued

| Wave Number ($cm^{-1}$) | n | k |
|---|---|---|
| 1.4387986D+04 | 1.328938 | 2.9633991D-08 |
| 1.4487719D+04 | 1.329106 | 2.6533231D-08 |
| 1.4588143D+04 | 1.329278 | 2.4705301D-08 |
| 1.4689263D+04 | 1.329452 | 2.3003300D-08 |
| 1.4825181D+04 | 1.329690 | 2.1766577D-08 |
| 1.4927944D+04 | 1.329869 | 2.0979259D-08 |
| 1.5031420D+04 | 1.330052 | 2.0313752D-08 |
| 1.5135612D+04 | 1.330238 | 1.9399482D-08 |
| 1.5275661D+04 | 1.330490 | 1.7774203D-08 |
| 1.5381546D+04 | 1.330683 | 1.6741337D-08 |
| 1.5488166D+04 | 1.330877 | 1.6061649D-08 |
| 1.5631476D+04 | 1.331144 | 1.5696042D-08 |
| 1.5739829D+04 | 1.331345 | 1.5516371D-08 |
| 1.5885467D+04 | 1.331619 | 1.5024158D-08 |
| 1.5995580D+04 | 1.331826 | 1.4716012D-08 |
| 1.6143586D+04 | 1.332106 | 1.3989112D-08 |
| 1.6255488D+04 | 1.332317 | 1.3298117D-08 |
| 1.6405898D+04 | 1.332598 | 1.2381981D-08 |
| 1.6519618D+04 | 1.332813 | 1.1318533D-08 |
| 1.6672472D+04 | 1.333100 | 9.6336340D-09 |
| 1.6788040D+04 | 1.333316 | 7.7230731D-09 |
| 1.6943378D+04 | 1.333609 | 6.3648789D-09 |
| 1.7100153D+04 | 1.333902 | 5.2214382D-09 |
| 1.7258379D+04 | 1.334200 | 4.4339434D-09 |
| 1.7378008D+04 | 1.334425 | 3.8440599D-09 |
| 1.7538805D+04 | 1.334729 | 3.4339198D-09 |
| 1.7701090D+04 | 1.335035 | 3.1317720D-09 |
| 1.7864876D+04 | 1.335344 | 2.8693937D-09 |
| 1.8030177D+04 | 1.335656 | 2.6594397D-09 |
| 1.8197009D+04 | 1.335972 | 2.4422501D-09 |
| 1.8365383D+04 | 1.336292 | 2.2687683D-09 |
| 1.8535316D+04 | 1.336615 | 2.0979259D-09 |
| 1.8706821D+04 | 1.336943 | 1.8870793D-09 |
| 1.8879913D+04 | 1.337273 | 1.7570744D-09 |
| 1.9054607D+04 | 1.337607 | 1.6397972D-09 |
| 1.9230917D+04 | 1.337944 | 1.5696042D-09 |
| 1.9408859D+04 | 1.338288 | 1.4614708D-09 |
| 1.9588447D+04 | 1.338635 | 1.2670395D-09 |
| 1.9815270D+04 | 1.339073 | 1.0784255D-09 |
| 1.9998619D+04 | 1.339430 | 9.2425146D-10 |
| 2.0183664D+04 | 1.339791 | 7.8485629D-10 |
| 2.0417379D+04 | 1.340248 | 7.3415903D-10 |
| 2.0606299D+04 | 1.340620 | 7.1579744D-10 |
| 2.0844909D+04 | 1.341093 | 7.0923497D-10 |

TABLE 1-Continued

| Wave Number ($cm^{-1}$) | n | k |
|---|---|---|
| 2.1037784D+04 | 1.341475 | 7.0111643D-10 |
| 2.1281390D+04 | 1.341961 | 7.2910511D-10 |
| 2.1527817D+04 | 1.342455 | 7.4953194D-10 |
| 2.1727012D+04 | 1.342858 | 7.5995897D-10 |
| 2.1978599D+04 | 1.343368 | 7.7945338D-10 |
| 2.2233099D+04 | 1.343889 | 8.0870503D-10 |
| 2.2490546D+04 | 1.344418 | 8.6854064D-10 |
| 2.2750974D+04 | 1.344956 | 9.3926933D-10 |
| 2.3014418D+04 | 1.345505 | 1.0180993D-09 |
| 2.3280913D+04 | 1.346066 | 1.0884040D-09 |
| 2.3550493D+04 | 1.346636 | 1.1689344D-09 |
| 2.3823195D+04 | 1.347219 | 1.2583172D-09 |
| 2.4099054D+04 | 1.347811 | 1.3390295D-09 |
| 2.4378108D+04 | 1.348417 | 1.4216417D-09 |
| 2.4717241D+04 | 1.349159 | 1.4886416D-09 |
| 2.5003454D+04 | 1.349793 | 1.5804841D-09 |
| 2.5292980D+04 | 1.350438 | 1.6626091D-09 |
| 2.5644840D+04 | 1.351231 | 1.7611248D-09 |
| 2.6001596D+04 | 1.352046 | 1.8398827D-09 |
| 2.6302680D+04 | 1.352740 | 1.9399482D-09 |
| 2.6668587D+04 | 1.353594 | 2.0313752D-09 |
| 2.7039584D+04 | 1.354470 | 2.1173378D-09 |
| 2.7415742D+04 | 1.355370 | 2.2171248D-09 |
| 2.7797133D+04 | 1.356295 | 2.3162751D-09 |
| 2.8183829D+04 | 1.357247 | 2.4198595D-09 |
| 2.8575905D+04 | 1.358224 | 2.5280761D-09 |
| 2.8973436D+04 | 1.359231 | 2.6533231D-09 |
| 2.9444216D+04 | 1.360441 | 2.7656049D-09 |
| 2.9853826D+04 | 1.361513 | 2.8826382D-09 |
| 3.0269134D+04 | 1.362616 | 2.9839404D-09 |
| 3.0760968D+04 | 1.363990 | 3.0816985D-09 |
| 3.1260794D+04 | 1.365376 | 3.1899960D-09 |
| 3.1768741D+04 | 1.366812 | 3.3249885D-09 |
| 3.2284941D+04 | 1.368287 | 3.5464198D-09 |
| 3.2809529D+04 | 1.369839 | 3.8263980D-09 |
| 3.3342641D+04 | 1.371437 | 4.1475358D-09 |
| 3.3884416D+04 | 1.373098 | 4.4034203D-09 |
| 3.4514374D+04 | 1.375086 | 4.7950169D-09 |
| 3.5075187D+04 | 1.376902 | 5.4049309D-09 |
| 3.5727284D+04 | 1.379072 | 5.7914878D-09 |
| 3.6391504D+04 | 1.381341 | 6.2920207D-09 |
| 3.7068072D+04 | 1.383726 | 6.8515707D-09 |
| 3.7757219D+04 | 1.386239 | 7.4437220D-09 |
| 3.8459178D+04 | 1.388881 | 7.9944786D-09 |

TABLE 1-Continued

| Wave Number ($cm^{-1}$) | n | k |
|---|---|---|
| 3.9174188D+04 | 1.391674 | 8.6057781D-09 |
| 3.9994475D+04 | 1.394993 | 9.3065806D-09 |
| 4.0831939D+04 | 1.398535 | 9.9035328D-09 |
| 4.1686938D+04 | 1.402321 | 1.0490354D-08 |
| 4.2559841D+04 | 1.406358 | 1.0710017D-08 |
| 4.3451022D+04 | 1.410702 | 1.1010072D-08 |
| 4.4463127D+04 | 1.415921 | 1.1582176D-08 |
| 4.5498806D+04 | 1.421603 | 1.2699603D-08 |
| 4.6558609D+04 | 1.427828 | 1.9988957D-08 |
| 4.7643099D+04 | 1.434685 | 3.8440599D-08 |
| 4.8752849D+04 | 1.442296 | 6.7110449D-08 |
| 5.0003453D+04 | 1.451724 | 1.1010072D-07 |
| 5.1286138D+04 | 1.462543 | 1.8496525D-07 |
| 5.2601727D+04 | 1.475183 | 3.6223478D-07 |
| 5.4075432D+04 | 1.491881 | 1.2495112D-06 |
| 5.5590426D+04 | 1.513343 | 5.9950132D-05 |
| 5.7147864D+04 | 1.543062 | 8.3905445D-04 |
| 5.7411646D+04 | 1.549412 | 1.1824700D-03 |
| 5.8076442D+04 | 1.568183 | 2.0035037D-03 |
| 5.8884366D+04 | 1.605555 | 3.9975154D-03 |
| 5.9566214D+04 | 1.635062 | 3.9975154D-02 |
| 6.0255959D+04 | 1.647245 | 7.2408599D-02 |
| 6.0953690D+04 | 1.653100 | 1.0394178D-01 |
| 6.1659500D+04 | 1.652917 | 1.3514194D-01 |
| 6.2517269D+04 | 1.650184 | 1.6702833D-01 |
| 6.3241185D+04 | 1.641473 | 2.0220419D-01 |
| 6.4120958D+04 | 1.620422 | 2.3377074D-01 |
| 6.4863443D+04 | 1.596861 | 2.5810127D-01 |
| 6.5765784D+04 | 1.559942 | 2.7719803D-01 |
| 6.6680677D+04 | 1.521276 | 2.7719803D-01 |
| 6.7608298D+04 | 1.489551 | 2.6411322D-01 |
| 6.8548823D+04 | 1.469275 | 2.4087412D-01 |
| 6.9502432D+04 | 1.460977 | 2.1666569D-01 |
| 7.0469307D+04 | 1.461485 | 1.9265937D-01 |
| 7.1449633D+04 | 1.471129 | 1.6779930D-01 |
| 7.2443596D+04 | 1.496271 | 1.4216417D-01 |
| 7.3451387D+04 | 1.536403 | 1.3328772D-01 |
| 7.4644876D+04 | 1.586268 | 1.4886416D-01 |
| 7.5683290D+04 | 1.619420 | 1.8697784D-01 |
| 7.6913044D+04 | 1.633849 | 2.3921596D-01 |
| 7.8162780D+04 | 1.626822 | 2.8760084D-01 |
| 7.9432823D+04 | 1.606068 | 3.2195127D-01 |
| 8.0723503D+04 | 1.584638 | 3.3868046D-01 |
| 8.2035154D+04 | 1.570304 | 3.4897165D-01 |

TABLE 1-Continued

| Wave Number ($cm^{-1}$) | n | k |
|---|---|---|
| 8.3368118D+04 | 1.560870 | 3.5957554D-01 |
| 8.4722741D+04 | 1.553435 | 3.7050165D-01 |
| 8.6297855D+04 | 1.548070 | 3.8263980D-01 |
| 8.7700082D+04 | 1.543211 | 3.9883214D-01 |
| 8.9330548D+04 | 1.535363 | 4.1475358D-01 |
| 9.0991327D+04 | 1.528933 | 4.3031862D-01 |
| 9.2682982D+04 | 1.523589 | 4.4852860D-01 |
| 9.4406088D+04 | 1.516305 | 4.7074980D-01 |
| 9.6161228D+04 | 1.506677 | 4.9293555D-01 |
| 9.7948999D+04 | 1.493473 | 5.1854941D-01 |
| 1.0000000D+05 | 1.476628 | 5.4298789D-01 |
| 1.0209395D+05 | 1.455868 | 5.7516194D-01 |
| 1.0423174D+05 | 1.425425 | 6.0504844D-01 |
| 1.0641430D+05 | 1.387639 | 6.2920207D-01 |
| 1.0864256D+05 | 1.346760 | 6.4385807D-01 |
| 1.1117317D+05 | 1.302663 | 6.5281503D-01 |
| 1.1376273D+05 | 1.259495 | 6.5734013D-01 |
| 1.1641260D+05 | 1.214969 | 6.5734013D-01 |
| 1.1912420D+05 | 1.173382 | 6.4534232D-01 |
| 1.2189896D+05 | 1.140628 | 6.2920207D-01 |
| 1.2502590D+05 | 1.111682 | 6.1346550D-01 |
| 1.2823306D+05 | 1.087685 | 5.9812250D-01 |
| 1.3152248D+05 | 1.068724 | 5.8585500D-01 |
| 1.3520726D+05 | 1.049744 | 5.8048385D-01 |
| 1.3899526D+05 | 1.020921 | 5.8585500D-01 |
| 1.4288940D+05 | 0.981692 | 5.7914878D-01 |
| 1.4689263D+05 | 0.941801 | 5.6336536D-01 |
| 1.5135612D+05 | 0.903527 | 5.3553782D-01 |
| 1.5631476D+05 | 0.866994 | 5.0325737D-01 |
| 1.6143586D+05 | 0.840575 | 4.5581661D-01 |
| 1.6672472D+05 | 0.830901 | 4.1189844D-01 |
| 1.7258379D+05 | 0.831628 | 3.7392986D-01 |
| 1.7864876D+05 | 0.835295 | 3.4977611D-01 |
| 1.8535316D+05 | 0.835240 | 3.3097115D-01 |
| 1.9230917D+05 | 0.830957 | 3.1534805D-01 |
| 1.9998619D+05 | 0.820742 | 2.9977136D-01 |
| 2.0844909D+05 | 0.805579 | 2.7656049D-01 |
| 2.1727012D+05 | 0.797007 | 2.4142939D-01 |
| 2.2750974D+05 | 0.797737 | 2.0882868D-01 |
| 2.3823195D+05 | 0.802291 | 1.7980019D-01 |
| 2.5003454D+05 | 0.809997 | 1.5338756D-01 |
| 2.6302680D+05 | 0.819753 | 1.3025372D-01 |
| 2.7797133D+05 | 0.830720 | 1.0934279D-01 |
| 2.9444216D+05 | 0.842171 | 9.0738197D-02 |

TABLE 1-Continued

| Wave Number ($cm^{-1}$) | n | k |
|---|---|---|
| 3.1260794D+05 | 0.854141 | 7.4608815D-02 |
| 3.3342641D+05 | 0.866493 | 6.0644322D-02 |
| 3.5727284D+05 | 0.878766 | 4.8505406D-02 |
| 3.8459178D+05 | 0.890837 | 3.8175976D-02 |
| 4.1686938D+05 | 0.902694 | 2.9497835D-02 |
| 4.5498806D+05 | 0.913973 | 2.2273586D-02 |
| 5.0003453D+05 | 0.924583 | 1.6360258D-02 |
| 5.5590426D+05 | 0.934744 | 1.1635636D-02 |
| 6.2517269D+05 | 0.944124 | 7.9577473D-03 |
| 7.1449633D+05 | 0.952792 | 5.1735678D-03 |
| 7.6913044D+05 | 0.956954 | 4.0718347D-03 |
| 8.3368118D+05 | 0.960953 | 3.1462276D-03 |
| 9.0991327D+05 | 0.964778 | 2.3702281D-03 |
| 1.0000000D+06 | 0.968416 | 1.7449788D-03 |

* The data in the first and third columns are in Fortran, double precision, exponential notation. For example, 5.0D-04 means $5.0 \times 10^{-4}$.

Fig. 23. The final spectrum of $n(\nu)$ from 0 to $10^6$ $cm^{-1}$.

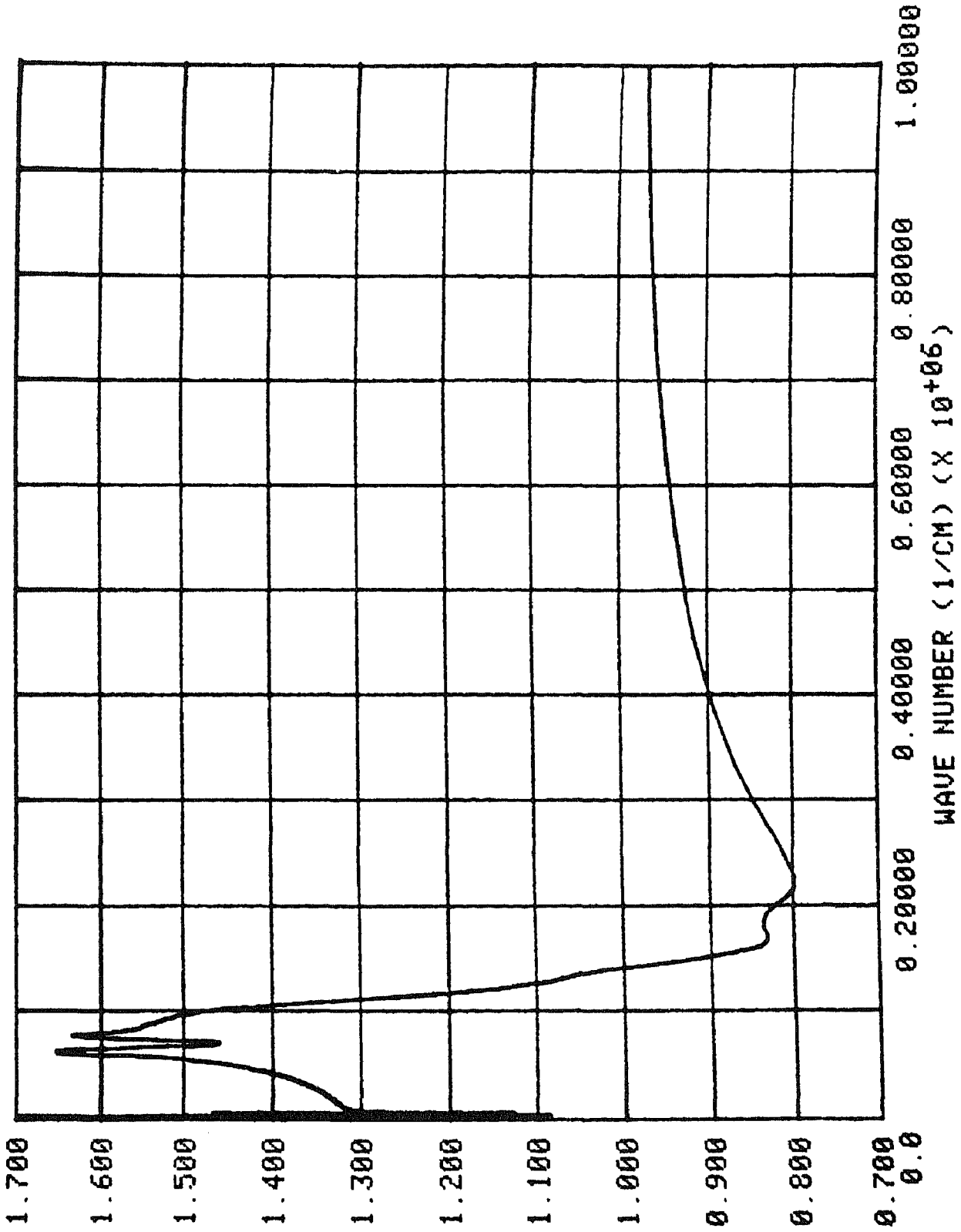
REAL PART OF N
1.700
1.600
1.500
1.400
1.300
1.200
1.100
1.000
0.900
0.800
0.700
0.0
0.20000
0.40000
0.60000
0.80000
1.00000
WAVE NUMBER (1/CM) (X 10+06)

Fig. 24. The final spectrum of $n(\nu)$ from 0 to $10^5$ $cm^{-1}$.

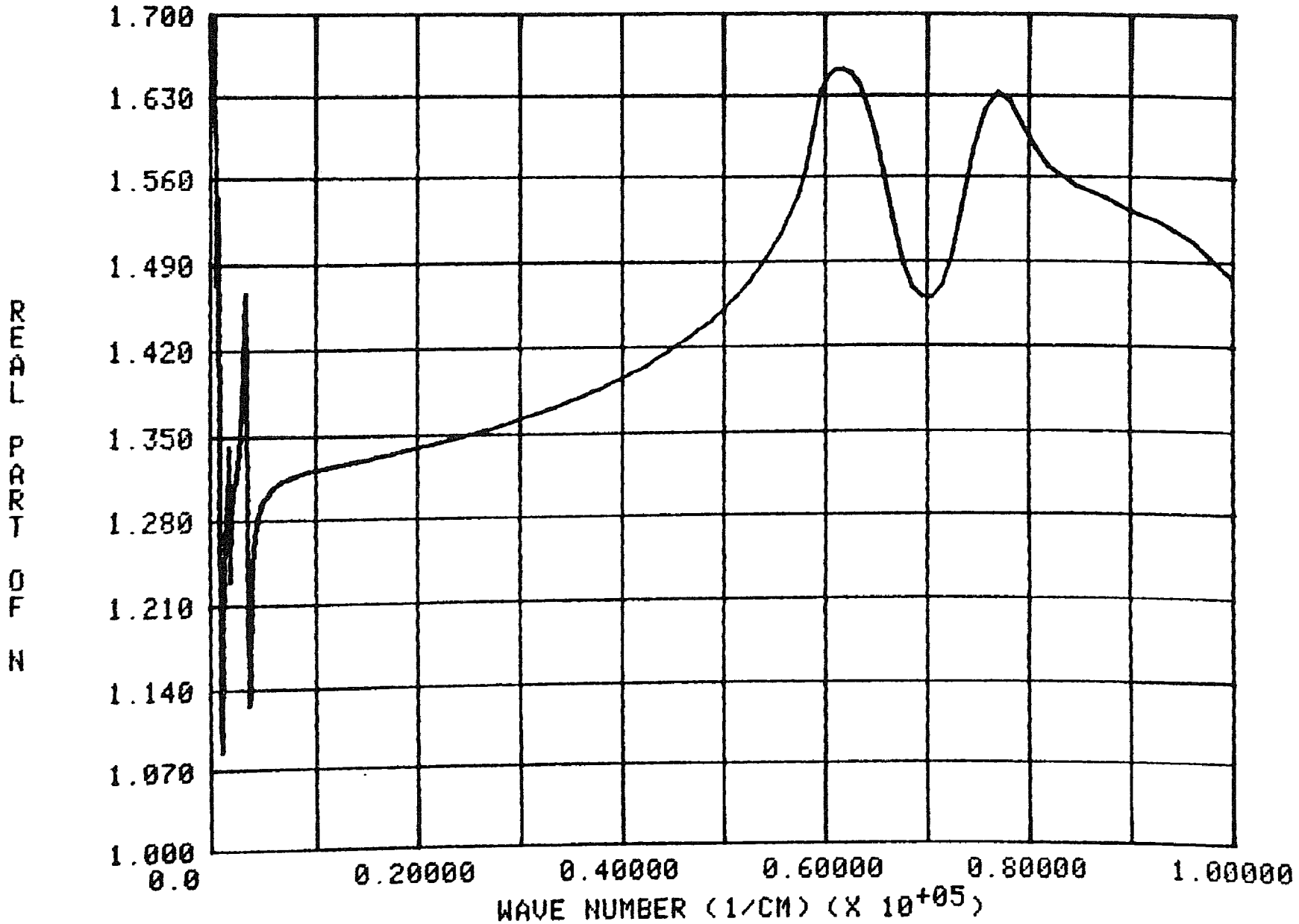
1.700
1.630
1.560
1.490
1.420
1.350
1.280
1.210
1.140
1.070
1.000
REAL PART OF N
0.0
0.20000
0.40000
0.60000
0.80000
1.00000
WAVE NUMBER (1/CM) (X 10+05)

Fig. 25. The final spectrum of $n(\nu)$ from 0 to $10^4$ $cm^{-1}$.

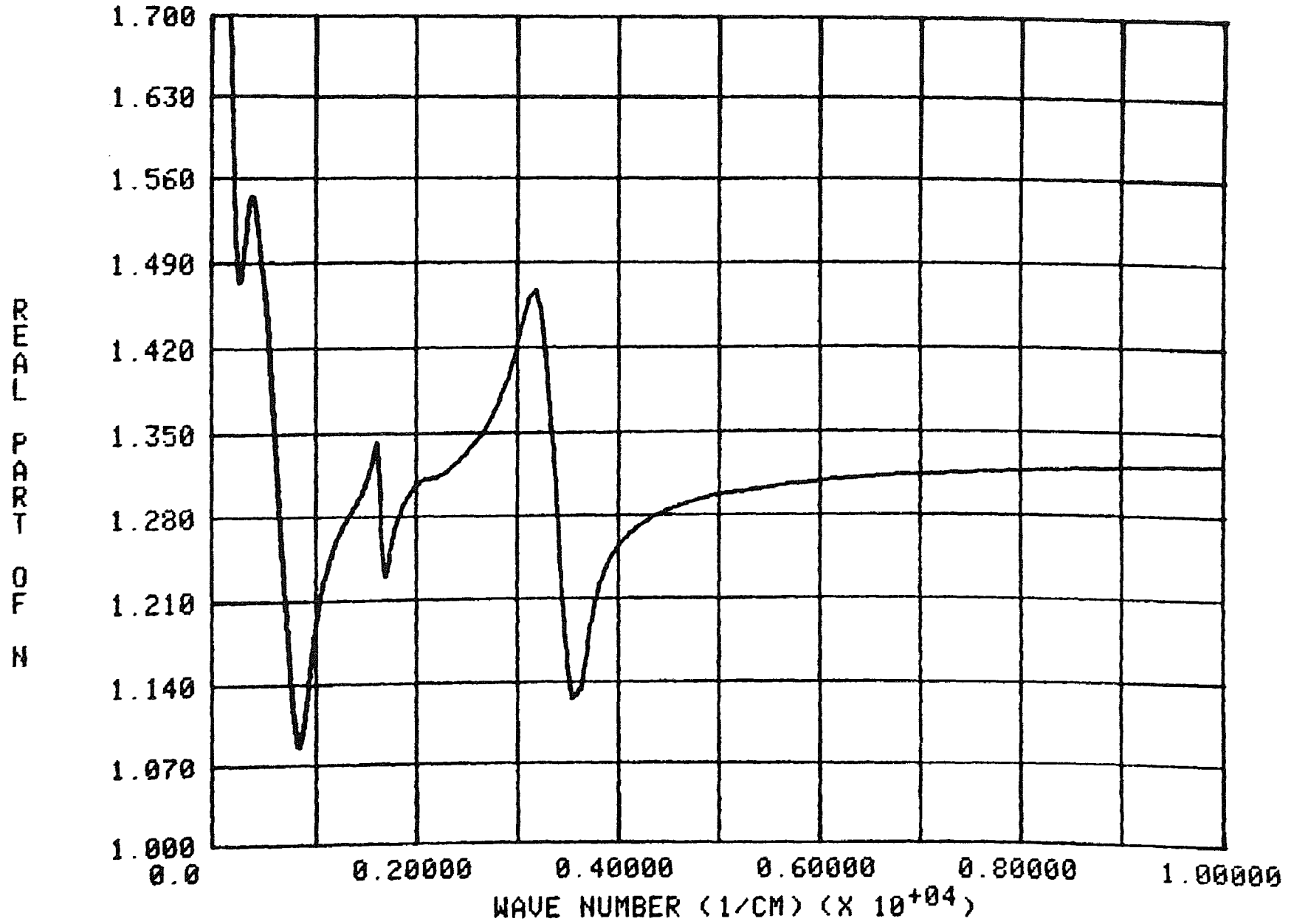
1.700
1.630
1.560
1.490
1.420
1.350
1.280
1.210
1.140
1.070
1.000
REAL PART OF N
0.0
0.20000
0.40000
0.60000
0.80000
1.00000
WAVE NUMBER (1/CM) (X 10+04)

Fig. 26. The final spectrum of $n(\nu)$ from 0 to $10^3$ $cm^{-1}$.

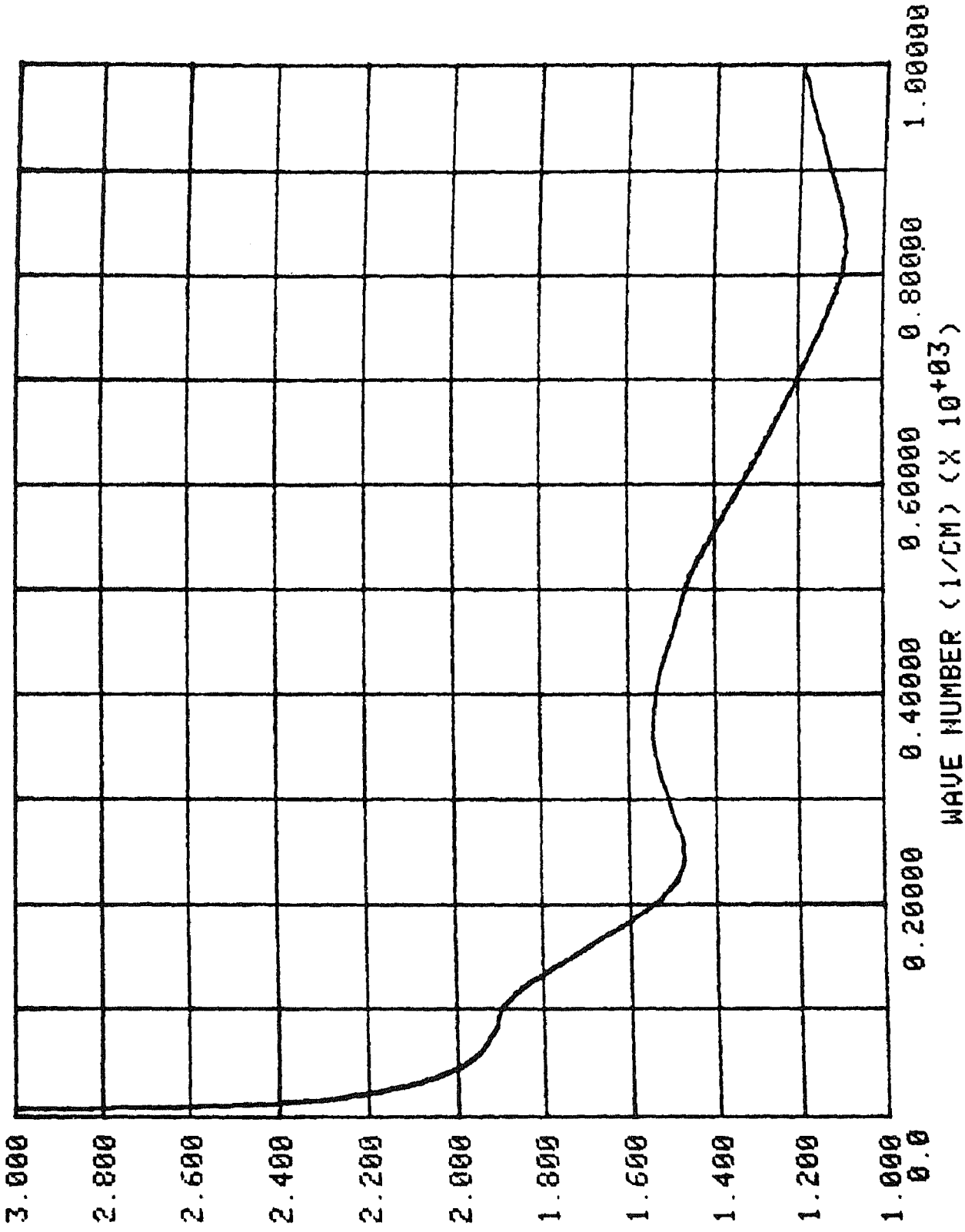
REAL PART OF N
3.000
2.800
2.600
2.400
2.200
2.000
1.800
1.600
1.400
1.200
1.000
0.0
0.20000
0.40000
0.60000
0.80000
1.00000
WAVE NUMBER (1/CM) (X 10+03)

Fig. 27. The final spectrum of $n(\nu)$ from 0 to $10^2$ $cm^{-1}$.

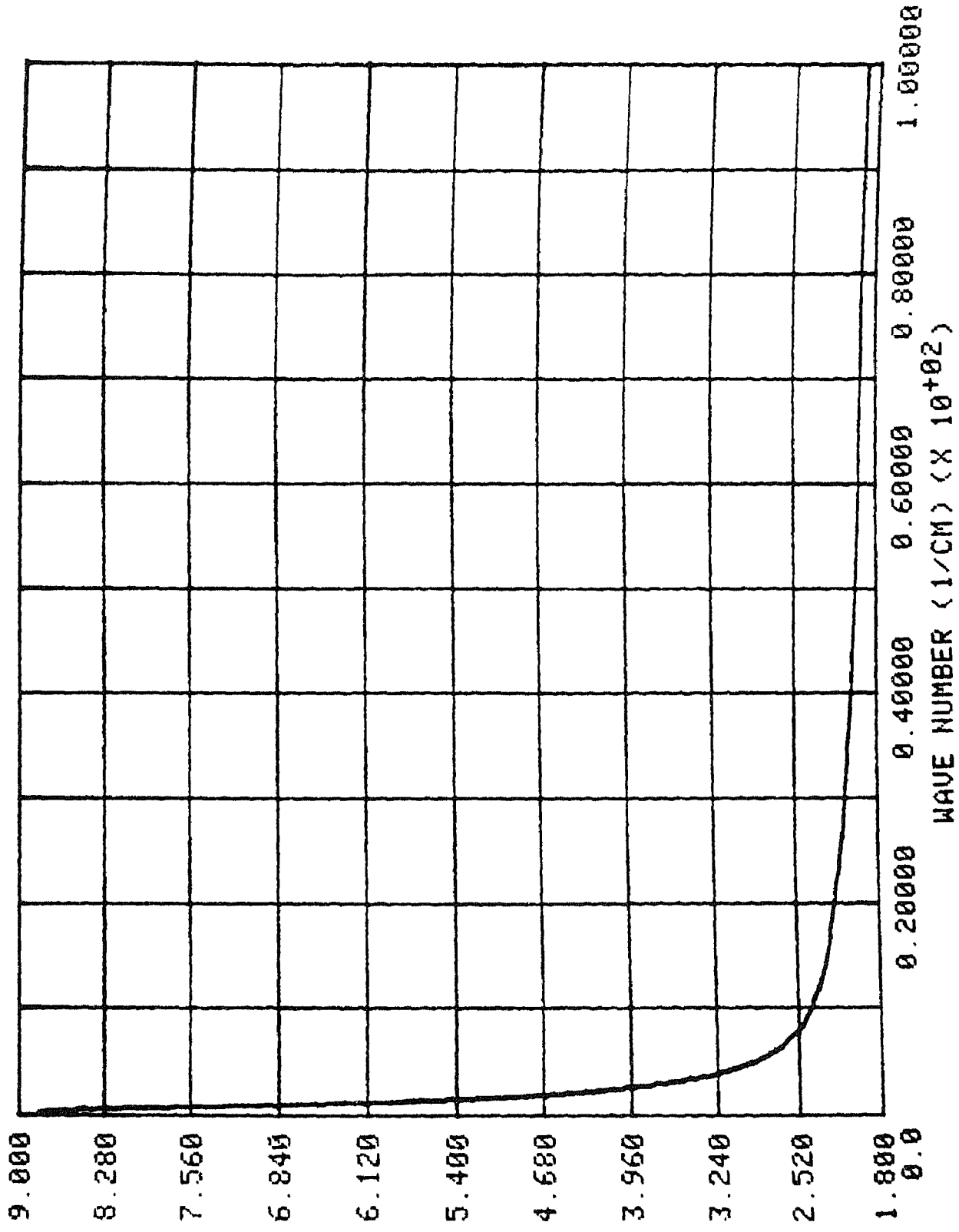
9.000
8.280
7.560
6.840
6.120
5.400
4.680
3.960
3.240
2.520
1.800
0.0
0.20000
0.40000
0.60000
0.80000
1.00000
WAVE NUMBER (1/CM) (X 10+02)
REAL PART OF H

Fig. 28. The final spectrum of $n(\nu)$ from 0 to 10 $cm^{-1}$.

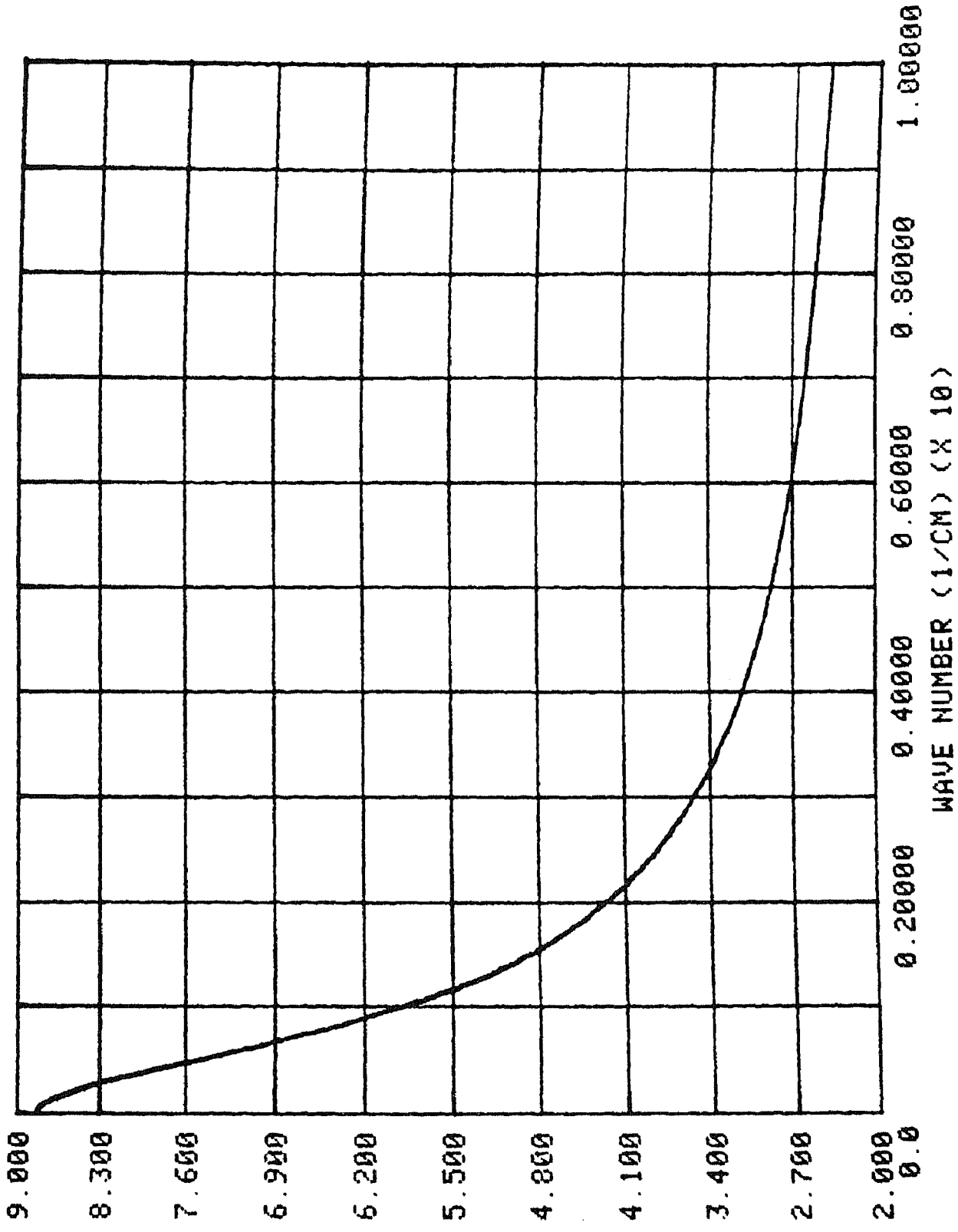
9.000
8.300
7.600
6.900
6.200
5.500
4.800
4.100
3.400
2.700
2.000
0.0
0.20000
0.40000
0.60000
0.80000
1.00000
WAVE NUMBER (1/CM) (X 10)
REAL PART OF H

Fig. 29. The final spectrum of $n(\nu)$ from 0 to 1 $cm^{-1}$.

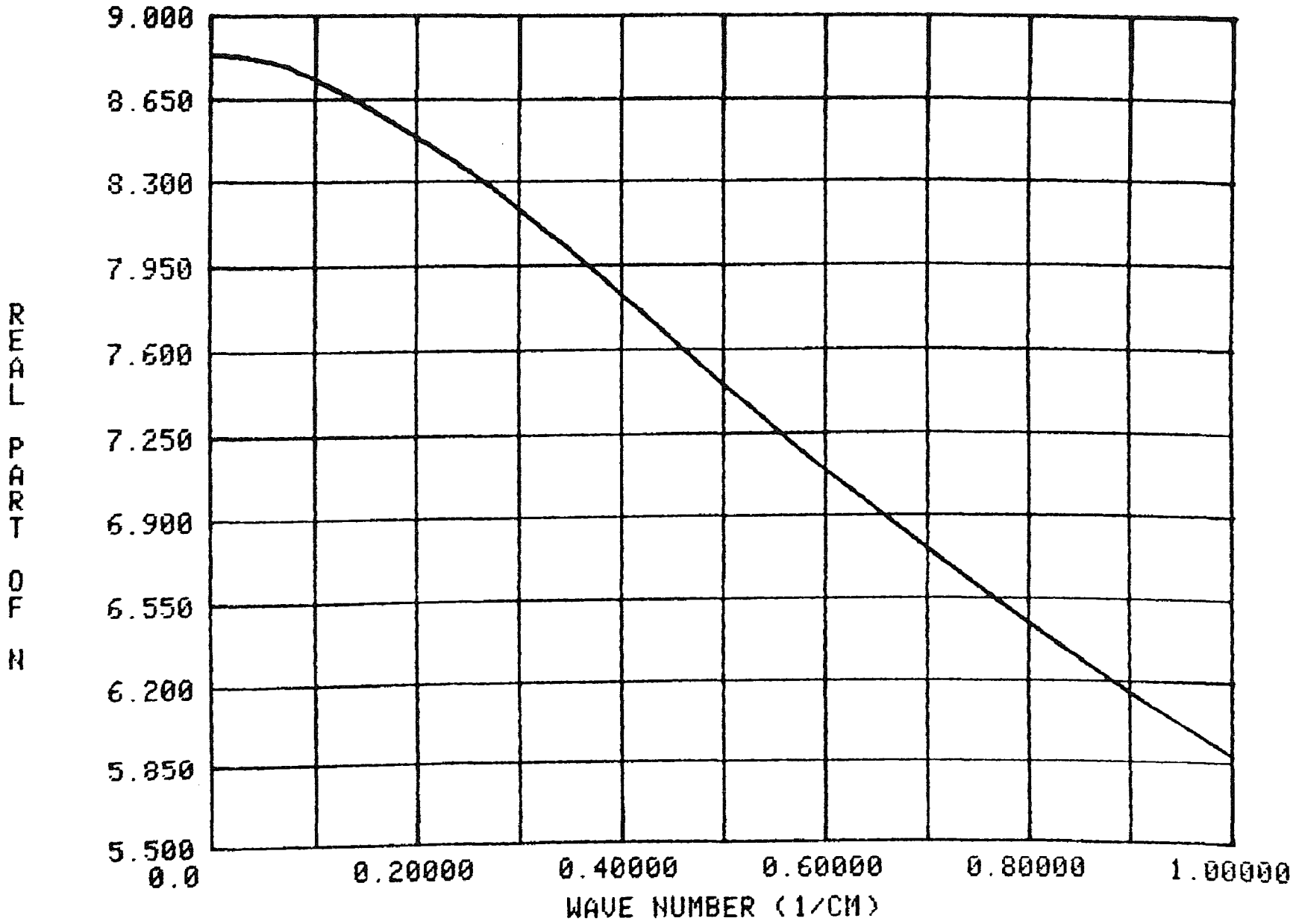
9.000
8.650
8.300
7.950
7.600
7.250
6.900
6.550
6.200
5.850
5.500
REAL PART OF N
0.0
0.20000
0.40000
0.60000
0.80000
1.00000
WAVE NUMBER (1/CM)

Fig. 30. The final spectrum of $n(\nu)$ from 0 to $10^{-1}$ $cm^{-1}$.

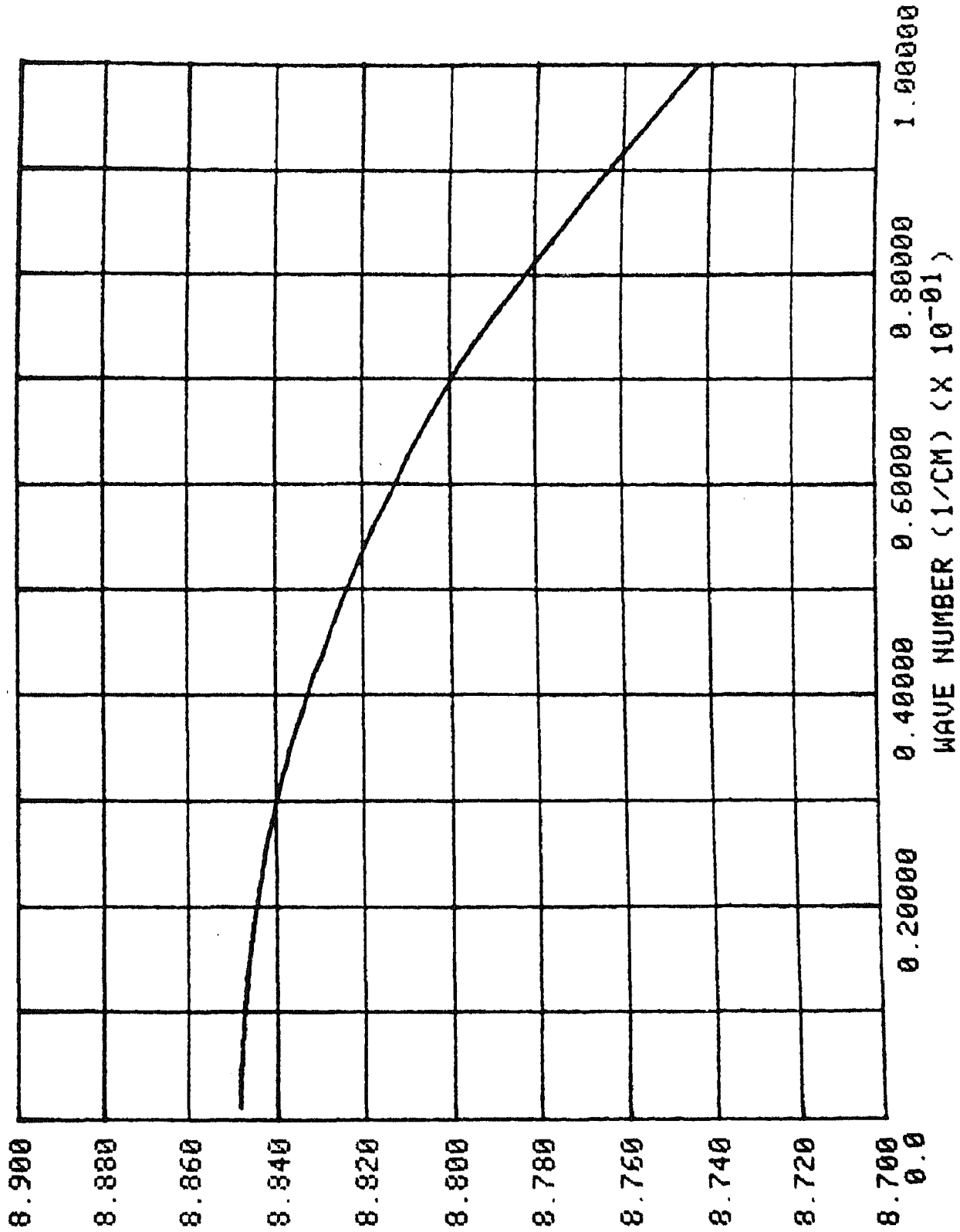
REAL PART OF N
8.900
8.880
8.860
8.840
8.820
8.800
8.780
8.760
8.740
8.720
8.700
0.0
0.20000
0.40000
0.60000
0.80000
1.00000
WAVE NUMBER (1/CM) (X 10-01)

# CHAPTER VI

## CONCLUSION

The process of obtaining the complex refractive index of water began with the acquisition of an absorption spectrum that spanned approximately 14 decades, from $10^{-6}$ to $10^{8}$ $cm^{-1}$. This spectrum comprised smoothly joined data from various sources, and was adjusted within experimental error until an electronic sum rule yielded proper results. This spectrum was appropriately Fourier transformed to give the real part of the complex refractive index. Calculations over several regions were joined to create a smooth spectrum over the range $10^{-3}$ to $10^{6}$ $cm^{-1}$. The result was a complete and self-consistent spectrum of both real and imaginary parts of the complex refractive index over 9 decades.

To address the question of error in the calculation of $n(\nu)$, the literature was again consulted to find sufficient data for comparison. The following four spectral locations were chosen: 10 $cm^{-1}$, $5x10^{2}$ $cm^{-1}$, $2x10^{3}$ $cm^{-1}$, and $1x10^{4}$ $cm^{-1}$. The procedure was to average the data, then find the percent difference between the mean and the results obtained in this research.

At 10 $cm^{-1}$, the data of Downing and Williams, Afsar and Hasted, and Zolotarev et al.[28] yielded a mean value of 2.588.

The value obtained in this research was 2.399, a difference of 7.6 percent. In the paper by Downing and Williams, 10 $cm^{-1}$ was the lowest frequency point of their calculations. Their paper stated that the data become "coarse at the lowest frequencies."[29] Further, they obtained optical constants for their calculations from Ray,[30] whose data were presented graphically and not in tabular form, thereby allowing for considerable inaccuracy. The work by Afsar and Hasted used a Fourier transform spectrophotometer. As a result, their calculations for the low endpoint of the range, which is near 10 $cm^{-1}$, are subject to the same problems as are outlined in Chapter IV above. The data of Zolotarev et al. are a result of Kramers-Kronig calculations, equivalent to the Fourier transform method. The data used are sparse in the region of 10 $cm^{-1}$, thus raising the objection that resolution in that range was not good. Considering all the above factors, one might well conclude that the results of the present study are more accurate at 10 $cm^{-1}$ than the values used for comparison.

At $5x10^{2}$ $cm^{-1}$, values by Hale and Querry, Downing and Williams, Pontier and Dechambenoy,[31] Rusk et al.,[32] and Zolotarev et al. gave a mean of 1.473. The present work gives 1.468, a difference of 0.4 percent. The same authors reported data at $2x10^{3}$ $cm^{-1}$ which gave a mean of 1.323. The present work gives 1.306, a difference of 1.3 percent. At $1x10^{4}$ $cm^{-1}$, data of Hale and Querry, Pontier and Dechambenoy, and Zolotarev et al. gave a mean of 1.325. The present study gives 1.322, a 0.2 percent difference. These values are much closer

to those of the comparison works than at lower wave number regions. To the extent that they differ, it is believed that the use of such a broad ranged and self-consistent absorption spectrum as is illustrated in Figure 3 gives more reliable results. Considering the uncertainty, however, it is probably reasonable to say that the values of $n(\nu)$ are accurate only to three significant figures.

One might hope that the future will bring more efficient algorithms for the computation of a spectrum over a broad range. The ideal would be a single calculation over a very large range with very fine divisions among the data. This would give a spectrum accurate near the endpoints and high in resolution, one which is entirely self-consistent. Hopefully, the present work is a small step in that direction.

## REFERENCES


1. George M. Hale and Marvin R. Querry, Appl. Opt. 12, 555 (1973).
2. J. M. Heller, Jr., R. N. Hamm, R. D. Birkhoff, and L. R. Painter, J. Chem. Phys. 60, 3483 (1974).
3. Harry D. Downing and Dudley Williams, J. Geophys. Res. 80, 1656 (1975).
4. O. V. Kopelevich, Opt. Spektrosk. 41, 666 (1976) [Opt. Spectrosc. 41, 391 (1976)].
5. M. N. Afsar and J. B. Hasted, J. Opt. Soc. Am. 67, 902 (1977).
6. Marvin R. Querry, Phillip G. Cary, and Richard C. Waring, Appl. Opt. 17, 3587 (1978).
7. A. C. Tam and C. K. N. Patel, Appl. Opt. 18, 3348 (1979).
8. Kenneth S. Cole and Robert H. Cole, J. Chem. Phys. 9, 341 (1941).
9. Arne Engstrom, X-ray Microanalysis in Biology and Medicine (Elsevier, Amsterdam, 1962), p. 9.
10. Reference 9, pp. 10-11.
11. J. Lenoble and B. Saint-Guilly, Compt. Rend. 240, 954 (1955).
12. L. R. Painter, R. D. Birkhoff, and E. T. Arakawa, J. Chem. Phys. 51, 243 (1969).
13. Charles W. Robertson and Dudley Williams, J. Opt. Soc. Am. 61, 1316 (1971).
14. P. Debye, Polar Molecules (Chemical Catalogue, New York, 1929).

15. Reference 14, p. 94.

16. Reference 14, p. 85.

17. Reference 8, p. 346.

18. J. B. Hasted, in Water, a Comprehensive Treatise, edited by Felix Franks (Plenum, New York, 1972), pp. 276-289.

19. J. H. Hubbell, Nat. Stand. Ref. Data Ser., Nat. Bur. Stand. 29 (1969).

20. Reference 9, pp. 10-11.

21. J. D. Jackson, Classical Electrodynamics (Wiley, New York, 1975), p. 218.

22. C. W. Peterson and Bruce W. Knight, J. Opt. Soc. Am. 63, 1238 (1973).

23. Reference 21, pp. 284-5 and 314-15.

24. R. V. Churchill, J. W. Brown, and R. F. Verhey, Complex Variables and Applications (McGraw-Hill, New York, 1974), pp. 88-93.

25. D. W. Berreman and F. C. Unterwald, Phys. Rev. 174, 791 (1968).

26. Reference 25, p. 792.

27. E. O. Brigham, The Fast Fourier Transform (Prentice-Hall, Englewood Cliffs, 1974), pp. 94-97.

28. V. M. Zolotarev, B. A. Mikhailov, L. I. Aperovich, and S. I. Popov, Opt. Spektrosk. 27, 790 (1969) [Opt. Spectrosc. 27, 430 (1969)].

29. Reference 3, p. 1657.

30. Peter S. Ray, Appl. Opt. 11, 1836 (1972).

31. L. Pontier and C. Dechambenoy, Ann. Geophys. 22, 633 (1966).

32. A. N. Rusk, D. Williams, and M. R. Querry, J. Opt. Soc. Am. 61, 895 (1971).

VITA

David Jay Segelstein was born on December 21, 1949, in New York City. After moving to Kansas City, Missouri, in 1952, he was educated in local public schools and graduated from Southwest High School in 1967. In 1971, he graduated from Columbia University with a Bachelor of Arts degree in Sociology.

Mr. Segelstein attended the University of Missouri-Kansas City Law School, receiving the Juris Doctor degree in 1975. Thereafter, he practiced law until 1978, when he returned to the University of Missouri-Kansas City to study Physics. Upon completion of his degree requirements, Mr. Segelstein plans to continue his education in a doctoral program at Princeton University beginning in September, 1981.